Effect of Alkali Treatment on the Microstructure and Tensile Properties of Abaca Fiber

Ming Cai

Tokushima University

ABSTRACT

Natural fibers are increasingly being used in fiber-reinforced composites (FRCs) due to their high tensile strengths, light weight, low cost and non-toxicity. Abaca, also known as Manila hemp, is a native plant of the Philippines where it is grown as a commercial crop. Abaca fiber has a high cellulose content and very good mechanical properties, including a high tensile strength and high Young's modulus. Chemically modified abaca fibers demonstrate enormous potential as natural reinforcing agents in composite materials, though little work to date has been reported on the effect of different chemical treatments on abaca fiber structure, composition and mechanical strength, motivating a detailed investigation.

This thesis systematically explored the effects of alkali concentration and treatment time on the microstructure and tensile properties of abaca fibers. Further, the interfacial bonding mechanism in abaca fiber-reinforced epoxy was also studied. Scanning electron microscopy (SEM), X-ray diffraction (XRD), Fourier transform-infrared spectroscopy (FT-IR), fiber tensile tests and fiber composite pull-out tests were used to obtain a detailed picture of different alkali treatments on abaca fiber properties and composite performance.

The effect of NaOH concentration and treatment time on the mechanical properties of abaca fibers was first investigated. Abaca fibers were immersed in 3, 5, 7, 9, 11, 13 and 15 wt. % aqueous NaOH solutions for 5 min, and 5, 10 and 15 wt.% aqueous NaOH solutions for 5, 10, 15, 20, 25 and 30 min. The mechanical properties of the fibers increased after each alkali treatment. The highest Young's modulus and tensile strength was achieved after 7 wt.% NaOH treatment for 5 min. The effect of treatment time on fiber properties was modest compared to the effect of alkali concentration.

The effect of NaOH concentration (5, 10 and 15 wt. %) and treatment time on abaca fiber microstructure and chemical composition was subsequently studied. The abaca fibers were

immersed in different NaOH solutions for specific times, rinsed with water and dried. The morphology of the treated abaca fibers were then characterized in detail. After alkali treatment, it was found by SEM that the lumen (the hollow core in the center of the elementary abaca fibers) had completely disappeared due to the swelling of surrounding cell walls. The abaca fiber bundles also became twisted after 10 and 15 wt. % NaOH treatments. The XRD measurements revealed that cellulose I in the abaca fibers was partially transformed to cellulose II after 15 wt. % NaOH treatments. Meanwhile, FT-IR analysis revealed that the alkali treatments caused gradual removal of the binding materials, such as hemicelluloses and lignin from the abaca fibers, resulting in the separation of abaca fiber bundles into individual elementary fibers. The Young's modulus of the abaca fibers treated with 5 wt. % NaOH for 30 minutes increased by 30-40% compared to the native fibers, whereas the Young's modulus of fibers treated with 10 and 15 wt. % NaOH decreased by 20-25% and 25-30%, respectively, compared to the native fibers. A non-linear behavior was observed in the stress-strain curves of the abaca fibers after 10 and 15 wt. % alkali treatments, which is explained by alkali-treated fiber twisting.

The effect of NaOH treatment on the abaca fiber-epoxy interface was then studied. The crystallinity index, microstructure, surface morphology, chemical composition, and mechanical characteristics of the untreated and alkali-treated abaca fibers were evaluated, along with the interfacial adhesion with epoxy and interfacial shear strength (IFSS). Results showed that the degree of crystallinity in the abaca fibers increased by 12% following 5 wt. % NaOH treatment for 2 hours. This treatment also increased the tensile strength and the Young's modulus (increased by 37.8%) of the fibers. However, the Young's modulus of abaca fibers decreased by 34% and 49% after 10 and 15 wt. % NaOH treatments for 2 hours, respectively, indicating that strong alkali treatments negatively impacted fiber stiffness and suitability for use in composite applications. The 5 wt. % NaOH treatment improved the

interfacial shear strength (IFSS) of abaca fiber-reinforced epoxy by 32 %. It can be concluded that pre-treatment of raw abaca fibers with 5 wt. % NaOH is highly beneficial for the fabrication of abaca fiber-reinforced composites.

Results guide the development of improved abaca fiber-reinforced composites for automotive and other high-value applications.

ACKNOWLEDGEMENTS

First and foremost, I am greatly indebted to my supervisor professor Hitoshi Takagi for all his ideas, encouragements, and supports, without whom this work would not have been completed. I have benefited in many ways from his considerable experience and knowledge.

I would like to express my appreciation to professor Yan Li, who is my supervisor in Tongji University, China. Without her support, I would miss this opportunity to study at Tokushima University as a double degree student.

I would also like to express my gratitude to associate professor Antonio N. Nakagaito for helping me and for always being there to discuss on my experimental results.

I would like to express my sincere thanks to the professor Masahiro Katoh of the Department of Chemical Science and Technology, and to Mr. Tomoyuki Ueki of the Center for Technical Support for their experimental supports.

I would like to express my thanks to Dr. Jana Frank, Dr. Geoffrey I.N. Waterhouse, and Mr. Jie Xu for helping me a lot on my papers. I would also like to thank Dr. Kazuya Kusaka, Dr. Chizuru Sasaki, professor Tatsuya Okada, Mr. Satoshi Sugano, and professor Yasuhiro Mizutani for their help and experimental support.

I am grateful to my committee members who are PhD student Noor Hisyam Noor Mohamed, PhD student Rosni binti Yusoff, Norfarlysa binti Zinodin, Shoma Maluyama,Kohei Fujii, Hiroki Ishikawa, Hiroaki Genta, Taishi Kitahama, Takaya Miyazaki, Yuya Muneta, Koutaro Lemura, Masayuki Tezuka, Seiji Shoji, Rikuto Kitadani, Hiroyuki Kinii, Takahiro Matsui, Sotaro Kanzawa, Kou Ikenaga, Takuhiro Kodama, Yoshitaka Ueno, Yutaka Otsuka, Kenya Nishimura, Hayato Sakaki, Ryoji Matsuda, and Shota Yuki from the Ecomaterial Science Laboratory for helping me with my experiments, working hard together, and their encouragement and insightful comments for the brainstorming discussion at journal club we

have had in the past two years. I also would like to thank office staffs Ms. Michiko Shinohara, Ms. Sawa Asada et al.

Special thanks are due to my family members for their strong support and encouragement during my study. I thank all my colleagues and friends for their strong help, valuable advice, and discussions during my study.

Finally, I would like to acknowledge with gratitude the financial support of the Double-Degree Exchange Program between Tokushima University (Japan) and Tongji University (China).

CONTENTS

LIST OF TABLES

LIST OF FIGURES

Chapter 1 General Introduction

1.1 Research background

In recent decades, natural fibers have been used as reinforcing material in thermoset or thermoplastic matrixes to make green composites. Advantages of natural fibers in industrial applications are their light weight, low cost, and nontoxic characteristics, coupled with biodegradability and high specific stiffness. Due to the advantages of the natural fibers, they have been attracting the attention of both academic and industrial worlds [1-4]. At present, natural fibers are suitably applicable for building industries, aerospace, sport, packaging and automobiles [5].

As reinforced materials, there are two basic types of fibers: natural fibers and synthetic fibers, as shown in Figure 1.1. Many researchers have studied composites based on these fibers [6, 7]. Currently, synthetic fibers like glass, carbon, and aramid are widely used in polymer-based composites. Compared with the synthetic fibers, natural fibers have a lot of advantages as mentioned above; however, the weaknesses of natural fibers are high water absorption and weaker interfacial bonding with polymeric matrix. These are the reasons why natural fibers have not replaced the synthetic fibers in high-load applications. Their application is still limited to interior parts such as in door panels and seat backs [8]. In order to tap and develop the industrial potential application of natural fibers, their surface modification is becoming an important field of research which focuses on the improvement of fiber-matrix interfacial adhesion.

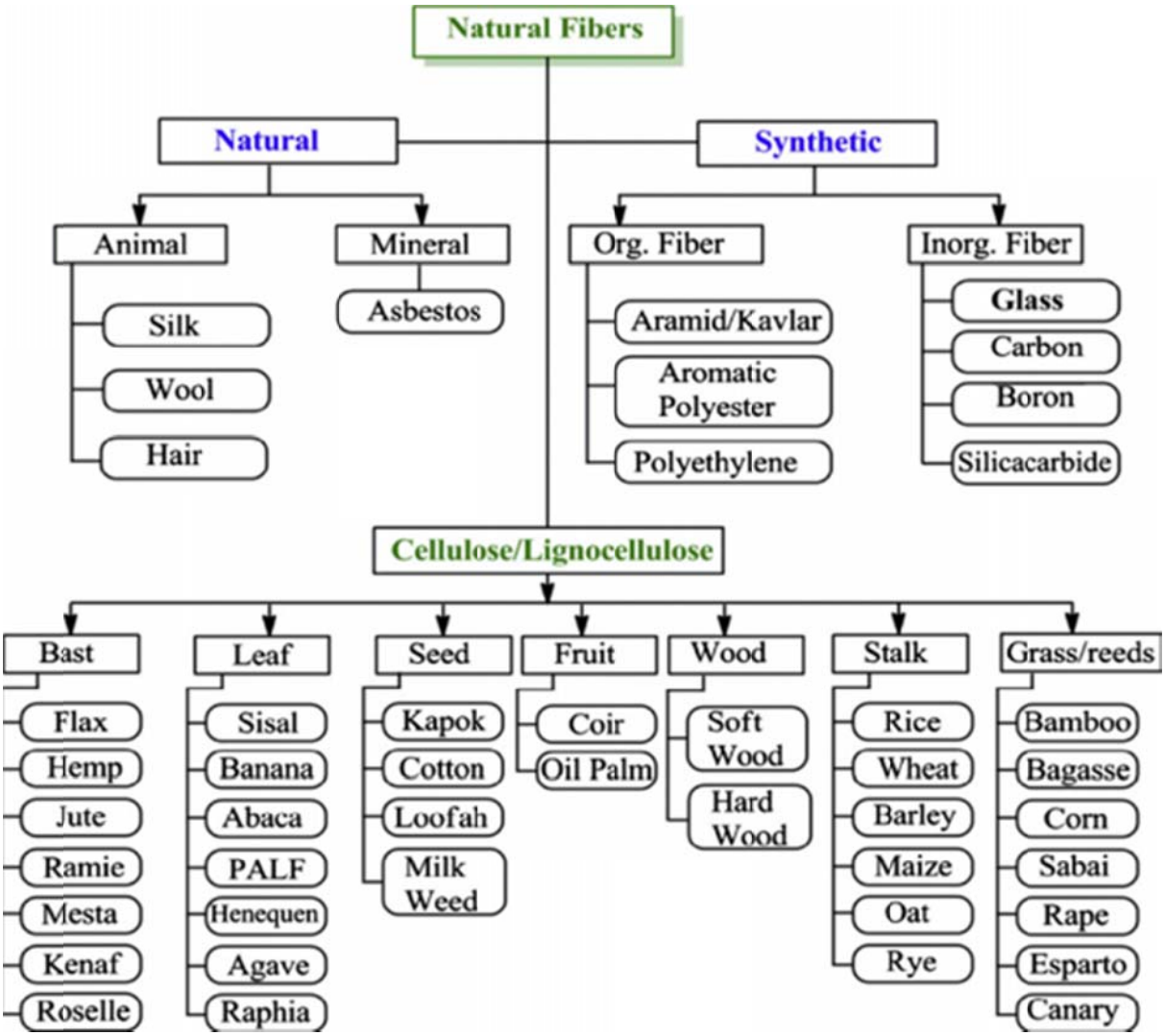

Figure 1.1 Classification of natural and synthetic fibers [9].

The outcome of the modification depends on the physical, chemical, and morphological properties of fibers [10-14]. The cross-sectional area of the fibers is one of the parameters that influence the physical properties of natural fibers. Especially, the lumen in the cross-sectional area of the fiber affects the thermal conductivity of the natural fiber reinforced composites, as is reported by Liu et al. [7, 15].

Moreover, to better understand the microstructure, mechanical properties, chemical composition and surface adhesive bonding of natural fibers is needed for developing natural fiber-reinforced composites. The components of natural fibers include cellulose,

hemicelluloses, lignin, pectin, waxes, and water soluble substances [16], which will be introduced in the next chapter.

1.2 Objective

A focus of this work is the understanding of microstructure and mechanical properties of abaca by different alkali concentration with different treating time. Furthermore, we also investigated their chemical components and crystalline structure related to alkali treatment. From these studies, several objectives were established. They are as follows:

1. To evaluate mechanical properties of alkali-treated abaca fibers by different concentration and different treatment times compared with untreated abaca fibers.
2. To explore why the lumen of fiber disappears after alkali treatment, and to explain how the lumen was affected.
3. To assess how the fiber was twisted by alkali treatment, and to explain how the fiber twisting occurred by alkali treatment.
4. To evaluate the crystallinity of cellulose in alkali-treated abaca fiber by XRD and to explain the transformation of cellulose I to cellulose II.
5. To demonstrate that the chemical components of hemicellulose, lignin and pectin et. al. were removed, using FT-IR after alkali treatment.
6. To investigate the interfacial adhesion of alkali-treated abaca fibers by different concentrations, comparing to untreated abaca fibers.

1.3 Scope of project

This research provides a comprehension of lumen shrinking after alkali treatment. The mechanical behavior of alkali-treated abaca fiber is studied and the interfacial properties of fiber reinforced composite is also evaluated.

1.4 Chapter outline

Chapter 2 is titled, “Literature Review” and outlines abaca fibers and types of chemical treatments for plant fibers. It describes the advantages and challenges of abaca fiber.

Chapter 3 is titled, “Influence of Different Alkali Concentrations on Morphology and Tensile Properties of Abaca Fibers”. It describes the results of SEM, FT-IR, XRD, and tensile testing of alkali-treated abaca fibers and offers a discussion of the results.

Chapter 4 is titled, “Influence of Different Alkali Treatment Time on Morphology and Tensile Properties of Abaca Fibers”. It describes the results of the SEM and tensile testing of the alkali-treated abaca fibers.

Chapter 5 is titled, “Influence of Alkali Treatment on Internal Microstructure and Tensile Properties of Abaca Fibers”. It discusses the mechanism of the effect of the microstructure and mechanical properties of alkali-treated abaca fibers. It also demonstrates the conversion of cellulose I to cellulose II as a means of alkali treatment. Moreover, its relationship with the structural form of cellulose was studied.

Chapter 6 is titled, “Influence of Alkali Treatment on interfacial bonding in abaca fiber composites”. It conducted the evaluation of interfacial properties of alkali-treated abaca fibers reinforced epoxy.

Chapter 7 is titled, “Conclusions and Suggestions for Future Work”. It furnishes a summary of the results of this study and suggests directions for future work, e.g. measurement of the MFA and the application of cellulose II

The “Appendix” provides a supplement of Chapter 3. It gives the details of the tensile results and microstructure of the abaca fibers.

Chapter 2 **Literature Review**

2.1 Introduction

Natural fibers are environmentally friendly in nature. They are grouped based on their origins from plants, animals or minerals. In present, plant fibers are being used as reinforcement in polymeric materials [13, 17]. Plant fibers consist of continuous hollow cells which have different sizes, shapes, and arrangements in different types of fibers such as bamboo, hemp, flax, ramie, sisal, jute, abaca, etc. [12, 18]. Many studies have been attempted on mechanical properties of natural fibers and incorporated into various thermosets (epoxy, phenolic and polyester) and thermoplastics (PLA and PHA) [19-21]. During those studies, the adhesion has been emphasized as it plays significant role between the fiber-matrix in the final mechanical properties of the composites. However, natural fiber contains large amount of hydroxyl group in the fibers, it tends to be active polar hydrophilic material. The weak interfacial bonding can result from hydrophilic fiber and hydrophobic matrix. This in turn leads to impaired mechanical properties of the composites. The weak interfacial bonding can be remedied by chemical modification of fibers by making it less hydrophilic. Meanwhile, the mechanical properties of composite can be improved after chemical treatment according to the literature [22-24].

In this chapter, the chemical components and the structure of the natural fiber are reviewed. Meanwhile, the abaca fiber which is the subject in this research has been reviewed. A review of the chemical modification for natural fibers was also conducted in order to collect related information. In the end of this chapter, the research focus has been reminded.

2.2 Natural fibers and their chemical components

A single natural filament generally has a diameter on the order of about 10 μm and is itself a type of natural composite material. Each fiber contains a primary cell wall and three secondary cell walls. The cell walls are made up of a lignin-hemicellulose matrix and microfibrils, which are oriented in different directions in each cell wall. The microfibrils each have a diameter of the order of 10 nm, and are made up of around 30-100 cellulose molecules [25,26]. These microfibrils have been found to possess better mechanical properties for manufacturing composites alone than combined in an individual fiber. Filaments are bonded into a bundle by lignin and then attached to the stem by pectin. The lignin and the pectin are both weaker polymers than the cellulose, so they must be removed if the fibers are going to be effective as composite reinforcements. Most of the pectin is removed when the bundles are separated from the rest after alkali treatment.

These cells are cemented together by an intercellular substance, which is isotropic and non-cellulosic in nature [25]. Individual cells consist of primary wall and secondary wall as shown in Figure 2.1 [26]. The secondary wall is made up by three layers and the thick middle layer determines the mechanical properties of the fiber. The layers differ in the composition and orientation of cellulosic microfibrils. The angle between the fiber axis and the microfibrils is called microfibrillar angle [14]. The microfibrillar angle, or the average angle at which the microfibrils are oriented off of the axis of the filament, is thought to be responsible for a number of mechanical properties of the fiber, as smaller angles generally lead to higher strength and stiffness and larger angles to better ductility. Among plant species, and even fibers of the same species, the fiber cell walls differ in their compositions and their microfibrillar angles. The central hollow structure of each cell is named lumen [27].

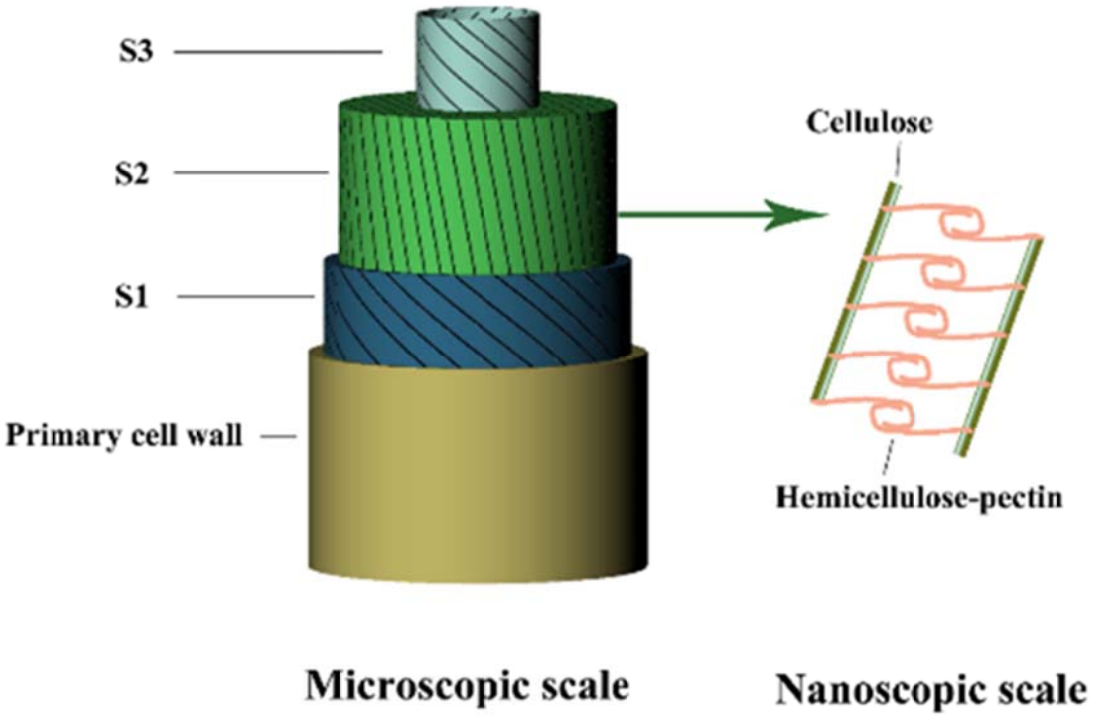

Figure 2.1 The structure of natural fibers [26]

Plant-based natural fibers consist of cellulose, hemicelluloses, lignins, pectin, and waxy substances [13]. Table 2.1 lists some plant fibers and their chemical composition [16, 28]. Cellulose is the main component, which is responsible for the determination of the mechanical properties of plant fibers [13]. Lignins and hemicelluloses also affect the characteristic properties of the fibers due to the hydroxyl groups in their molecular structure [29].

Table 2.1 Composition of natural fibers [16]

Fiber	Cellulose (%)	Hemicelluloses (%)	Lignin (%)	Pectin (%)	Ash (%)
Flax	71	18.6-20.6	2.2	2.3	--
Kenaf	31-57	21.5-23	15-19	--	2-5
Jute	45-71.5	13.6-21	12-26	0.2	0.5-2
Hemp	57-77	14-22.4	3.7-13	0.9	0.8
Ramie	68.6-91	5-16.7	0.6-0.7	1.9	--
Bamboo	60.8	6.8	32.2	--	--
Abaca	56-63	15-17	7-9	--	3
Sisal	47-78	10-24	7-11	10	0.6-1

Natural fibers from plants can be grouped into bast, leaf, seed or fruit fibers. The elementary unit of a cellulose macromolecule is the anhydro D-glucose, which contains three hydroxyl (-OH) groups as shown in Figure 2.2(a) [27]. The hydroxyl groups form hydrogen bonds inside the macromolecule itself (intramolecular) and between other cellulose macromolecules (intermolecular) [30]. Cellulose microfibrils have amorphous and crystalline domains and a high degree of organization. Cellulose fibers interact with water molecules on the surface and the bulk. Moisture from the atmosphere comes into contact with the fibers hydroxyl groups forming hydrogen bonds with water molecules [25]. All these factors play an important role when the fiber is in contact with the matrix which affect the interface adhesion of the composites.

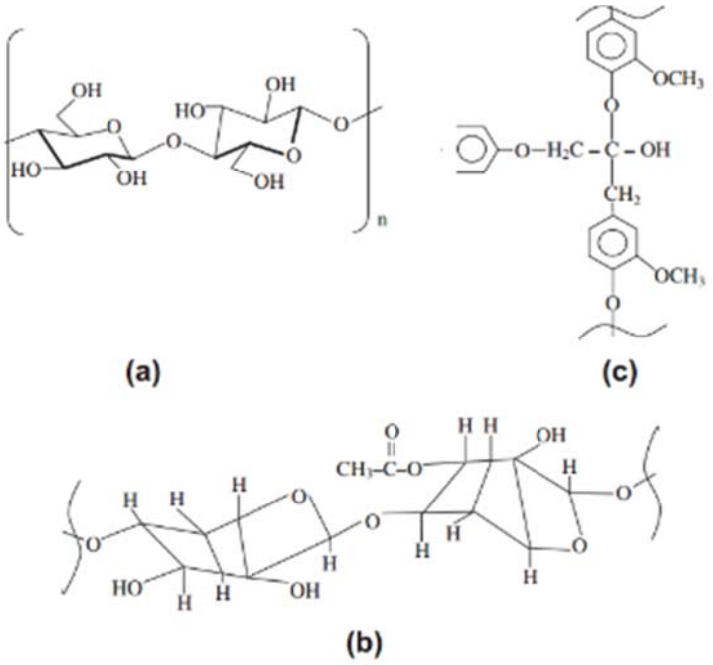

Figure 2.2 Chemical structure of (a) cellulose (b) hemicellulose and (c) lignins [27]

Hemicelluloses have varied chemical structure and occur mainly in the primary cell wall with branched polymers carbon sugars [13]. One type of the hemicelluloses is shown in Figure 2.2(b) [27]. Hemicellulosic polymers are branched, fully amorphous and have a significantly lower molecular weight than cellulose. Because of its open structure containing many hydroxyl and acetyl groups, hemicellulose is partly soluble in water and hygroscopic [16]. Hemicelluloses in fibers are sensitive to react with NaOH [25].

Lignins are amorphous, highly complex, aromatic structure polymers of phenylpropane units, but they have the lowest water sorption of natural fiber components [16]. One type of lignin is shown in the Figure 2.2(c) [27].

Pectin structure is complex, their side chains are often cross-linked with the calcium ions and arabinose sugars [13]. Pectin is soluble in water only after a partial neutralization with alkali or ammonium hydroxide [17].

Waxes are the part of the fibers that can be extracted with organic solutions. Waxy materials consist of different types of alcohols, which are insoluble in water as well as in several acids [17].

2.3 Abaca fibers

Among all the natural fiber-reinforcing materials, abaca appears to be a promising material because it is low cost and abundantly available. Abaca fibers are extracted from the stalks of plants. Abaca belongs to the Musasea family of plant native to Asia and is planted in humid areas including the Philippines and east Indonesia. The Philippines is the world's largest source and supplier of abaca fibers for cordage and pulp for specialized paper. It supplies 85% of the global abaca fiber market [31].

2.3.1 Properties of abaca fibers

The need for using abaca fibers in place of the traditional glass fiber partly or fully as reinforcing agents in composites stems from their characteristics:

- Lower specific density (1.25 g/cm^3) and higher specific Young's modulus (48.5 GPa) of abaca compared with those of glass (2.5 g/cm^3 and 28 GPa, respectively).
- Abaca fiber is 100% bio-degradable.
- It has good insulating and antistatic properties, as well as low thermal conductivity.

2.3.2 Advantages of abaca fibers

Abaca is considered one of the strongest plant fibers. Abaca fiber has high tensile strength, and is resistant to rotting, and its specific flexural strength is near to that of glass fiber [32].

2.3.3 Uses and application of abaca fibers

Abaca is a versatile plant with several uses. Abaca fibers are removed from the abaca's stalk to produce products such as tea and coffee bags, sausage casing paper, currency notes

(Japan's yen banknotes contain up to 30% abaca), cigarette filter papers, medical/food preparation/disposal papers, high-quality writing paper and more.

Currently abaca is being used for interior trim parts in the automotive industry as a filling material. However, it can also be used for structural applications in automotive industry given its strong tensile strength. Nowadays, abaca fiber reinforced composites are gaining interest due to their innovative application in under-floor of Daimler AG vehicles [5, 32, 33].

Abaca fibers reinforced polypropylene thermoplastic composites have been used in automobile body parts of Mercedes Benz. It can be used to reduce the weight of automotive parts and to facilitate more environmentally friendly production and recycling of the car parts. Owing to the extremely high mechanical strength of the fiber as well as its length, abaca offers great potential for different industrial applications even in highly stressed components.

2.4 Advantages and disadvantages of natural fibers

The majority of natural plant fibers have been utilized for composite. The strengths and Young's modulus of plant fibers have been recognized and utilized. Seat backs, boot liners and aviation interior are some of the present applications that take advantage of the good mechanical properties of plant fibers. Furthermore, there are several other advantageous characteristics that plant fibers have over traditional fibers. Plant fibers are typically derived from the renewable plants which is significantly cheaper and subjected less to economic fluctuations. Meanwhile, the lower density of cellulose plant fibers can be a half of traditional fiber such as glass fiber. Therefore, the resulting plant fiber reinforced composites can be lighter than traditional composites. They are more efficient systems and have lower costs with material transportation. Plant fibers use as non-toxic materials can be occupationally safer compared to glass fibers which can cause allergic reaction, irritation to the respiratory

system or skin irritation. Plant fibers are also known as being biodegradable, environmentally friendly and sustainable.

However, the disadvantages of natural fibers still exist for composite reinforcement. The first difference compared to traditional fiber-reinforced composite is the processing and manufacture of plant fibers. This may require companies to develop new methods and machines for manufacture of natural fiber reinforced composite for widespread implementation.

Secondly, the synthetic fibers can be repeatedly produced with bearing structure. However, the plant fiber-reinforced composites show large scatter in properties due to varying fiber properties due to growing conditions, harvesting and processing techniques. Thirdly, the more serious problem with using plant fibers in composites is their strong water absorption. It leads to the poor interfacial adhesion by hydrophilic plant fiber with hydrophobic matrix. Therefore, for plant fiber to be successful used, it is essential that weaknesses are addressed in terms of efficient solution by thorough research.

2.5 Fiber-Matrix adhesion

A strong interface adhesion of natural fiber-matrix is needed for high strength properties of composites, due to the effective stress transfer from the matrix to the fiber. Many research related to natural fibers-reinforced composites that there is weak adhesion between the hydrophilic fiber and hydrophobic matrices. Interface adhesion is one of the key technology of composite materials. Meanwhile, mechanical properties of the composites improve with interface adhesion [25]. However, the main chemical composition of plant fiber is cellulose which contains a large number of hydroxyl groups. It leads to the incompatibility between hydrophilic fiber and hydrophobic matrix, further weak interfacial adhesion and eventually low mechanical properties. Therefore, it is crucial to obtain improved interfacial properties

and mechanical properties of plant fiber reinforced composites so that more applications could be realized. Furthermore, these hydroxyl groups of the plant fiber could be removed by chemical modification.

2.6 Chemical modification of natural fibers

The chemical modification is a common way to improve the mechanical properties of natural fiber-reinforced composites.

Natural fibers are hydrophilic due to hydroxyl groups in their structure which are easy to react with water molecules. Therefore, natural fibers are incompatible with hydrophobic polymer resins because hydrophilic fibers absorb moisture. This is the reason for poor interfacial adhesion between the polar, hydrophilic fiber and the non-polar, hydrophobic matrix [25]. Interface adhesion between hydrophilic natural fibers and the hydrophobic polymer resins can be improved by chemical surface treatment. Chemical pretreatments can clean the fiber surface, stop the moisture absorption process and increase the surface roughness to increase the interlocking with the matrix [14].

When the fiber is subjected to chemical treatment, the hydroxyl groups are broken and replaced by a new reactive functional group. The hydrophilic character of the fiber is therefore reduced, which results in improved fiber-matrix adhesion characteristics of the composites. Therefore, the problem can be solved by treating natural fibers with suitable chemicals to decrease the number of hydroxyl groups on the fiber surface. Several chemical treatment methods have been introduced as the following.

2.6.1 Alkali treatment

Alkali treatment of natural fibers is known to improve stiffness, strength, and dynamic flexural modulus of the composites [32]. Alkali treatment of cellulosic fibers, also called

mercerization, is a classic method to improve interfacial bond strength and adhesion between the matrix and the fibers [29].

In addition, alkali treatment leads to fibrillation which causes the breaking down of the natural fiber bundle into elementary fibers. Due to the mercerization process, it also takes out certain portion of hemicelluloses, lignin, pectin and other chemical components [13]. Therefore, the aspect ratio is increased and a rough fiber surface topography is developed [13, 29]. When the hemicelluloses as bonding materials are removed, the interfibrillar region becomes less dense and less rigid, making the fibrils more capable of rearranging themselves along the direction of tensile deformation. In contrast, softening of the interfibrillar matrix negatively affect the fiber bundle under tensile deformation [17].

Moreover, moisture resistance of the fiber is improved because hydrophilic hydroxyl groups are partially removed [13]. Fiber-matrix adhesion consequently improves. Alkali treatment changes the orientation of highly packed crystalline cellulose order and forms amorphous region by swelling the fiber cell wall. The (OH) groups present among the molecules from the fiber are broken down by alkali treatment, then reacting with water molecules (H-OH). The remaining reactive molecules form fiber-O-Na groups and water molecules. Thus, the (OH) group was moved out from the fiber structure [27]. This process is described in the following reaction [16, 29]:

$$\text{Fiber-OH} + \text{NaOH} \longrightarrow \text{Fiber-O}^{-}\text{Na}^{+} + \text{H}_2\text{O} \qquad (1)$$

The efficiency of the alkali treatment depends on the type, concentration, and time of the alkaline treatment. The immersion in alkaline solution leads to formation of high amounts of voids and makes the surface rougher. The effective surface area is increased, which improves mechanical interlocking between the fibers and the matrix [30]. The alkali treated fibers have better tensile properties compared to the untreated fibers. The presence of crystalline

celluloses is higher in treated fibers than untreated fibers. The alkali treated natural fibers have good mechanical properties which are comparable to the man-made fibers [25].

2.6.7 Silane treatment

Silane treatment is an effective method to chemically modify both the hydroxyl groups of cellulose and the functional groups of the matrix. Silane is a coupling agent which improve the degree of cross-linking in the interface region and offer better bonding [29].

Coupling agents are molecules possessing two functions. The first is to react with the OH groups of cellulose and the second is to react with functional groups of the matrix. The silane molecules act as a bridge between the matrix and the cellulose. The organo-functional group bonds between the hydrophilic fiber and hydrophobic matrix are formed through a siloxane bridge. The general chemical formula of silane is $X_3Si\text{-}R$ [25, 30]. R is a reactive group that reacts with the resin, and X is a group, which reacts with hydroxyl groups of the cellulose surface [30]. Silane coupling agents form a bridge to bond the cellulose fibers to the matrix by covalent bonds.

2.6.8 Acetylation treatment

Acetylation is an effective way to reduce the moisture absorption by the fibers. It esterifies the hydroxyl groups on the fiber surface [25].

Acetylation consists of a reaction introducing an acetyl functional group (CH_3COO^-) to replace the OH^- of cellulose. The fibers become hydrophobic because they are treated with acetic anhydride substitutes. The polymer hydroxyl groups react with the acetyl groups (CH_3COOH) [16]. Acetylation is based on the reaction between the cell wall hydroxyl groups and acetic or propionic anhydride at elevated temperature. The reaction of acetic anhydride with the fiber is shown below [16, 31]:

$$\text{Fiber-OH} + CH_3 - C(=O) - O - C(=O) \longrightarrow CH_3 - \text{Fiber} - OCOCH_3 + CH_3COOH \qquad (2)$$

It is possible to speed up acetylation by using a catalyst. The hydroxyl groups are acetylated in different ways. The moisture absorption by the cell wall is reduced if the hydroxyl groups in the cellulose are substituted with acetyl groups. The acetylation was used in surface treatment of natural fiber-reinforced composites in several studies [31].

2.6.9 Benzoylation treatment

Benzoylation is an important chemical treatment method in organic synthesis. Benzoylation treatment uses benzoyl chloride ($C_6H_5C=OCl$) to reduce the hydrophilic nature of the treated fiber and improve fiber matrix adhesion, thereby increasing the strength of the composite [16]. It also enhances thermal stability of the fiber. Before the benzoylation treatment alkali pretreatment is used to activate the hydroxyl groups of the fiber. Then the fiber is soaked in benzoyl chloride solution for 15 min. Afterwards ethanol solution is necessary for 1 h to remove benzoyl chloride that adhered to the fiber surface followed by washing with water and oven drying [13].

2.6.10 Other chemical treatments

Isocyanate is a compound containing the isocyanate functional group –N=C=O, which is highly reactive with the hydroxyl groups of cellulose and lignin in fibers and reduce the hydrophilic tendency [34].

Permanganate is a compound that contains permanganate group MnO_4^-. The potassium permanganate ($KMnO_4$) solution has been used in most permanganate treatments. As a result, the hydrophilic tendency of the fibers was reduced by permanganate treatment; therefore, the water absorption of fiber-reinforced composite decreased [16].

2.7 Research focus

The purpose of this study is thus to clarify the effect of alkali treatment on the microstructure and mechanical properties of abaca fibers. However, there have been many studies on alkali

treatment of natural fibers but very limited information is available on the effect of lumen size of the alkali treated-abaca fiber. More importantly, the hollow microstructure of natural fiber affects the thermal conductivity, sound absorption, mechanical properties etc. of the natural fiber-reinforced composites. Therefore, it is important to explore the effect of the alkali treatment on microstructure and mechanical properties of the natural plant fibers. The interfacial properties were also assessed in this thesis.

Chapter 3 Influence of Different Alkali Concentrations on Morphology and Tensile Properties of Abaca Fibers

3.1 Abstract

Abaca, also known as Manila hemp, is native to the Philippines, where it is grown as a commercial crop. It belongs to the Musasea family and is cultivated for ropes and fibers. The abaca fiber is a natural fiber with highest cellulose content. In this study, the effects of alkali treatments on mechanical properties and microstructure of abaca fibers are discussed. Abaca fibers were soaked in the aqueous solution of sodium hydroxide at the concentration from 3 to 15 wt.% for 5 minutes and subsequently subjected to tensile tests and observations by scanning electron microscopy (SEM) to assess morphological changes caused by the alkali treatment. Fourier transform-infrared spectroscopy analysis demonstrated that the treatment led to the gradual removal of lignin and hemicelluloses from the abaca fibers. The cellulose crystallinity of abaca fibers was analyzed by an X-ray diffraction method. SEM images revealed that the lumen size decreased and shrunk with increasing alkali concentration. The tensile strength of the alkali-treated abaca fibers was higher than that of the untreated ones. The Young's modulus increased with increasing alkali concentration up to 7 wt.% and then decreased. However, the strain at break decreased below 7 wt.% and then increased. The lumen size started to decrease from 7 wt.% alkali concentration.

3.2 Introduction

During the last decade, the natural plant fibers have been popularly used for the industrial production of biodegradable materials based on their environmentally friendly and high specific mechanical properties [35]. In engineering, the natural fiber-reinforced thermoplastics or thermosets composites have been used in various industrial markets, such

as aeronautic and building industries. Especially, it has been used in automobile industry such as door panels, seat backs, headliners, package trays, dashboards, and interior parts [33, 36]. In recent years, many investigations have been done to analyze the different properties of different natural fibers in different ways [12]. H. Takagi and others had researched and contributed with the recent developments of natural fiber composites [1, 37].

One difficulty that has prevented the use of natural fibers is the lack of good adhesion with polymeric matrices. In particular, the great moisture sorption of natural fibers adversely affects adhesion with hydrophobic matrix leading to premature ageing by degradation and loss of strength. Interfacial adhesion and resistance to moisture absorption of natural-fiber composites can be improved by treating these fibers with suitable chemical reactions. In fact, many studies have been reported concerning the chemical treatments of natural fibers [18, 38-40].

Gomes et al. [41] analyzed the mechanical properties of alkali-treated curaua fiber reinforced cornstarch-based resin. It was found that the tensile strength of the treated fibers decreased in comparison to untreated fibers, whereas the fracture strain increased two to three times after alkali treatment. Boopathi et al. [42] studied the Borassus fruit fibers treated with 5, 10 and 15 wt.% NaOH solutions. It was found that the 5 wt.% NaOH treatment significantly improved tensile properties of the Borassus fruit fibers than other alkali concentrations.

The study by Mylsamy and Rajendran [43] focused on the Agave Americana natural fibers. In their study it was found that hemicellulose, lignin, and wax content of the fibers were reduced by the alkali treatment. The surface smoothness and impurity removal of the fiber were also observed. Sghaier et al. [44] studied the characteristics of doum palm fiber after chemical treatment and found that the alkali treatment removed only the residual impurities, not affecting the microfibrils of cellulose.

Although a great deal of research over the past decade has demonstrated the efficiency of the use of chemical treatment of natural fibers, little work has been conducted on the morphology and the internal structure of the fiber affected by the chemical treatment.

The objective of this chapter was to study the abaca fiber was treated by different alkali concentrations and evaluate the changes in the morphology and mechanical properties of abaca fiber. The morphological properties show that the lumen was gradually shrunk by different alkali concentrations. The tensile strength showed the peak at 7 wt.% NaOH treatment, Young's modulus increased with increased concentration until 7 wt.%, then decreased with increased the alkali concentration, and the strain at break increased with increased alkali concentration over 7 wt.% NaOH treatment. The FT-IR and XRD analyses were conducted for the chemical components and crystallinity.

3.3 Materials and Experimental

3.3.1 Materials

Single fiber bundles were extracted from untreated and treated abaca fibers to carry out tensile tests. Single fiber bundle was bonded to a paper with rectangular holes of 10 mm in length, as shown in Figure 3.1.

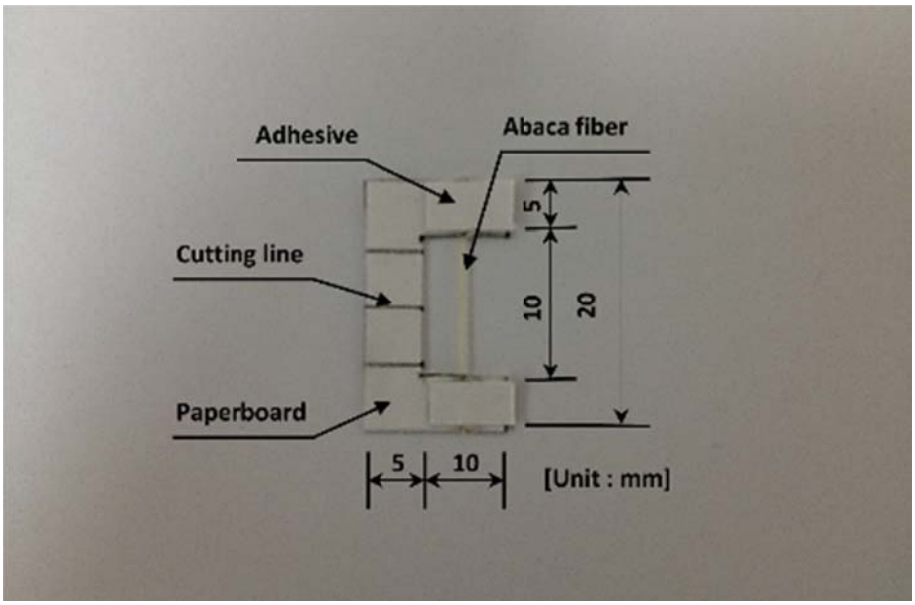

Figure 3.1 Tensile-test specimen of abaca fiber

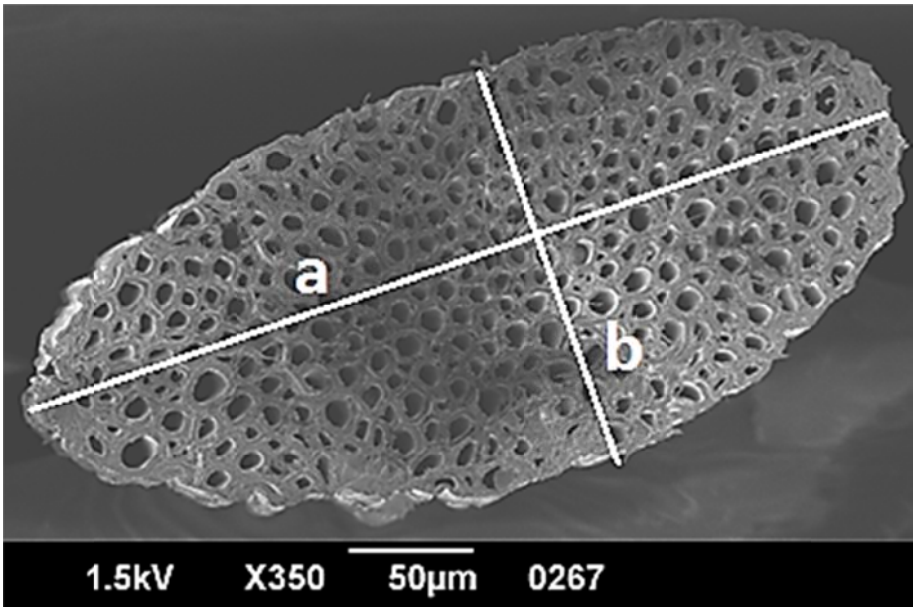

Figure 3.2 Typical cross-section of abaca fiber bundle

The abaca fibers in the present work were supplied from the Philippines. It was found that the cross section of abaca fiber bundle is not completely circular (Figure 3.2), thus fiber cross sectional area (A) is determined approximately by a formula as follows:

$$A = \frac{\pi ab}{4}$$

Where *a* and *b* are dimensions in Figure 3.2. They were measured by digital microscope VHX-600(Keyence, Japan).

The diameter (*d*) of abaca fiber is calculated approximately as follows:

$$d = \sqrt{ab}$$

The length of abaca fibers exceeded 20 mm and diameters varying from 200 to 400 μm were selected carefully to be used in this study.

3.3.2 Alkali treatment of abaca fiber

The abaca fibers were treated with different NaOH concentration (3, 5, 7, 8, 9, 10, 11, 13 and 15 wt.%) for 5 min under vacuum condition. The fibers were taken out of the solution, washed several times with fresh water to take away NaOH sticking on the fiber surface. Then the fibers were dried in the vacuum drying oven for 2 hours at 80^{o} C. The reaction of sodium hydroxide with abaca fiber is described as follows:

$$\text{Abaca-OH} + \text{NaOH} \rightarrow \text{Abaca-O}^{-}\text{Na}^{+} + \text{H}_2\text{O} \quad (1)$$

3.3.3 Mechanical properties of single fiber bundle

According to the preparation procedure described in ASTM D 3822 standard, the fiber bundles were glued to paper frames with 10 mm gauge length. Following the standard, tensile tests of abaca fibers were carried out on a universal testing machine (Instron model 5567). The tests were performed using a load cell of 500 N at a cross head speed of 1.0 mm/min. Before each testing, the edge of the supporting paper was cut in the middle. The gauge length was set at 10 mm. The specimens that fractured at the end of the paper frame or near the glued clamp were excluded from the data for the tensile test. Tensile strength was obtained from the maximum stress of stress-strain curves and the Young's modulus (E) was provided by the tangent at the origin of the stress-strain curve.

3.3.4 Micro-structural examination of fracture cross section of abaca fiber

The cross section of the test specimens was examined by scanning electron microscopy (PCSEM) (JEOL-JSM-6390). Each sample was deposited on carbon tape mounted on stubs and then gold-coated. Specimens were observed at an accelerating voltage of 5 kV and emission current of 47 μA. Specimens were analyzed at magnifications of 350 X for different alkali concentrations.

3.3.5 Fourier Transform Infrared Spectrometry (FT-IR)

The Fourier Transform Infrared Spectrometry was performed using the Thermo Fisher Scientific NICOLET IS10 spectrometer at room temperature. The infrared spectra of untreated fiber and after treatment fiber were measured by scratching a fiber with a knife and collecting some powdered sample. Then potassium bromide (KBr), which acts as a reagent, was mixed (at a ratio; KBr: Sample =100:1) with sample with a mortar and pestle. The mixture was then taken in a dice of specific dimensions. The pellet was formed by pressing with a hand press machine and was placed on the sample holder. The IR spectrum obtained in this study is presented in the results and discussion section.

3.3.6 X-ray Diffractometer (XRD)

The XRD data was obtained at room temperature on a Rigaku SmartLab X-Ray Diffractometer (Rigaku Corporation, Japan), equipped with the Cu K X-ray source. X-ray tube was operated at 45 kV and 200 mA with a detector placed on a goniometer scanning the range from 5º to 50º, at a scan speed of 2º/min, with the wave length $\lambda = 1.54059$Å.

3.4 Results and Discussion

3.4.1 SEM of the cross section of the abaca fibers

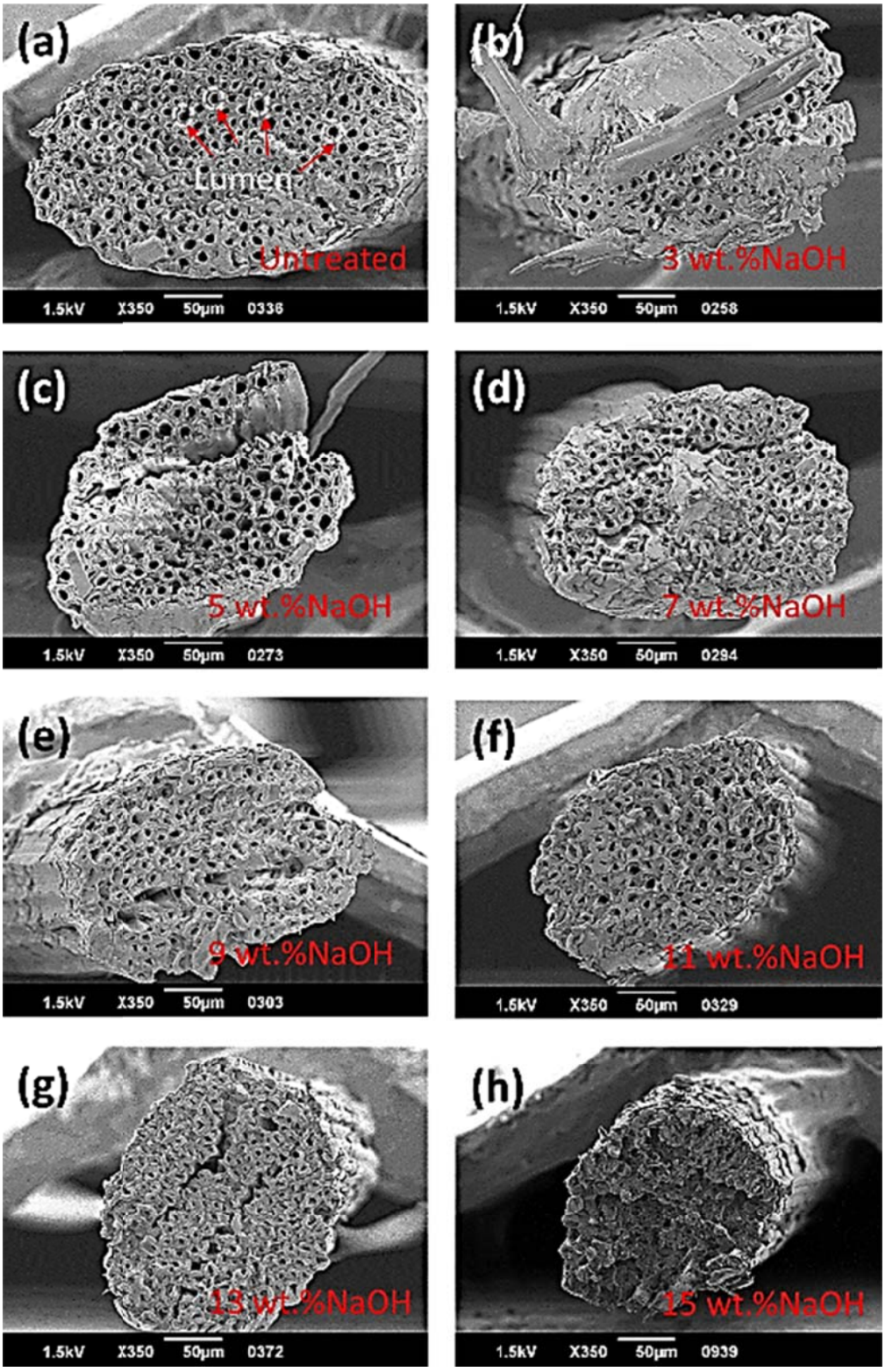

Figure 3.3 The cross-section of untreated and alkali-treated abaca fibers at different concentrations for 5 min.

Cross section of untreated and alkali-treated abaca fibers was observed using a scanning electron microscope. Figure 3.3(a) – (h) show SEM photographs of untreated fiber and 5 min treated fiber with 3, 5, 7, 9, 11 13 and 15 wt.% NaOH solution. It can be seen that the lumen is observed in the cross section of the untreated fiber (Figure 3.3(a)). During the alkali treatment, the lumen size was gradually decreased with increasing the alkali concentrations, as shown in the Figure 3.3(b) - (d). After higher than 7 wt.% NaOH treatment, the lumen was shrunk until disappearing when the alkali treatment reached 15 wt.% NaOH concentration (Figure 3.3(e) - (h)). As we can see the diameter of the fiber was decreased following this shrinkage. Moreover, the cell wall of each lumen swelled with increasing alkali concentrations. However, it has been reported that the differences of single fiber shape and lumen diameter strongly influence fiber density and mechanical and dimensional properties [18].

There are two possible reasons for lumen shrinkage and cell wall swelling. One possible reason may be that the pectin, hemicelluloses and lignin were removed from the abaca fiber during alkali treatment. Observations of the lumen of the cross section of the treated fiber revealed that the fiber is not truly a monofilament. It is a bundle of monofilaments bonded and covered by lignin. Therefore, alkali treatment is inferred to provoke removal of a great amount of lignin from the untreated fiber surface. Alkali treatment changes the bundle structure into an element structure, which comprises monofilaments that are barely bonded to each other by a small amount of lignin. Not only the chemical structure change mentioned above, but also such morphological change brings a decrease in strength of the fibers. Moreover, another possible reason for lumen shrinkage may be that the sodium ion entered the cell wall; the cell wall thickness increased and the lumen size decreased after alkali treatments [18, 45, 46].

3.4.2 Morphology of the untreated and treated abaca fibers

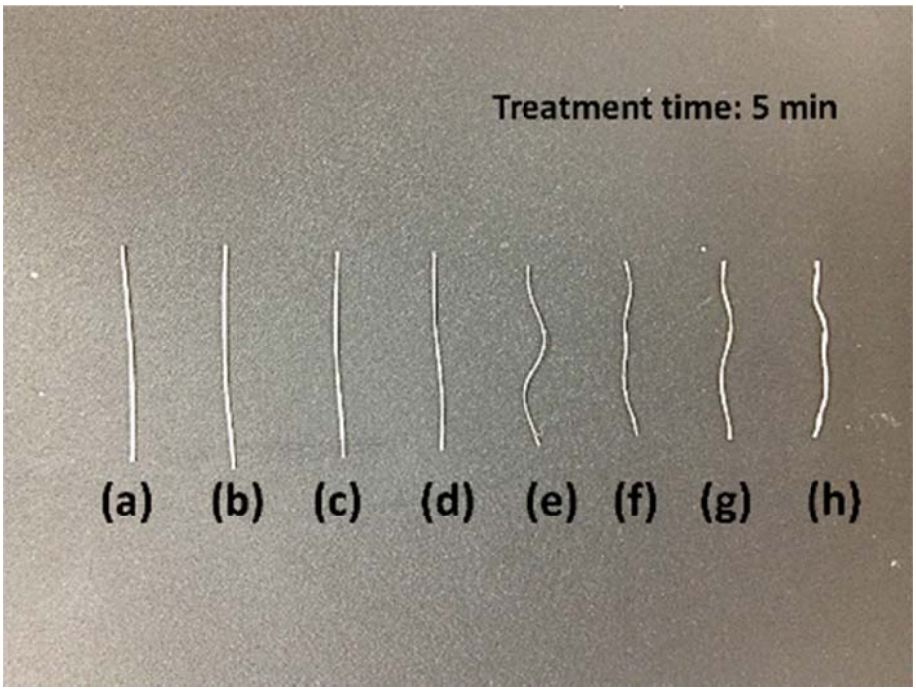

Figure 3.4 The sample of the untreated and alkali-treated abaca fibers (a) untreated, (b) 3 wt.% NaOH, (c) 5 wt.% NaOH, (d) 7 wt.% NaOH, (e) 9 wt.% NaOH, (f) 11 wt.% NaOH, (g) 13 wt.% NaOH, (h) 15 wt.% NaOH

Figure 3.4 shows the morphology of the untreated and alkali-treated abaca fibers. It can be seen that the abaca fibers are straight in the Fig 3.4 (a)-(d). However, after higher than 7 wt.% alkali treatment, twisting fiber bundles in the longitudinal direction was observed as shown in the Figure 3.4(e) - (h).

3.4.3 Mechanical properties of single fiber bundle

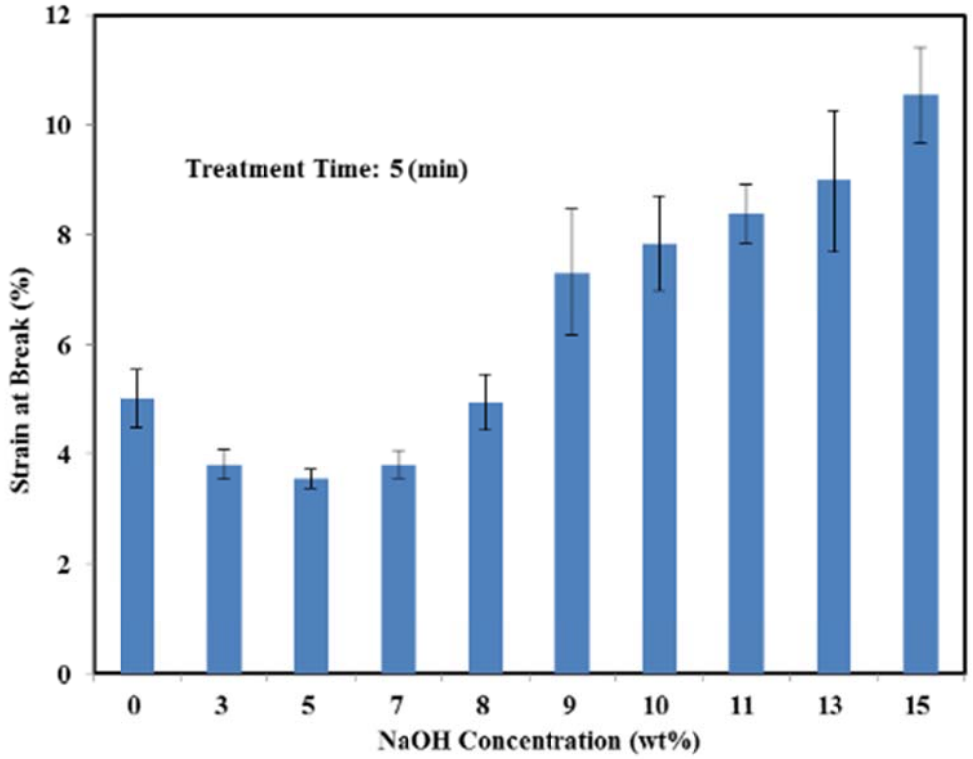

Figure 3.5 Strain at break curves of untreated and alkali-treated abaca fibers

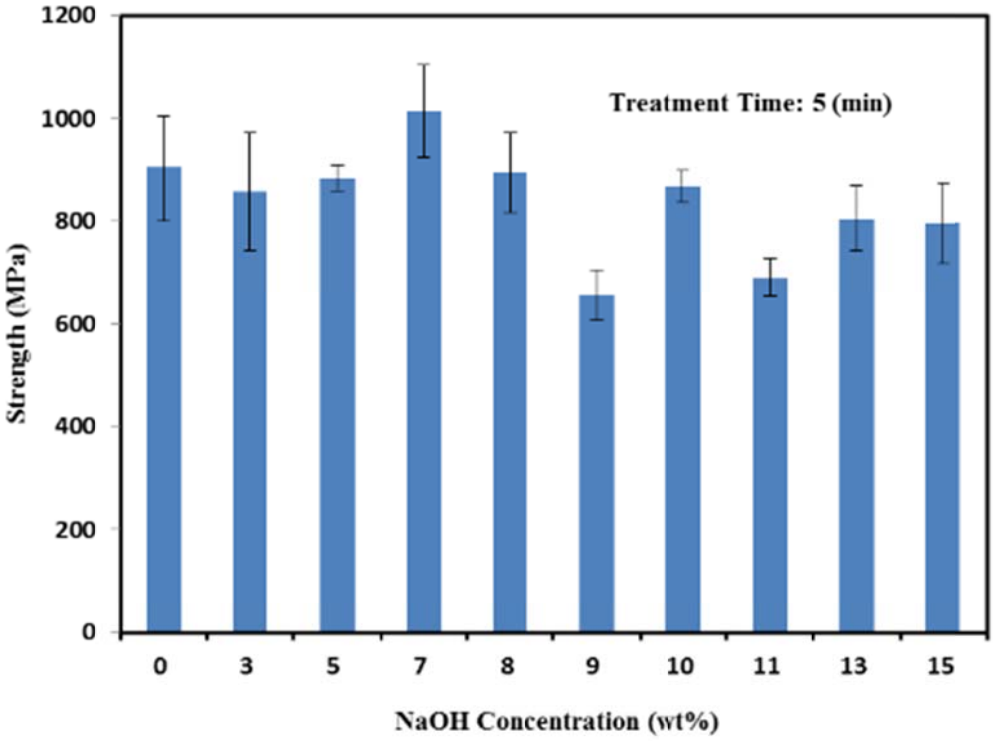

Figure 3.6 Tensile strength of untreated and alkali-treated abaca fibers

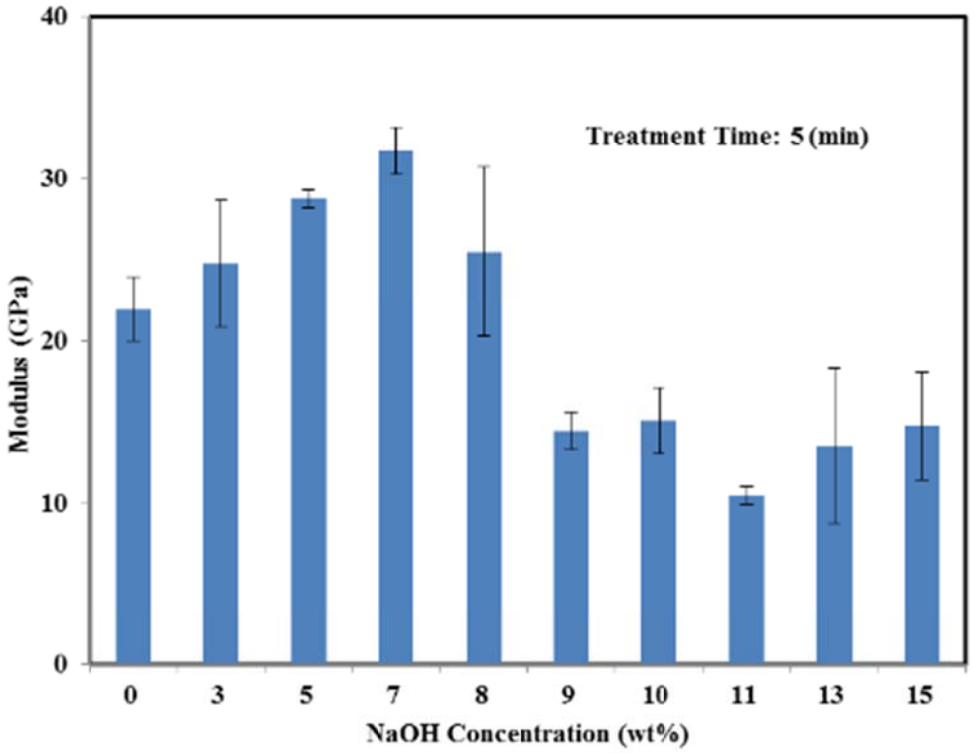

Figure 3.7 Young's modulus of untreated and alkali-treated abaca fibers

The tensile properties of untreated and alkali-treated abaca fibers are shown in Figure 3.5 to Figure 3.7 and Table 3.1 Tensile properties of untreated and alkali-treated abaca fibers. It can be seen that the strain at break increased with increasing the alkali concentrations greater than 7 wt.% NaOH treatment (Figure 3.5). The tensile strength shows ups and downs with increasing the alkali concentrations. The highest value of the tensile strength occurred at 7 wt.% NaOH treatment (Figure 3.6). The Young's modulus increased with increasing alkali concentrations below 7 wt.% and decreased linearly above 7 wt.% NaOH treatment (Figure 3.7).

A decrease in the Young's modulus and an increase in the strain at break occurred at concentrations greater than 7 wt.% NaOH treatment, and both changes were closely correlated with longitudinal contraction (as shown in Figure 3.4). The factors that influence these mechanical properties in the longitudinal direction of abaca fiber are apparently due to

changes in the structure of the cell wall and the morphology of the fiber as we mentioned in section 3.1.

There are two explanations, which can be offered for the contraction during the alkali treatment in the present report. One is the conformational change of cellulose chains in disordered or amorphous regions. The other one is, the structural changes in the microfibrils themselves are expected to affect the changes in the mechanical properties of abaca fiber. This led to an investigation of the dependence of the changes in crystal structure and degree of crystallinity in natural fiber as a function of NaOH concentration. In addition, the relationships between the changes in cellulose structure or longitudinal contraction, and the changes in the mechanical properties during alkali treatment have been reported [47, 48].

Table 3.1 Tensile properties of untreated and alkali-treated abaca fibers

NaOH concentration (%)	Tensile strength (MPa)	Young's modulus (GPa)	Elongation at break (%)
Untreated	900±100	22±2	5.0±0.5
3	860±110	25±4	3.81±0.28
5	883±24	28.7±0.6	3.55±0.17
7	1010±90	31.7±1.5	3.82±0.25
8	900±80	25±5	5.0±0.5
9	660±50	14.4±1.2	7.3±1.1
10	870±30	15±2	7.8±0.9
11	690±40	10.4±0.6	8.4±0.5
13	810±60	13±5	9.0±1.3
15	800±80	15±3	10.6±0.9

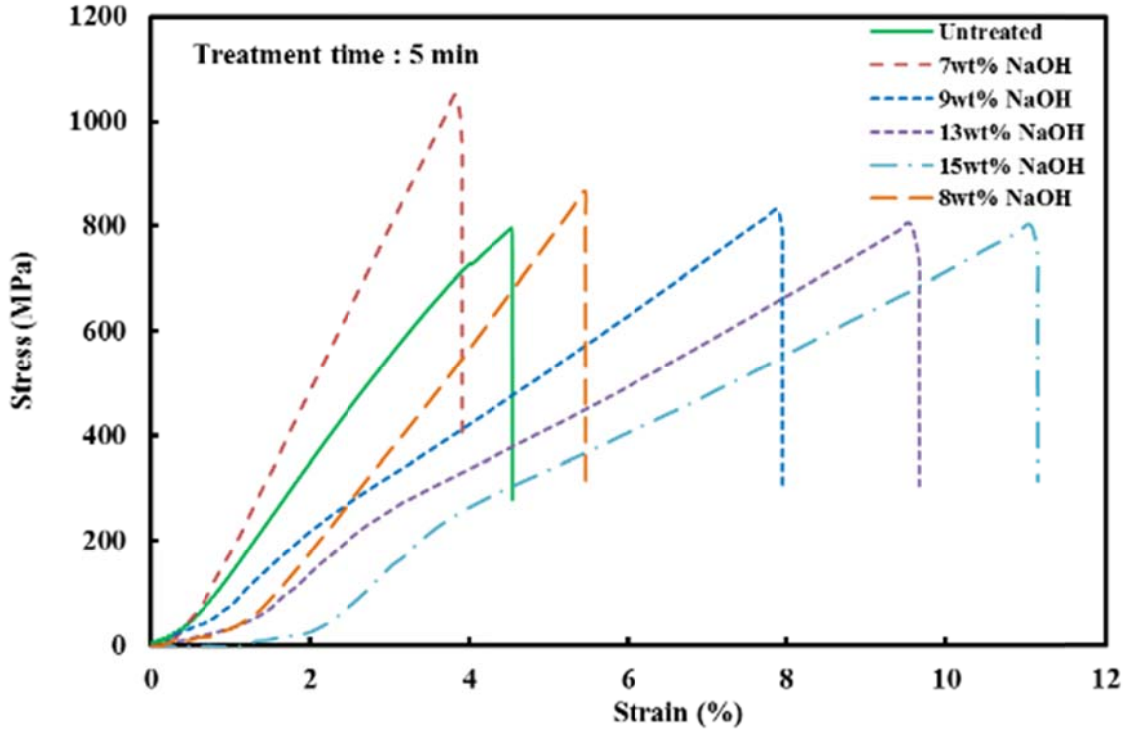

Figure 3.8 Stress-strain curves of untreated and alkali-treated abaca fibers

Typical tensile stress-strain curves of single untreated and alkali-treated abaca fiber bundle is shown in Figure 3.8. These curves show the influences of different alkali solution concentration on the mechanical properties of treated fibers. It is noted that the peak of the tensile strength and the Young's modulus is found at 7 wt.% alkali concentration. Over the 7 wt.% alkali-treated fibers, slopes of the stress-strain curves of the treated fibers are lower than that of the untreated fiber. The lower slope of the stress-strain curve typically implies lower tensile strength and Young's modulus. In addition, a non-linear behavior is observed in the earlier stage of the loading when the concentration is higher than 7 wt.% NaOH. As shown in the Figure 3.4, after treating with 3 and 5 wt. % alkali concentrations, abaca fibers were straight and their lumen sizes were similar to that of the untreated one. However, after alkali treatment of 7, 8 and 9 wt. % NaOH solution, abaca fibers were slightly twisted and the lumen started to shrink. After 11, 13 and 15 wt. % alkali treatments, they were completely

twisted and the lumen size decreased conspicuously. The reason for the change in tensile properties is that the morphology of alkali-treated abaca fibers changed with different alkali concentration. Another possible reason is that the mechanical properties increased with increasing degree of crystallinity. However, the non-linear behavior occurred around 1 to 3% of the strain and Young's modulus decreased above 7 wt. % alkali treatments as shown in Figure 3.7. The reason for this is that the alkali-treated abaca fibers were twisted above 7 wt.% alkali treatments.

3.4.4 Fourier Transform Infrared Spectrometry (FT-IR)

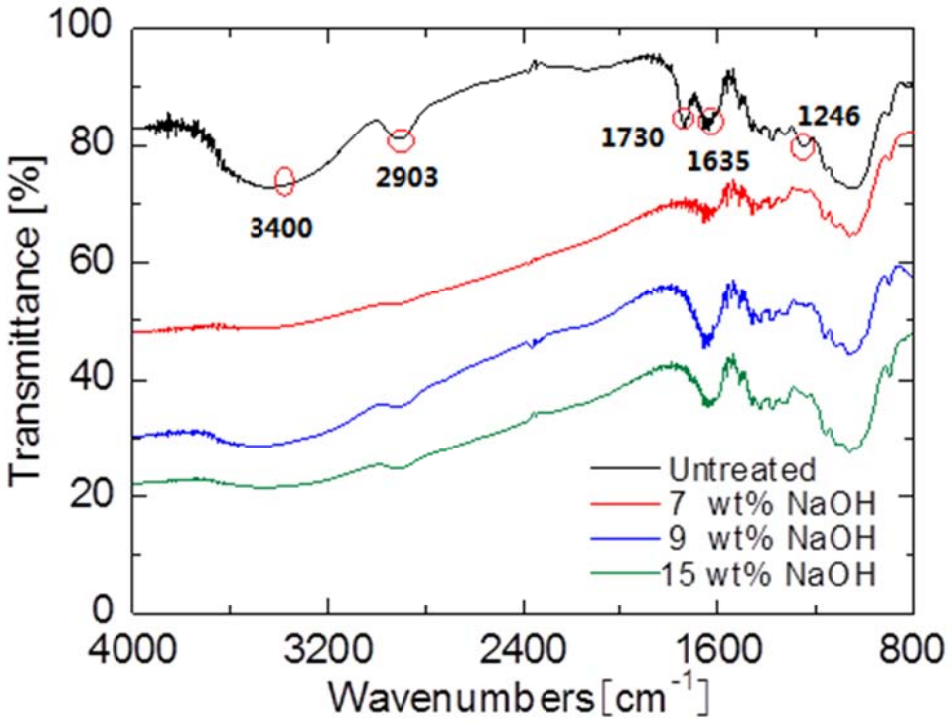

Figure 3.9 FT-IR spectra of abaca fibers before and after alkali treatment for 5 min

Table 3.2 FT-IR spectral data of abaca fibers [49-51]

Position/cm^{-1}	Band type	Possible Assignment
~3600-3200	⁻ OH	strong band from the cellulose, hemicellulose and lignin of abaca
~3000-2900	C–H	in aromatic rings and alkanes
~1730	C=O	most probably from the lignin and hemicelluloses
~1635	C=C	aromatic skeletal ring vibration due to lignin
~1246	=C–O–C=	aliphatic unsaturated carbonate

Figure 3.9 shows the FT-IR spectrum of abaca fiber at different NaOH concentration treatments. As discussed in chemical analysis, the main components in the abaca fiber are cellulose, hemicellulose and lignin. These three components are mainly composed of esters, aromatic ketones and alcohols, with different oxygen-containing functional groups.

The spectral data peaks as Table 3.2 shows, lignin present in the abaca fiber gives characteristic peaks at 1246, 1635 and 1730 cm^{-1} corresponding to the aromatic skeletal vibration and carbonyl group. The peak present at 1635 cm^{-1} in the spectrum corresponding to the raw fiber is due to the presence of C=C linkage, which is a characteristic group of lignin and at 1730 cm^{-1} is due to hemicellulose. The reduction in the peak intensity found at around 2903 cm^{-1} in alkali treated abaca fiber indicates the partial reaction of the C-H bonds. Alkali treatment reduces hydrogen bonding due to removal of the hydroxyl groups by reacting with sodium hydroxide. This result in the decrease of the –OH concentration, evident from the decreased intensity of the peak between 3300 and 3400 cm^{-1} bands compared to the

untreated fiber. From the FT-IR analysis, it has been concluded that the untreated fibers have a characteristic peak in between 1246 and 1730 cm^{-1}. These peaks are mainly due to the hemicellulose and lignin components.

3.4.5 X-ray diffraction

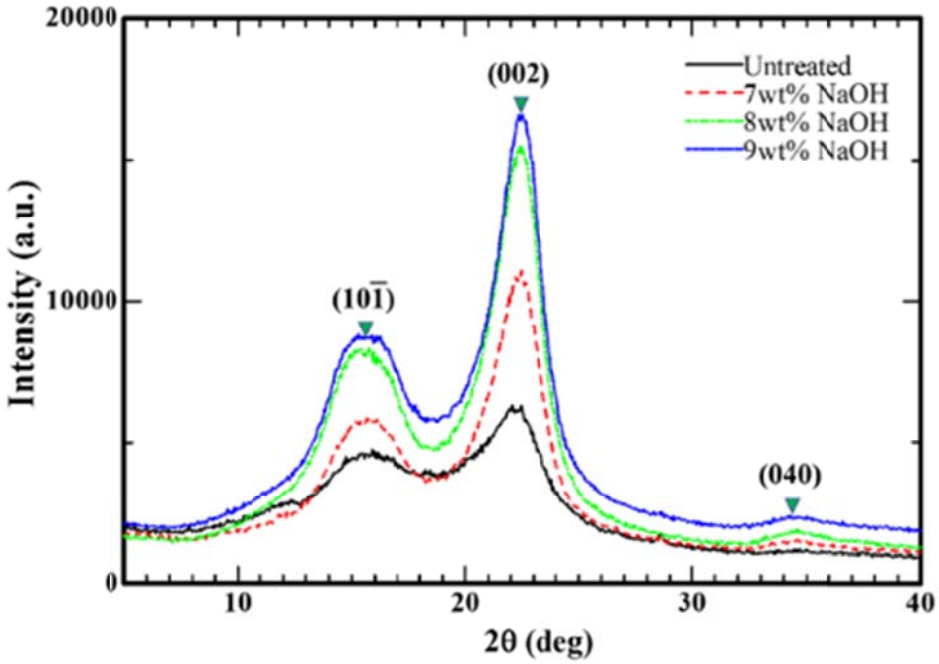

Figure 3.10 XRD spectra of abaca fibers before and after alkali treatment for 5 min

Figure 3.10 shows the change in the degree of crystallinity of alkali-treated abaca fiber measured by XRD. All of the XRD spectra show three main peaks around 15.7, 22.2 and 34.5°. These peaks are characteristic of cellulose crystallography and are assigned to (10$\bar{1}$), (002) and (040) reflections. After 7 wt. % alkali treatment, the peaks become sharp. At 9 wt. % alkali treatment, the peaks are the sharpest. The crystalline regions fraction may be increased with increasing alkali concentration.

3.5 Conclusions

In this study, abaca fibers were treated by NaOH solutions with different concentrations. The major changes in morphology, chemical and mechanical properties are summarized below:

(1) The lumen size decreased with increasing alkali concentration above 7 wt. %.

(2) The mechanical properties increased after alkali treatments. Young's modulus and tensile strength reached the highest value after 7 wt. % NaOH treatment for 5 min.

(3) The chemical components such as pectin, lignin and hemicelluloses were removed from the abaca fiber by alkali treatments.

Chapter 4 Influence of Different Alkali Treatment Time on Morphology and Tensile Properties of Abaca Fibers

4.1 Abstract

The natural fibers play a major role as reinforcement in composites due to their important properties such as lightweight, biodegradability and non-toxicity. Abaca fiber is one of such material with high cellulose content which is cheap and easily available. Extracted abaca fiber has good mechanical properties, such as high tensile strength and high Young's modulus. There has been some research on the tensile properties of natural fibers with little attention on the relationship between the variations of lumen size and tensile properties. In this study, the abaca fibers were treated with 5, 10 and 15 wt. % NaOH solution for different treatment times, and the effects of alkali treatments on the fiber properties were assessed and also the structural changes of lumen were observed.

4.2 Introduction

In recent years, interest in the use of the plant fibers has been increased as an eco-friendly material in construction, automobile and aircraft interior applications [8, 33, 36]. Abaca fiber is one of the plant fibers with high tensile strength [52]. Abaca fiber is also the first plant fiber to be used on the exterior of road vehicles as report by Bledzki et al. [52]. Meanwhile, abaca fiber-reinforced composites have been used for under-floor protection of passengers in Daimler AG vehicles [53] due to its efficient combination of strength and stiffness to weight ratios, its hollow tube form structure, relatively high shape factors which are important for the structural design of high strength structure applications.

Significant research has been carried out recently to study the physical and thermal properties of abaca fiber by Takagi et al.[15, 54]. However, the hollow structure of the fiber and the mechanical properties are rarely studied by the academic research.

Because of these concerns, this study investigates the microstructure and mechanical properties of the abaca fiber as the main focus when subjected to alkali solution treatment with different treatment times. It is through this research that the effect of the alkali treatment time will be ascertained.

4.3 Materials and experimental

The abaca fibers were treated with 5, 10 and 15 wt. % NaOH solution separately for 0 min, 5 min, 10 min, 15 min, 20 min, 25 min and 30 min under vacuum condition. The fibers were then washed with fresh water to take away NaOH sticking on the fiber surface. Then the fibers were dried in the vacuum drying oven for 2 hours at 80^{o}C.

4.3.1 Diameter measurement

The fiber cross sectional area (A) and the diameter of abaca fiber were measured by a digital microscope VHX-600 (Keyence, Japan). The abaca fibers whose length exceeded 20 mm and diameter varying from 240 μm to 280 μm were selected to be used in this study.

4.3.2 Tensile test

Tensile tests of abaca fibers were carried out on a universal testing machine (Instron model 5567). The tests were performed using a load cell of 500 N at a cross head speed of 1.0 mm/min. Before each test, the mean diameter was calculated from microscopic analysis. The gauge length was 10 mm. Determination of the Young's modulus (E) was provided by tangent at the origin of the stress-strain curves. Scanning Electron Microscopy images were taken by an SEM model JEOL-JSM-6390 and FESEM S4700.

4.4 Results and Discussion

4.4.1 The microstructure of the untreated and alkali-treated abaca fibers

The study of the surface morphology of fibers is important to understand the changes caused by alkali treatments. The SEM images revealed that the abaca fibers had multi lumen structure.

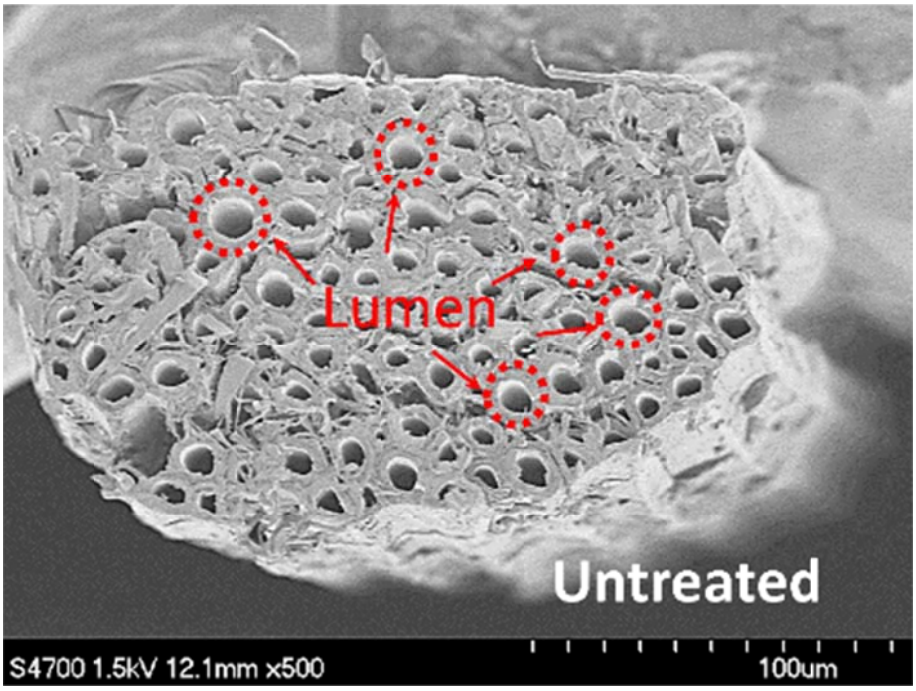

Figure 4.1 The microstructural cross-section of untreated abaca fiber

Figure 4.1 shows the cross-section of untreated abaca fiber after tensile test. It can be seen that fiber have an open lumen in the center of every elemental cell. The diameter of the untreated fiber is around 200-250 μm. The lumen size is around 10-25 μm with a cell wall thickness of polygonal cells of 2-4 μm. Whereas the lumen was collapsed after different times of alkali treatment.

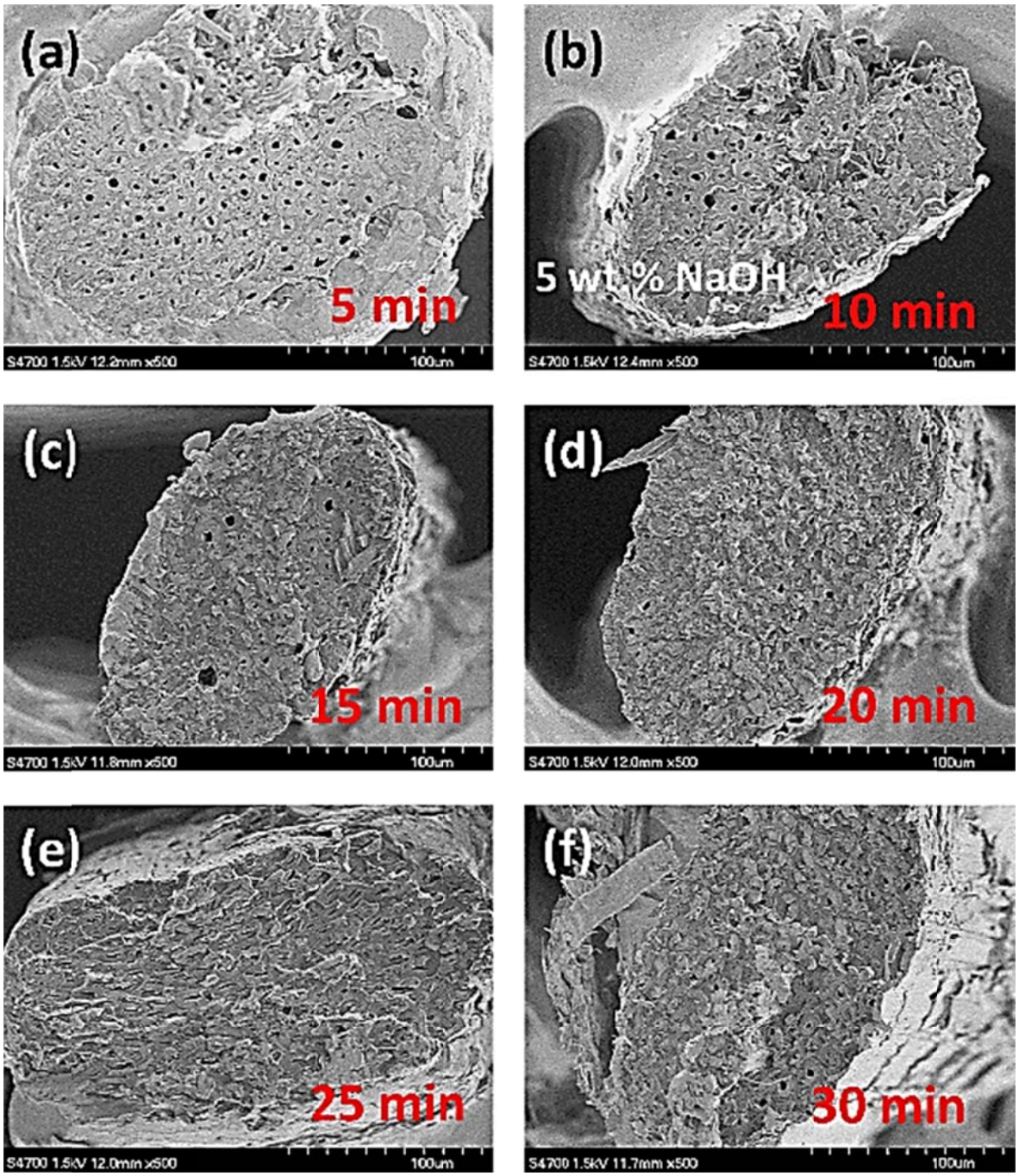

Figure 4.2 The microstructural cross-section of 5 wt. % alkali-treated abaca fibers

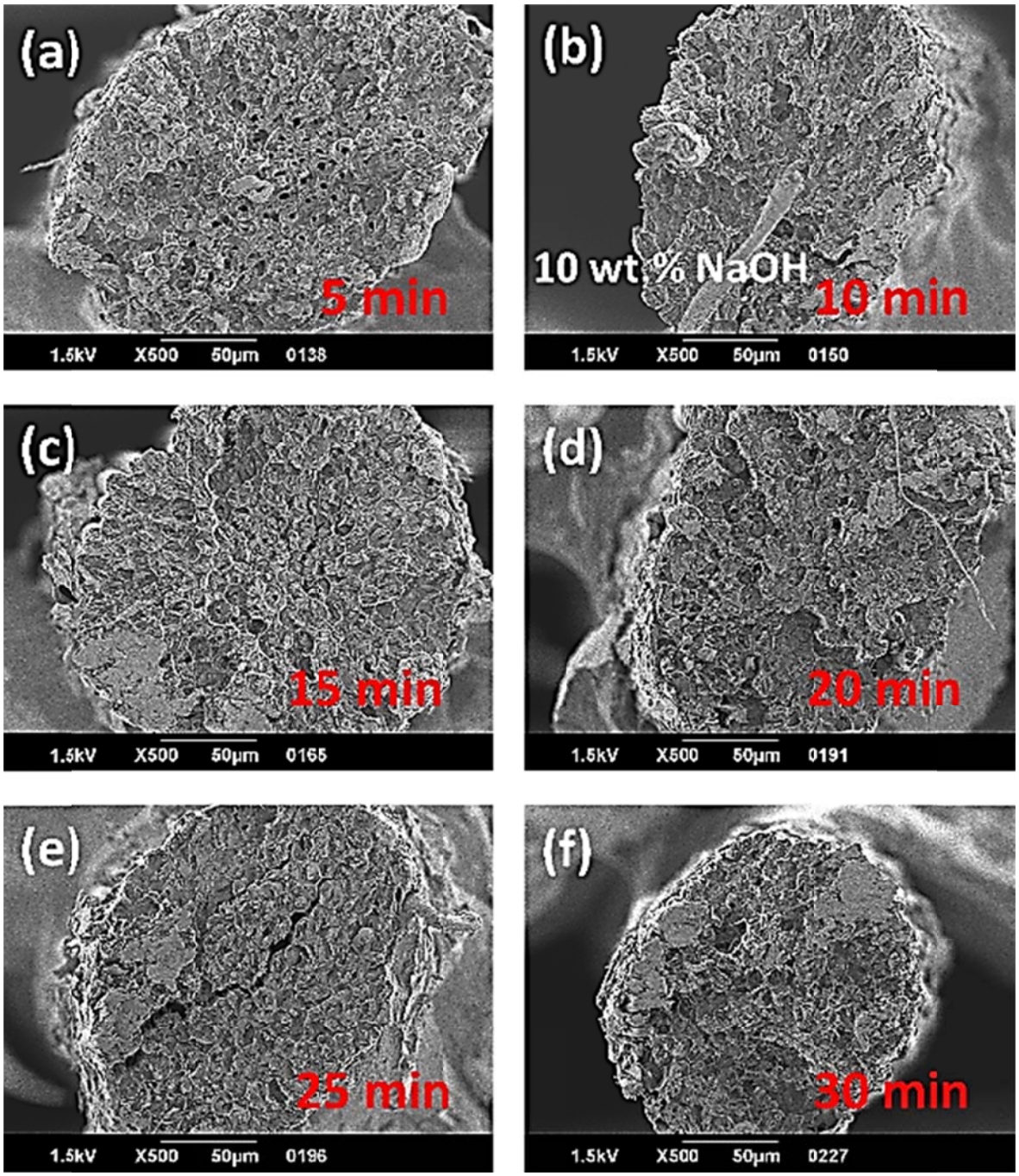

Figure 4.3 The microstructural cross-section of 10 wt. % alkali-treated abaca fibers

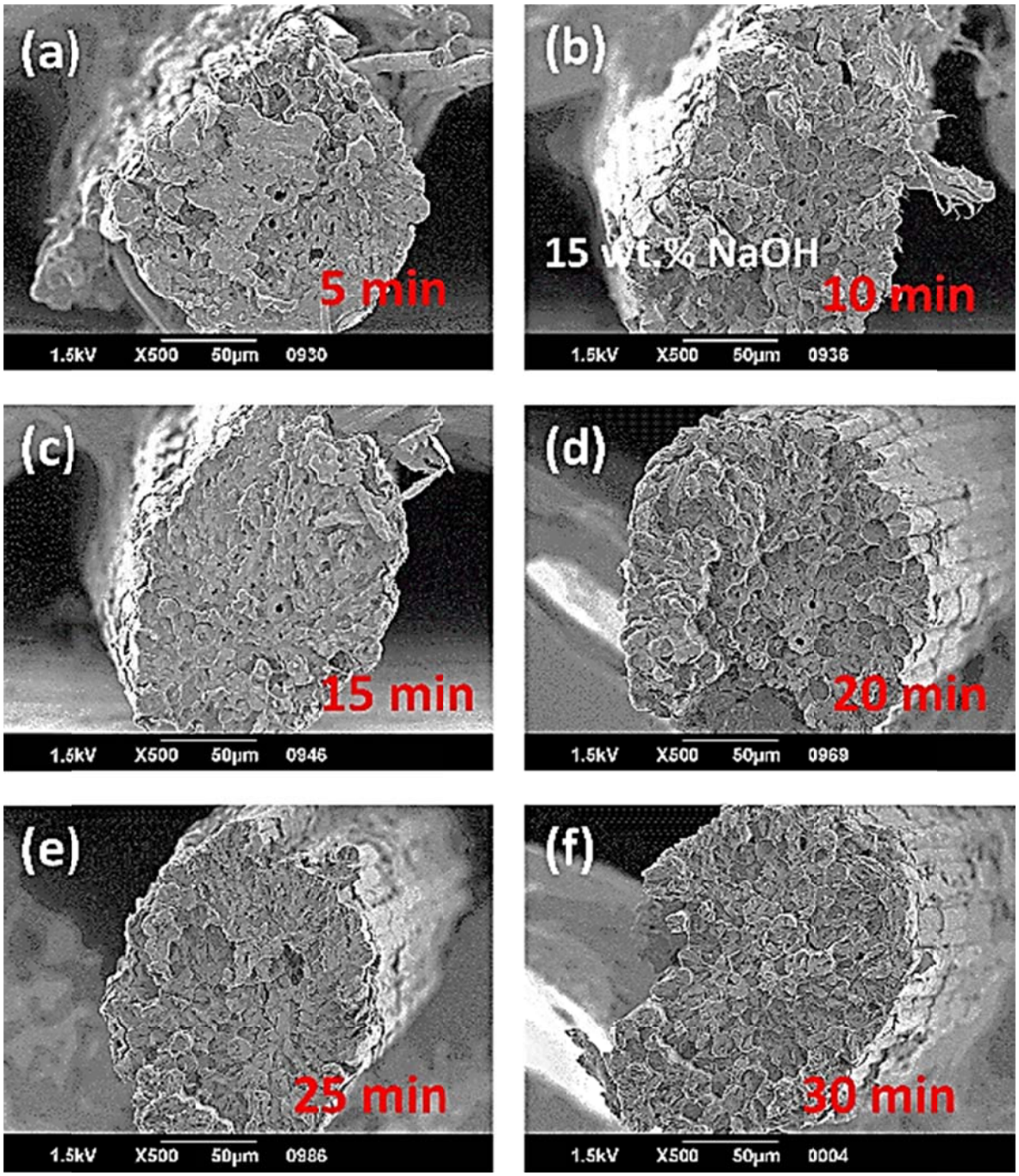

Figure 4.4 The microstructural cross-section of 15 wt. % alkali-treated abaca fibers

Figure 4.2 shows that the fiber lumen size decreased and completely collapsed during the different alkali treatment times with 5 wt. % alkali concentration. After 5 wt. % NaOH treatment, it can be seen that the lumen is shrunk and it is visible in the cross-section for 5 and 10 min. treated (Figure 4.2(a) - (b)) compared to the untreated fiber (Figure 4.1). After 15 min; we can see a few lumen in the cross-section of the abaca fiber (Figure 4.2(c)). Moreover, the lumen size almost collapsed during the alkali treatment process over 15 min. treatment (Figure 4.2(d) - (f)). Meanwhile, the cell wall of abaca fibers swelled with each alkali treatment time.

Figure 4.3 shows that the fiber lumen size decreased and completely collapsed during the different alkali treatment times with 10 wt. % alkali concentration. After 10 wt. % NaOH treatment, we can see that few lumen is visible in the middle of the cross-section for 5 min. treatment (Figure 4.3 (a)). This phenomenon may be attributed to the treatment time of only 5 min. when alkali solution penetrated from surface to inside. Thus, the lumen still exist in the middle of the cross-section of the fiber. However, the lumen completely collapsed during the alkali treatment time of more than 5 min. (Figure 4.3(b) - (f)). It means that the 10 wt. % NaOH concentration was adequate to completely collapse the lumen.

Figure 4.4 shows that the fiber lumen size decreased and completely collapsed during the different alkali treatment times with 15 wt. % alkali concentration. After 15 wt. % NaOH treatment, we can see that the minor lumen is visible in the middle of the cross-section for 5 min. treatment (Figure 4.4 (a)). This phenomenon is similar with 10 wt. % alkali concentration treatment. Meanwhile, the lumen almost completely collapsed during the alkali treatment time of more than 5 min. (Figure 4.4(b) - (f)). In addition, lumen exist in the cross-section of the fiber treated for 10-20 min. (Figure 4.4(b) - (d)). It is due to the non-uniform distribution of the fiber by alkali treatment.

4.4.2 The tensile properties of alkali-treated abaca fibers

Table 4.1 The tensile properties of the untreated and 5 wt. % NaOH-treated abaca fibers

NaOH treatment time (min)	Tensile strength (MPa)	Young's modulus (GPa)	Elongation at break (%)
Untreated	760±90	17.1±2.3	5.8±0.7
5	810±160	22±3	4.8±0.3
10	800±150	22±4	4.6±0.3
15	930±120	24±4	4.5±0.5
20	890±60	25.9±2.8	4.4±0.4
25	830±120	21.2±2.7	4.4±0.6
30	800±140	22±4	4.8±0.5

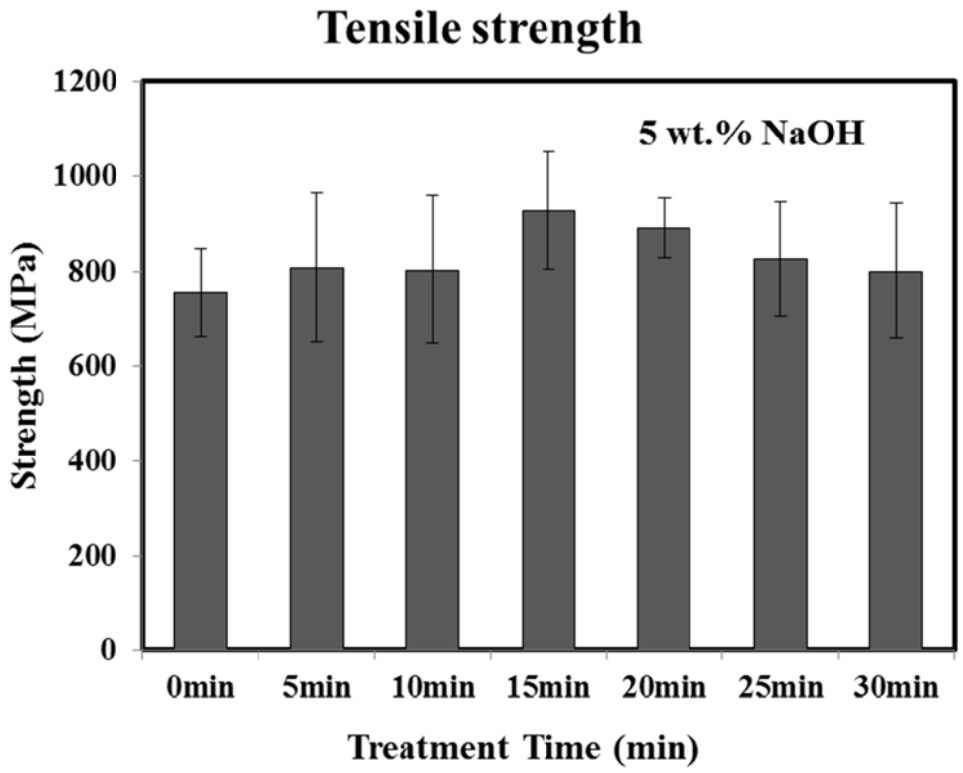

Figure 4.5 Tensile strength of 5 wt. % alkali-treated abaca fibers with different treatment times

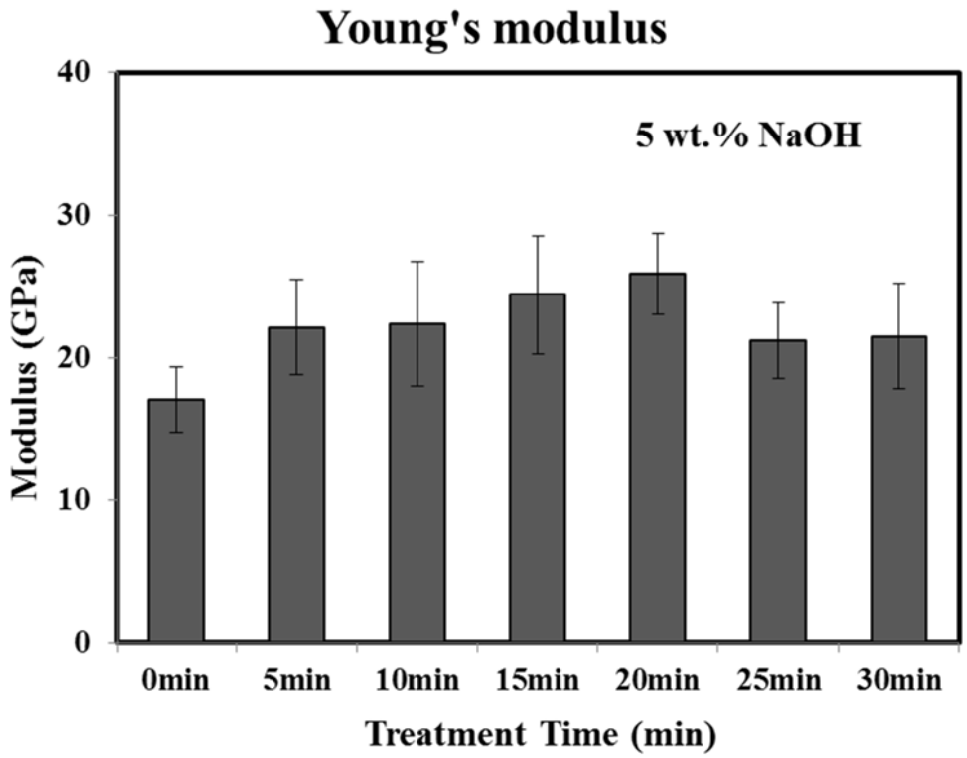

Figure 4.6 Young's modulus of 5 wt. % alkali-treated abaca fibers with different treatment times

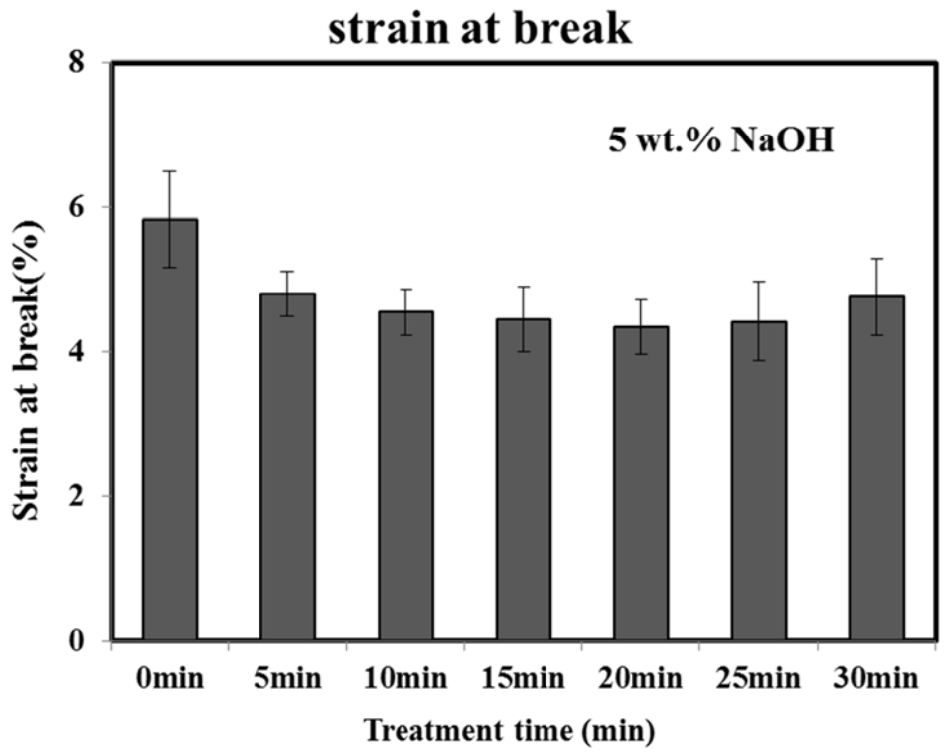

Figure 4.7 Strain at break of 5 wt. % alkali-treated abaca fibers with different treatment times

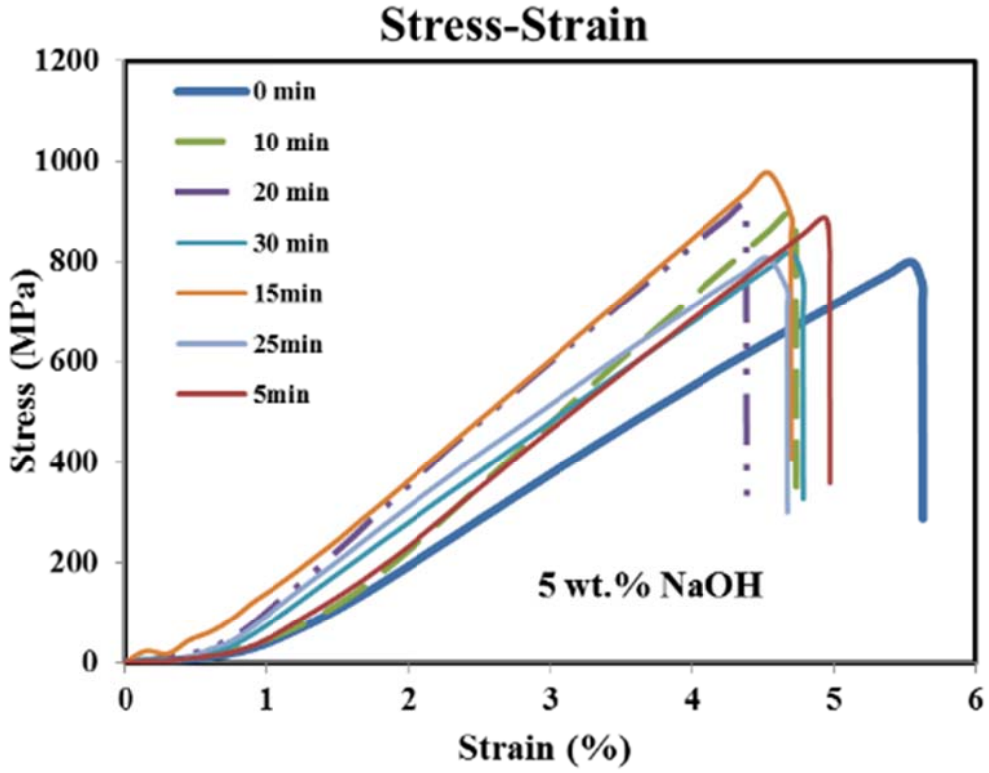

Figure 4.8 Stress-strain curves of 5 wt. % alkali-treated abaca fibers with different treatment times

One of the most important factors of natural fibers is high performance in mechanical properties. Figure 4.5 to Figure 4.8 and Table 4.1 show the results of mechanical tests for the 5 wt. % alkali-treated abaca fibers. The tensile strength slightly increased with increasing treatment time. The highest value of the tensile strength occurred after 15 min. alkali treatment (Figure 4.5). As shown in Figure 4.6, the Young's modulus increased with increasing treatment time after 5 wt. % NaOH treatment. The strain at break decreased for each treatment time after 5 wt. % NaOH treatment (Figure 4.7). The stress-strain curves are shown in the Figure 4.8, which show a linear behavior. From 0-0.3% of the strain, the curve fluctuates and changes after treatment time for 15 min.

Table 4.2 The tensile properties of the untreated and 10 wt. % NaOH-treated abaca fibers

NaOH treatment time (min)	Tensile Strength (MPa)	Young's Modulus (GPa)	Elongation at break (%)
Untreated	760±90	17.1±2.3	5.8±0.7
5	870±30	15.1±2.1	7.8±0.9
10	860±90	15±4	8.5±1.3
15	900±120	12.8±2.7	9.2±0.7
20	870±80	14.6±1.9	8±1
25	800±100	17.9±2.4	7.6±1.2
30	840±60	13.1±2.1	9±1

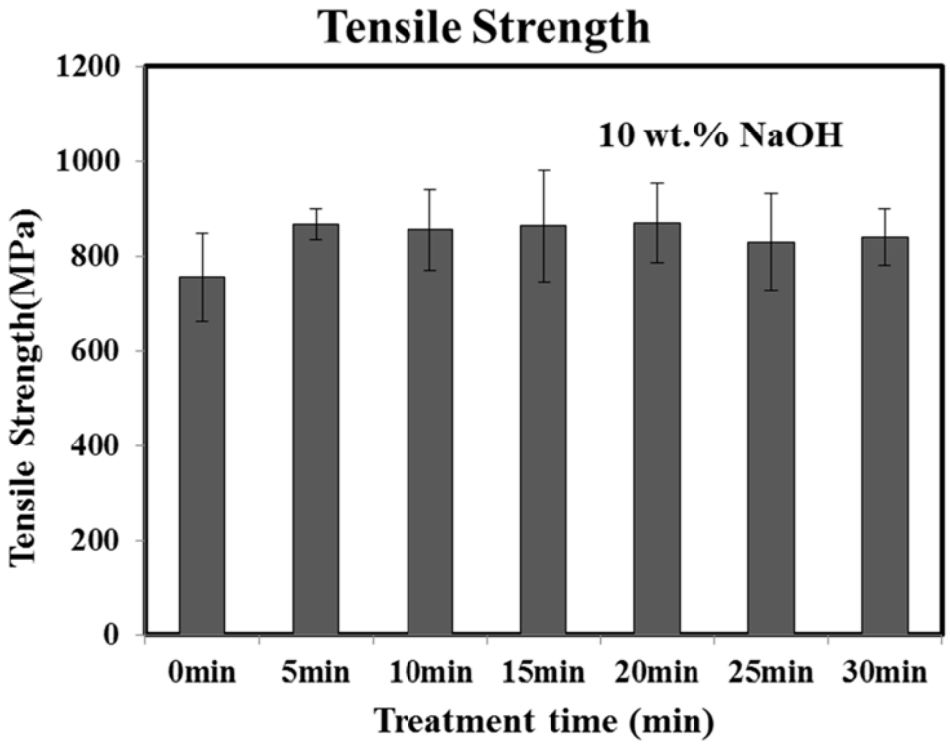

Figure 4.9 Tensile strength of 10 wt. % alkali-treated abaca fibers with different treatment times

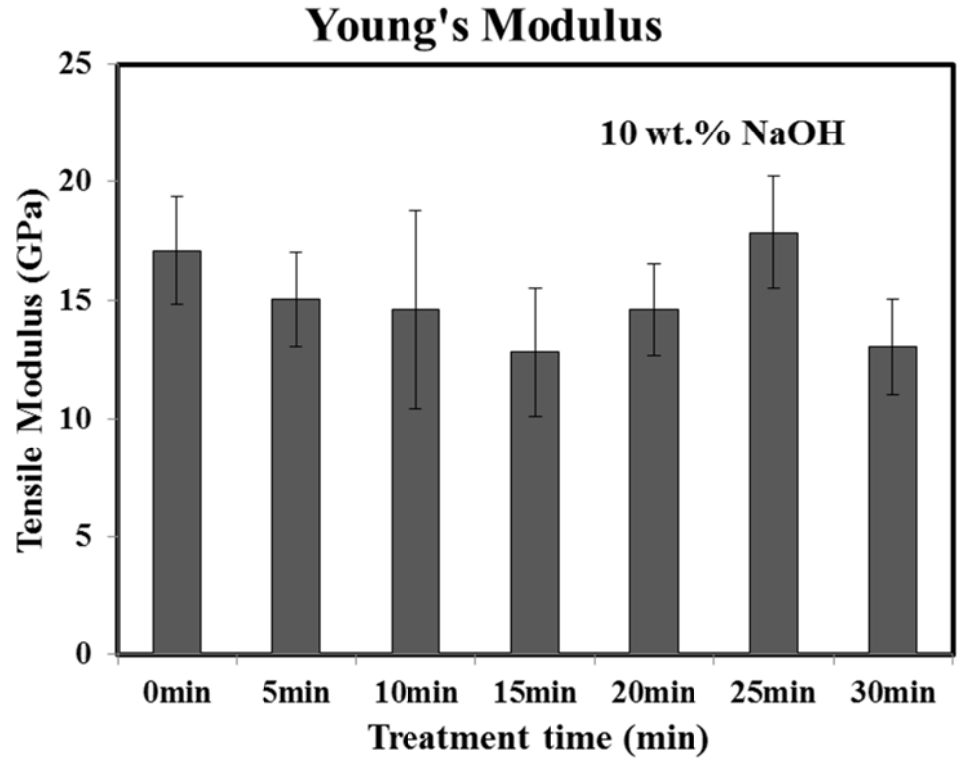

Figure 4.10 Young's modulus of 10 wt. % alkali-treated abaca fibers with different treatment times

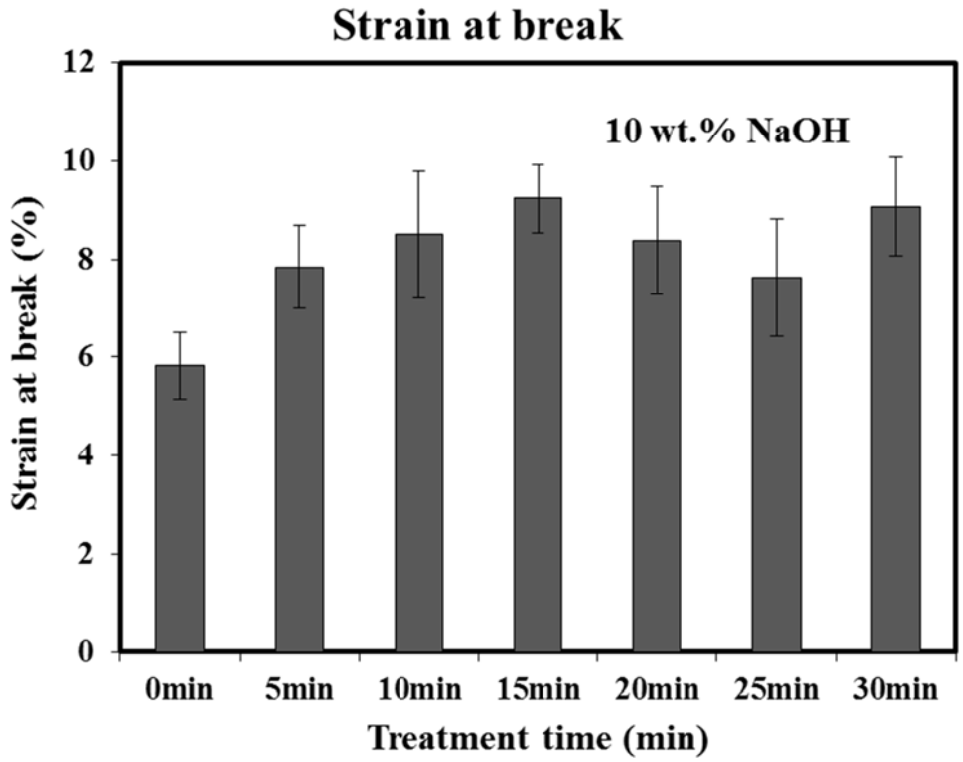

Figure 4.11 Strain at break of 10 wt. % alkali-treated abaca fibers with different treatment times

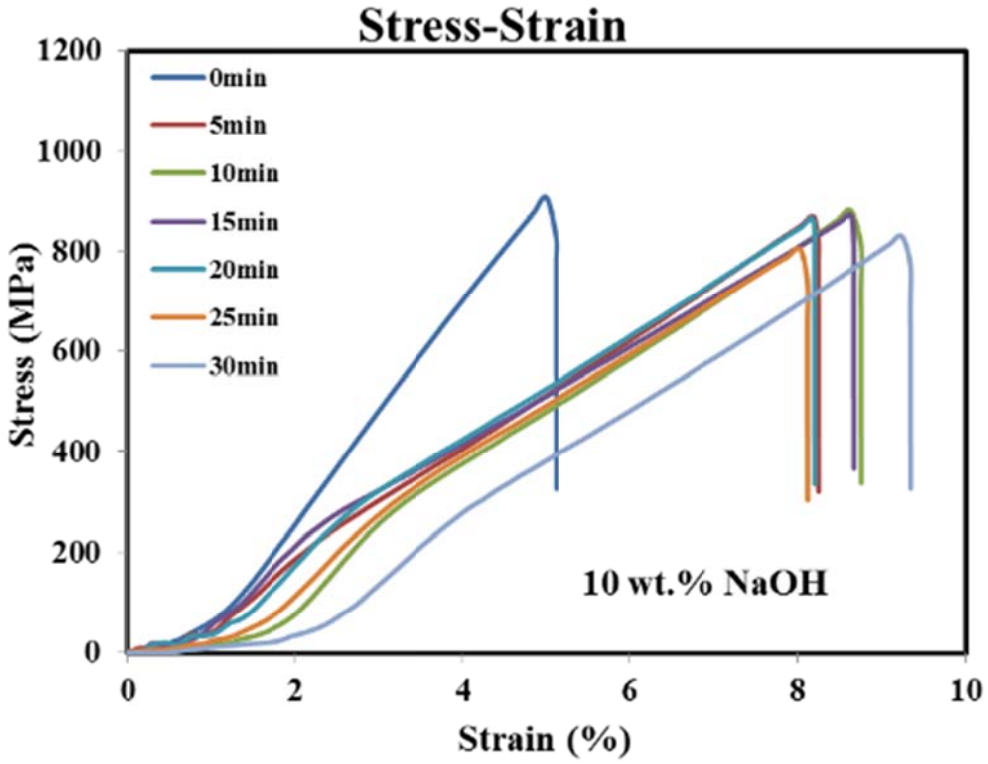

Figure 4.12 Stress-strain curves of 10 wt. % alkali-treated abaca fibers with different treatment times

The tensile properties of untreated and 10 wt. % alkali-treated abaca fibers are summarized in Figure 4.9 to Figure 4.12 and Table 4.2. After 10 wt. % NaOH treatment, the tensile strength increased by 15%. Meanwhile, the tensile strength is consistently unchanged in every treatment time (Figure 4.9). Figure 4.10 shows the Young's modulus after 10 wt. % NaOH treatment. It can be seen that the Young's modulus decreased with increasing treatment time. However, it is important to note that the Young's modulus increased after 25 min. treatment. The strain at break increased with increasing treatment time after 10 wt. % NaOH treatment (Figure 4.11). The stress-strain curves are shown in the Figure 4.12. We can see that the non-linear behavior occurred for every treatment time after 10 wt. % NaOH treatment. It is showing an initial steep increase followed by a weaker linear increase with strain above 1.5-3%. The non-linear behavior appears to be the result of fiber twisting, which will be studied in detail in Chapter 5.

Table 4.3 The tensile properties of the untreated and 15 wt. % NaOH-treated abaca fibers

NaOH treatment time (min)	Tensile Strength (MPa)	Young's Modulus (GPa)	Elongation at break (%)
Untreated	760±90	17.1±2.3	5.8±0.7
5	800±80	15±3	10.6±0.9
10	800±100	14.5±2.2	10.1±0.7
15	800±100	13±3	10.5±0.5
20	810±140	13±4	10.4±1.3
25	940±40	16.0±1.8	10.0±0.7
30	840±80	12±3	11.7±2.1

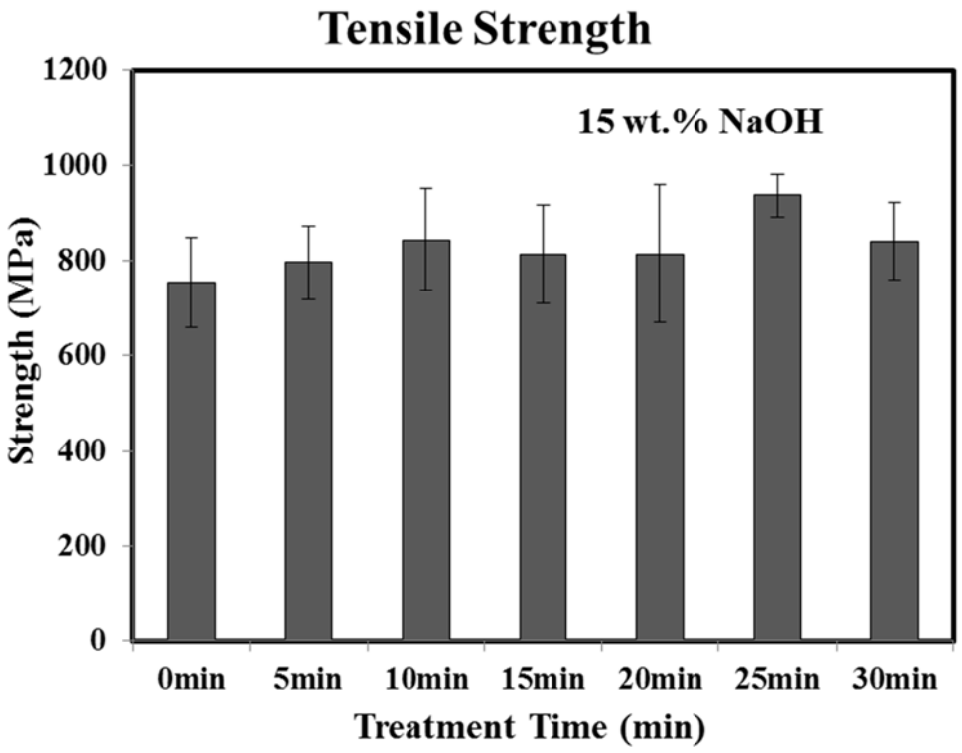

Figure 4.13 Tensile strength of 15 wt. % alkali-treated abaca fibers with different treatment times

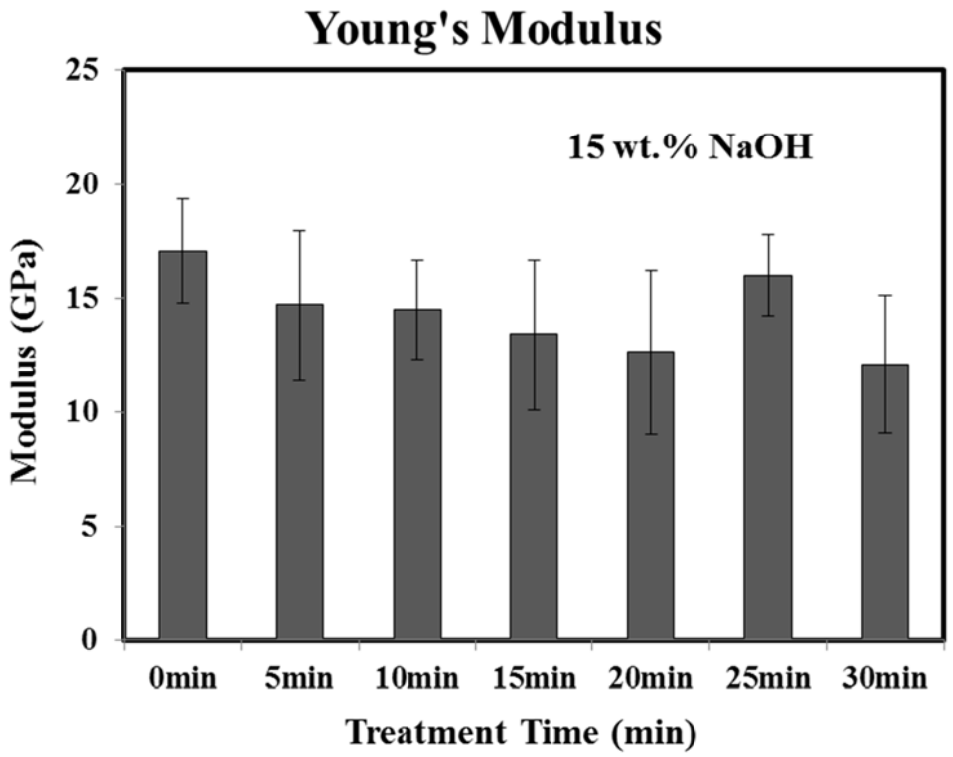

Figure 4.14 Young's modulus of 15 wt. % alkali-treated abaca fibers with different treatment times

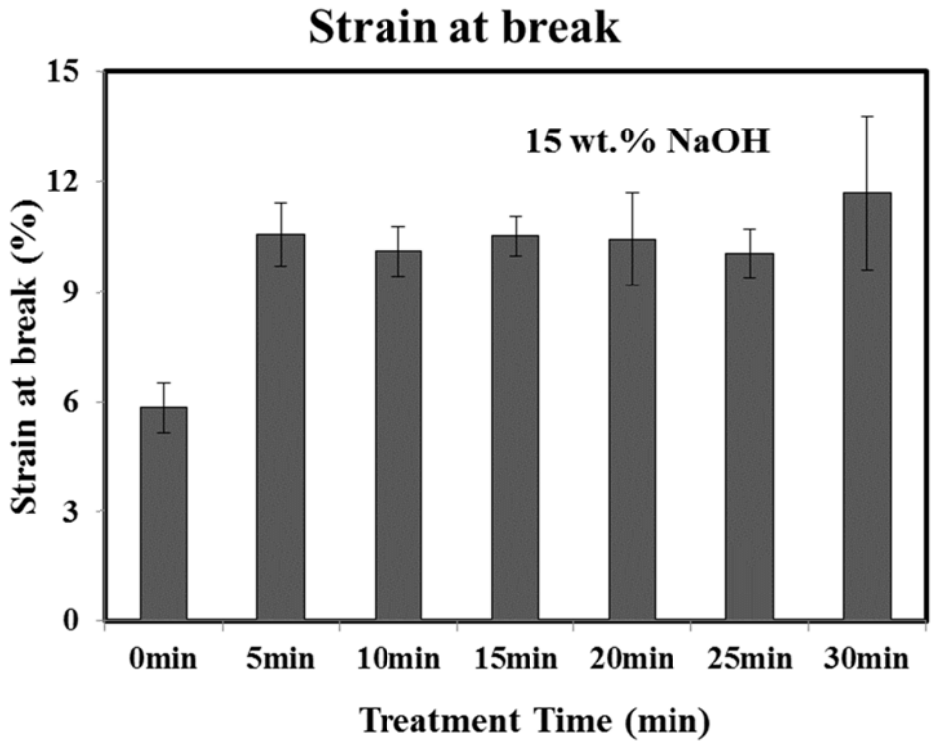

Figure 4.15 Strain at break of 15 wt. % alkali-treated abaca fibers with different treatment times

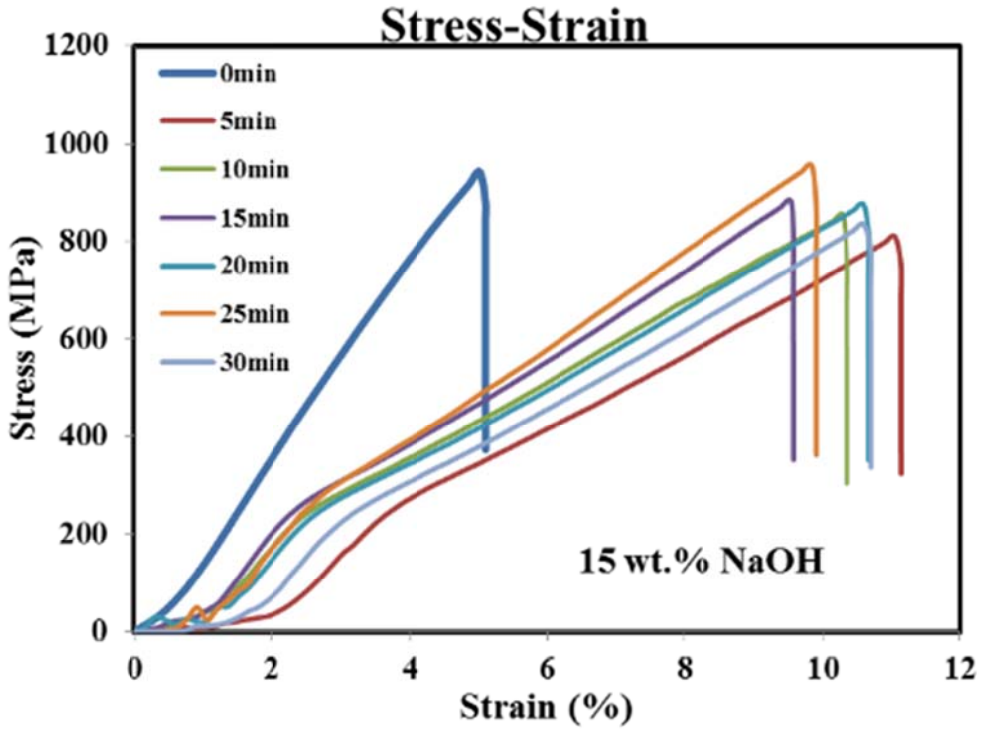

Figure 4.16 Stress-strain curves of 15 wt. % alkali-treated abaca fibers with different treatment times

The tensile properties of untreated and 15 wt. % alkali-treated abaca fibers are summarized in Figure 4.13 to Figure 4.16 and Table 4.3. After 15 wt. % alkali treatment, the tensile strength was maintained relative to the untreated fiber. The Young's modulus decreased during different treatment times (Figure 4.14). After treatment time of 25 min; the tensile strength and Young's modulus was higher than in other treatment times. The strain at break substantially increased after 15 wt. % alkali-treatment (Figure 4.15). Meanwhile, the strain at break leveled off irrespective of the treatment time. The stress-strain curves are shown in the Figure 4.16. The non-linear behavior also occurred for every treatment time after 15 wt. % NaOH treatment. The initial stress-strain curves of the treated fibers show flectional behavior due to the clamp swing.

Considering all different alkali concentrations and treatment times, a decrease in the Young's modulus and an increase in the strain at break occurred at concentrations greater than 10 wt. %. The factors that influence these mechanical properties in the longitudinal direction of

abaca fiber are apparently due to changes in the structure of the cell wall and the morphology of the fiber as we mentioned in Chapter 3.

4.5 Conclusions

In this study, abaca fibers were treated by 5, 10 and 15 wt. % NaOH solutions with different treatment times. The major changes in morphology and mechanical properties are summarized below:

(1) The lumen size decreased with increasing alkali concentration and treatment time.

(2) The tensile strength slightly increased after 5 and 10 wt. % and was maintained after 15 wt. % alkali treatments.

(3) The Young's modulus increased after 5 wt. % and decreased after 10 and 15 wt. % alkali treatments.

(4) The strain at break decreased after 5 wt. % and remarkably increased after 10 and 15 wt.% alkali treatments.

(5) The effect of treatment time is not evident compared to the effect of alkali concentration.

Chapter 5 Influence of Alkali Treatment on Internal Microstructure and Tensile Properties of Abaca Fibers

5.1 Abstract

The objective of this study is to investigate the effect of alkali treatment on the internal microstructure and tensile properties of abaca fibers. The abaca fibers were immersed in aqueous solutions of NaOH (5, 10 and 15 wt. %) for 30 min, rinsed and dried. The fibers were subsequently characterized by scanning electron microscopy, X-ray diffraction (XRD), Fourier transform-infrared spectroscopy (FT-IR) and tensile strength tests. The lumen is a hollow region in each elementary fiber of the abaca fiber bundles. It was found that the lumen of the abaca fibers completely collapsed after 10 and 15 wt. % NaOH treatment due to the swelling of the fibers. The fibers also became twisted after these alkali treatments. It was found that cellulose I in abaca fiber was partially transformed to cellulose II after 15 wt. % NaOH treatment, as evidenced by XRD measurements. FT-IR analysis indicated that the alkali treatment led to a gradual removal of binding materials; such as hemicelluloses and lignin from the abaca fibers, resulting in the separation of abaca fiber bundles into individual elementary fibers. The tensile strength of alkali-treated abaca fibers did not vary with alkali concentration. The Young's modulus of the abaca fibers treated with 5 wt. % NaOH solution increased by 41%, whereas those treated with 10 and 15 wt. % NaOH solution decreased by 24 and 29%, respectively. A non-linear behavior was observed in the stress-strain curves of the abaca fibers after 10 and 15 wt. % alkali treatments, which could be attributable to the twisting of the fibers.

5.2 Introduction

Due to economic incentives and increasing environmental awareness, natural fiber reinforced thermoplastic or thermoset composites have attracted many researchers' attention [1, 6, 15, 55]. The advantages of using natural fibers in industrial applications relate to their light weight, low cost, nontoxicity, biodegradability and high specific stiffness. These characteristics make natural fiber-reinforced composites suitable for application in automotive and aircraft industries. The European Union legislation implemented in 2006 has expedited the application of natural fiber-reinforced plastics in automobiles. Car manufacturers must make vehicles in such a way that more than 85% of the vehicle's total weight can be recycled [8]. Regarding potential industrial application, fiber strength is one of the most important characteristics. Natural fibers including sisal [56], flax [6], ramie [57], bamboo [58] and abaca [59] exhibit good strength and are thus suitable for fabrication of fiber-reinforced composites.

Abaca (i.e., Manila hemp) is a species of banana and grows as a commercial crop in the Philippines. Abaca fiber has a high tensile strength (600-900 MPa) and Young's modulus (30-50 GPa) [60, 61], higher values compared to other strong fibers, such as sisal fiber which possess a tensile strength of 511 - 635 MPa and Young's modulus between 9.4 - 22.0 GPa [28]. Abaca fiber reinforced composites have been used for under-floor protection of passengers Daimler AG vehicles [53]. Importantly, abaca fibers satisfy the stringent quality requirements of road transportation, especially resistance to influences such as dampness, exposure to the elements and stone strike [52]. Understanding the unique physical and chemical properties of abaca fibers, and the structure-function relationship of the fibers, is critical to their effective utilization in industrial applications.

A weakness of the natural fibers is their high-water absorption characteristics and weak interfacial bonding with the matrix material of composites. This is the reason why natural

fibers have not completely replaced conventional fiber materials in high-load applications. Natural fiber-reinforced composites have been used in the automotive industry, but their application is generally limited to parts such as door panels, seat backs and other interior panels [8]. Due to the large industrial potential of natural fibers, their surface modification is becoming an important field of research. The majority of research in the area of fiber improvement focuses on the fiber-matrix interfacial adhesion and decreasing water absorption [62-64].

Alkali treatment (i.e. mercerization) is one of the most popular and lowest cost methods used for surface modification of natural fibers. Many studies have reported that alkali treatment increases fiber surface area and improves the interfacial characteristics of the fiber in composites [10, 18, 38, 46, 65].

The lumen of natural fibers contributes to the high sound absorption performance [66] and also plays a greater role than crystal structure and chemical compounds, on the transverse thermal conductivity of unidirectional composites [7]. The lumen is a hollow structure in the center of the abaca fibers that strongly influences the properties of natural fibers. The effect of the alkali treatment on the lumen of abaca fibers, and in turn the mechanical strength of such alkali-treated fibers, has received little attention in the literature, motivating the current study.

This study aimed to explore the relationship between the internal microstructure and tensile properties of abaca fibers by alkali treatment. XRD and FT-IR were used to follow alkali-induced structural and chemical changes in the fibers, respectively. The obtained structural and chemical information, combined with mechanical tests on the same untreated and treated fibers, serve to guide the development of the surface modification processes of natural fibers for advanced composite applications.

5.3 Materials and Experimental

5.3.1 Materials

Abaca fibers were supplied from the Philippines. The abaca fibers were immersed in different aqueous NaOH solutions (5, 10 and 15 wt. %) for 30 min, under a vacuum of 13 kPa (98 Torr) applied to ensure complete penetration of the alkali solution into the pores of the fibers. The fibers were taken out of the NaOH solutions, and washed repeatedly with fresh tap water (until the pH of the wash water was 7) to remove residual NaOH from the abaca fibers. Finally, the abaca fibers were dried in a vacuum desiccator oven at 80ºC for 2 hours.

5.3.2 Morphological examination of abaca fibers

The fracture surface and lateral surface of untreated and alkali-treated (5, 10 and 15 wt. % NaOH solution) abaca fibers were examined by a scanning electron microscope JEOL-JSM-6390 (JEOL Ltd., Japan) as shown in Figure 5.1. Specimens were platinum-sputter coated before analysis, and the imaging was performed at an accelerating voltage of 1.5 kV.

Figure 5.1 The fiber microstructure was measured by SEM

5.3.3 XRD measurements

The XRD data was obtained at room temperature on a Rigaku MultiFlex X-Ray Diffractometer (Rigaku Corporation, Japan), equipped with a Cu K X-ray source. X-ray tube was operated at 40 kV and 20 mA with a detector placed on a goniometer scanning the range from 5º to 40º, at a scan speed of 2º/min. Table 2 shows the 2θ calculated using the following equations [67]:

$$2\theta = 2\sin^{-1}\left(\frac{n\lambda}{2d_{hkl}}\right) \quad (3)$$

$$\frac{1}{{d_{hkl}}^2} = \frac{1}{a^2}\frac{h^2}{\sin^2\beta} + \frac{1}{b^2}k^2 + \frac{1}{c^2}\frac{l^2}{\sin^2\beta} - \frac{2hl\cos\beta}{ac\sin^2\beta} \quad (4)$$

where θ is the angle of diffraction, n is an integer, λ is the wavelength of the X-ray ($\lambda = 1.5406$ Å), and d_{hkl} is the crystallite dimension in the direction perpendicular to the crystallographic plane $h\ k\ l$. The cellulose structure is monoclinic, namely $a \neq b \neq c$ and $\alpha = \gamma = 90° \neq \beta$.

5.3.4 FT-IR measurements

FT-IR was performed at room temperature (20−22ºC) using a Bio-Rad VARIAN FTS 3000MXT spectrometer (Varian, Inc., USA). The infrared spectra of untreated and 5, 10 and 15 wt. % concentration alkali-treated abaca fibers were measured using finely powdered samples. The powdered samples were mixed with KBr at a weight ratio of KBr : sample = 100 : 1. This mixture was then pelletized using a hand-operated press.

5.3.5 Mechanical characterization of abaca fibers

To carry out tensile tests, the fibers were split into parcels, of which three were treated with 5, 10 and 15 wt. % NaOH solution and one was an untreated control sample. Each treated or untreated abaca fiber was stuck on a paper frame, as shown in Figure 5.2.

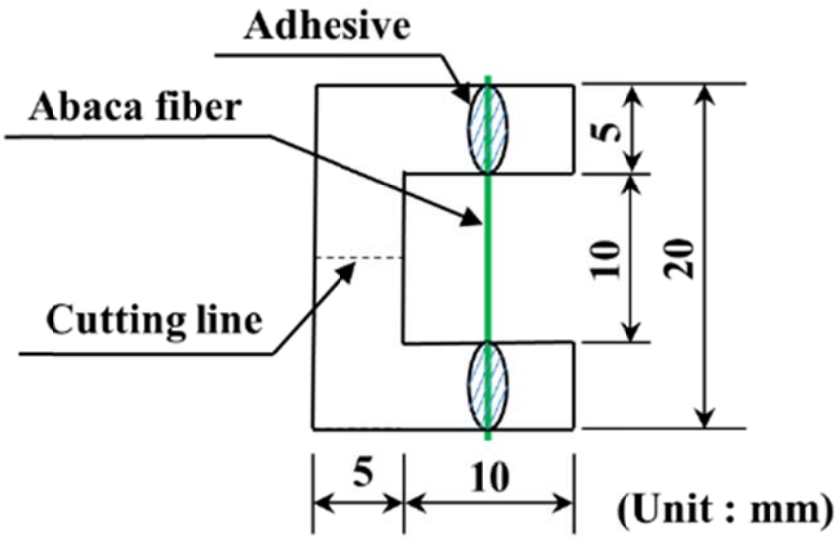

Figure 5.2 Tensile specimen of abaca fiber bundle was glued on a paper frame

The cross-section of abaca fibers was not completely circular (Figure 5.3), thus the average cross-sectional area (A) was calculated from two fiber diameters (*a* and *b*), by the following equation:

$$A = \frac{\pi ab}{4} \quad (5)$$

where *a* and *b* are the fiber diameters that run at right angles to each other, and measured by using a digital microscope VHX-600 (Keyence Corporation, Japan). Abaca fibers with the diameter around 200 µm were carefully selected and used in this study.

Tensile tests of abaca fiber bundles were carried out on a universal testing machine Instron model 5567 (Instron Corporation, USA). The abaca fiber bundle was glued on a paper frame with 10 mm gauge length. The tensile tests were performed using a load cell of 500 N at a cross head speed of 1.0 mm/min. Before each tensile test, the edge of the supporting frame was cut in the middle (as shown in Figure 5.2). The tensile strength was obtained from the maximum stress on the stress-strain curve. The Young's modulus was provided as the slope of the linear portion of the stress-strain curve. The strain at break was also obtained from the stress-strain curve.

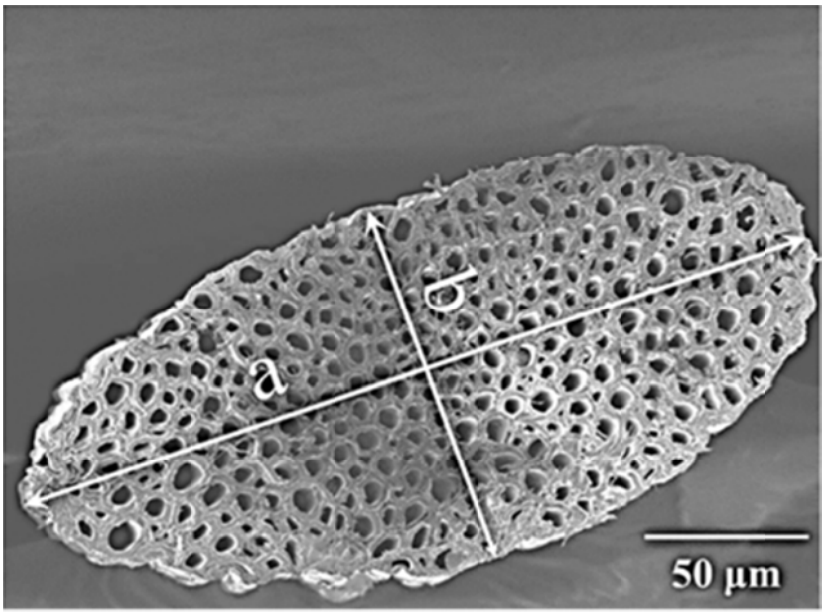

Figure 5.3 The SEM image of the cross-section of abaca fiber bundle

5.4 Results and Discussion

5.4.1 Morphology of alkali-treated abaca fibers

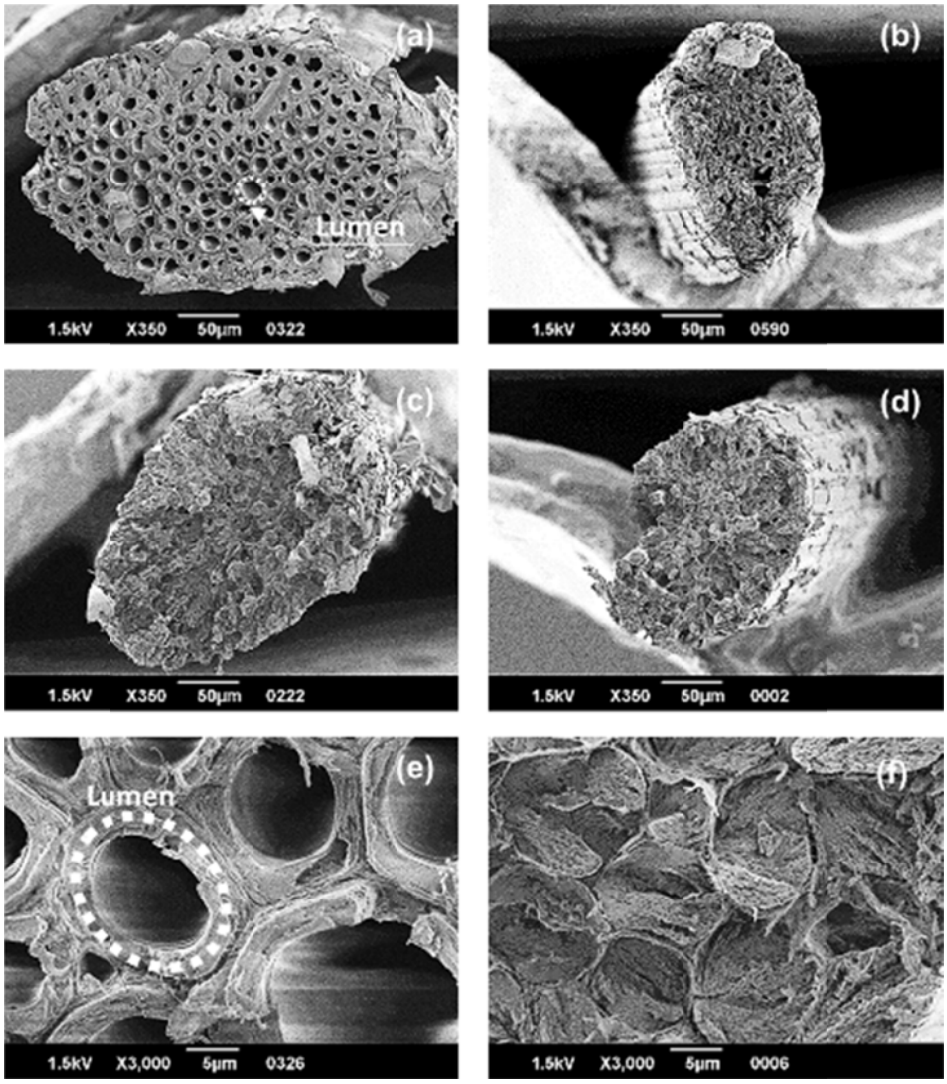

Figure 5.4 SEM images of fractured surfaces of abaca fiber bundles after tensile tests:(a) untreated abaca fiber bundle; (b), (c) and (d) abaca fiber bundles treated with 5, 10 and 15 wt. % NaOH solution for 30 min; respectively; (e) magnified image of untreated fiber bundle and (f) magnified image of 15 wt. % NaOH-treated fiber bundle.

SEM images (Figure 5.4(a) - (d)) show that the fiber lumen size decreased and completely disappeared during the alkali treatment process. Meanwhile, the cell wall of abaca fibers swelled with the increasing alkali concentration. The strong alkali treatment (10 and 15 wt. %) caused shrinkage in the cross section of the abaca fibers. In the case of untreated abaca fibers as shown in Figure 5.4(a) and (e), there is a large visible lumen in the center of every cell

(elementary fiber). The cross section of the fiber bundle is composed of polygonal cells of 10 – 25 μm in diameter with a cell wall thickness of 2 – 4 μm. The diameter of the alkali-treated fibers decreased by 20 – 40% compared to that of the untreated fibers. The lumen diameters of abaca fibers treated with 5 wt. % NaOH solution are in the range of 8 to 10 μm (Figure 5.4(b)), which is slightly smaller than that of untreated fibers (Figure 5.4(a)). The thickness of the cell wall is in a range of 2 to 6 μm. However, after alkali treatment with 10 and 15 wt. % NaOH solution, the lumen of abaca fibers was no longer visible and a large swelling of the cell walls was observed as shown in Figure 5.4(c) and (d). The cell wall thickness of 10 and 15 wt. % alkali-treated fibers is in a range of 6 to 20 μm. The lumen was collapsed after strong alkali treatment as shown in Figure 5.4(f). The swelling of abaca fibers due to alkali treatment, during which the natural crystalline structure of the cellulose relaxes, has already been described in the literature [45].

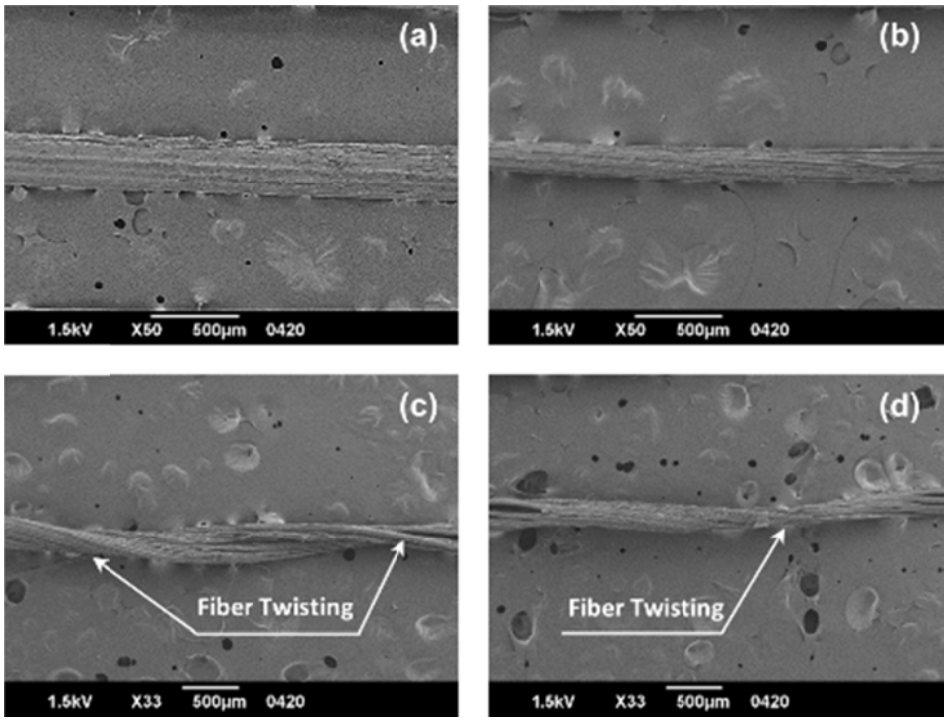

Figure 5.5 SEM images of surfaces of abaca fiber bundles:(a) untreated abaca fiber bundle; (b), (c) and (d) abaca fiber bundles treated with 5, 10 and 15 wt. % NaOH solution for 30 min; respectively.

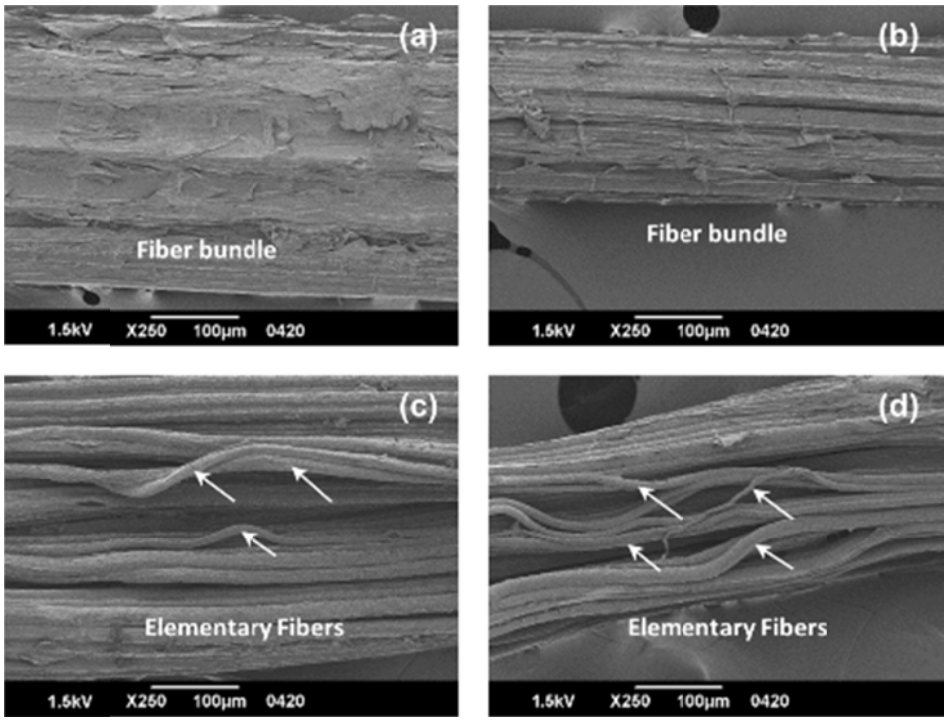

Figure 5.6 Magnified SEM images of the surfaces of abaca fiber bundles: (a) untreated abaca fiber bundle; (b), (c) and (d) abaca fiber bundles treated with 5, 10 and 15 wt. % NaOH solution for 30 min; respectively.

As shown in Figure 5.5(a) - (d), abaca fibers were twisted after strong alkali treatment. Figure 5.6(a) - (d) show that binding materials were removed from abaca fiber bundles after alkali treatment. In comparison to the untreated abaca fibers (Figure 5.5(a) and Figure 5.6(a)), the fibers were not twisted and surface materials were only slightly removed after 5 wt. % NaOH treatment (Figure 5.5(b) and Figure 5.6(b)). Nonetheless, after 10 and 15 wt. % NaOH treatment, the fiber bundles were significantly twisted and separated into elementary fibers as shown in Figure 5.5(c) and (d); and Figure 5.6(c) and (d). A possible explanation is that binding materials such as pectin, lignin and hemicelluloses were removed from abaca fibers during the alkali treatment, which led to fibrillation and breakdown of the fiber bundle into elementary fibers [14]. As shown in Figure 5.7, after 10 and 15 wt. % NaOH treatment, the twisting of the fiber bundles in the longitudinal direction was observed. This probably

occurred because of the longitudinal contraction of microfibrils, resulting in twisting of abaca fibers. Two factors influencing the twisting behavior of wood samples were reported by Nakano et al. [68]: one is an increase in the microfibril angle (MFA) and the other is the longitudinal contraction of microfibrils themselves. Nakano [69] has proposed a simplified mechanism of longitudinal contraction of wood samples. He suggested that the longitudinal contraction of microfibrils might be related to a reduction in the end-to-end distance of the chain segments in the amorphous region of the cellulose, and that the amorphous phase might be due to the defects caused by alkali penetrating the cellulose structure in the longitudinal direction during alkali treatment.

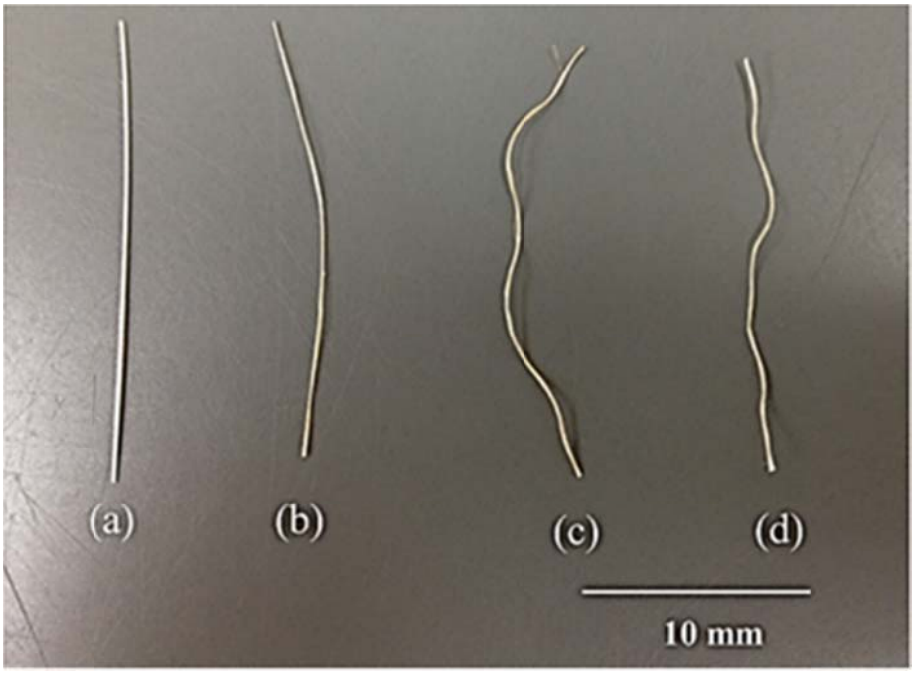

Figure 5.7 The morphological change of alkali-treated abaca fiber bundles: (a) untreated abaca fiber bundle; (b), (c) and (d) abaca fiber bundles treated with 5, 10 and 15 wt. % NaOH solution for 30 min; respectively.

5.4.2 X-ray diffraction crystallography of alkali-treated abaca fibers

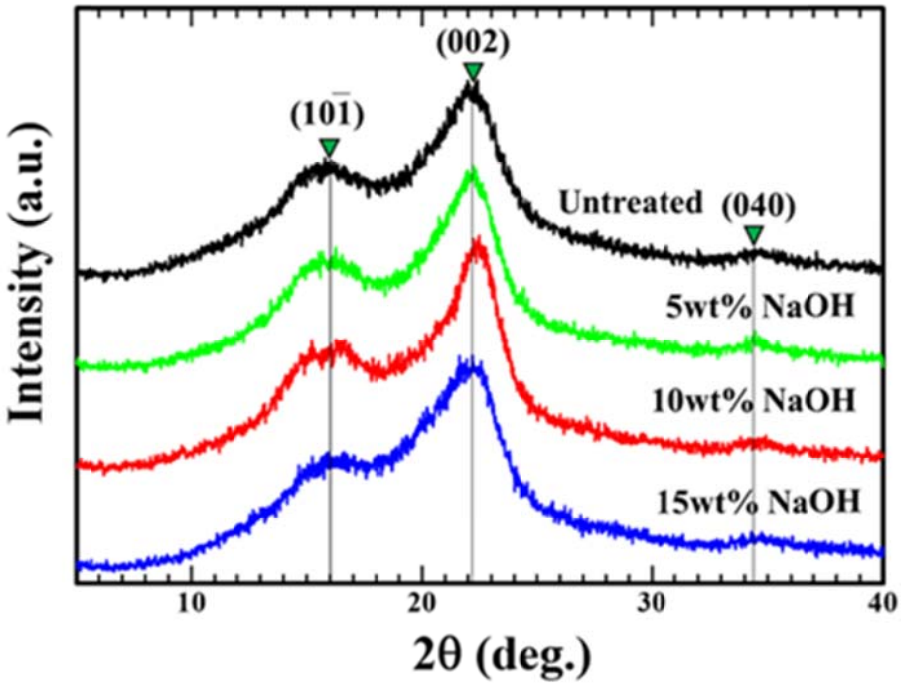

Figure 5.8 XRD diffractograms of the untreated and alkali-treated abaca fiber bundles for 30 min.

The lumen was collapsed and the cell wall was swelled during the alkali treatment (Figure 5.4(f)), compared to untreated abaca fibers (Figure 5.4(e)). These phenomena may be attributed to the increased spacing of the cellulose lattice. We analyzed the cellulose structure of the alkali-treated abaca fibers with XRD as shown in Figure 5.8. The spectrum of untreated abaca fibers shows three main peaks at 16.0, 22.2 and 34.5°. These peaks are attributed to the cellulose I crystalline structure and are assigned to $(10\bar{1})$, (002) and (040) reflections, respectively. In Table 5.1 [70, 71] the 2θ angle (calculated from Eqs. (1) and (2)) and lattice spacing parameters of Na-cellulose I, Na-cellulose IV, cellulose I and cellulose II are presented.

Table 5.1 Different cellulose types by crystallographic structure.

Cellulose type	**Lattice parameters (Å)**			**2θ (deg.)**		
	a	**b**	**c**	**$10\bar{1}$**	**002**	**040**
Na-Cellulose I	8.8	10.3	25.3			
Na-Cellulose IV	9.6	10.3	8.7			
Cellulose I	8.3	10.3	7.9	16.0	22.6	34.5
Cellulose II	8.1	10.3	9.1	20.2	22.2	34.5

(2θ is the angle of diffraction and was calculated from the lattice parameters. β is the inter-axial angle between **a** and **c**. Cellulose I, $\beta = 84°$. Cellulose II, $= 62°$. The geometry of both celluloses is monoclinic [71].)

The spectrum of the 5 wt. % alkali-treated abaca fibers shows the same cellulose I profile as the untreated ones (Figure 5.8). In the case of 10 wt. % alkali-treated fibers, the peak (002) became sharper than that of the untreated ones and double peaks were found around the peak ($10\bar{1}$). We assume that the 10 wt. % alkali treatment increased the cellulose crystallinity by removing some parts of chemical components, such as hemicelluloses, pectin, and lignins, thus the cellulose content increased, resulting in a sharper (002) peak. The 15 wt. % alkali treatment resulted in the increase in the full width at half maximum of the ($10\bar{1}$) and (002) peaks. Nishiyama et al. [72] described the mechanism of transformation of cellulose I structure into cellulose II structure during mercerization, where Na-cellulose I is an intermediate phase in the transformation. In 3 to 5 N (12 – 20 wt. %) NaOH solution, the cellulose I transforms to Na-cellulose I. After washing with fresh water, Na-cellulose I changes to Na-cellulose IV (without Na^+) and after drying Na-cellulose IV changes to cellulose II [18, 72]. In our study, the alkali-treated abaca fibers, cellulose I is not completely transformed into cellulose II even after alkali treatment higher than 12 wt. % (3N) NaOH. The spectrum of 15 wt. % alkali-treated abaca fibers indicates the coexistence of cellulose I

and cellulose II. It may be that only part of the cellulose I transforms into Na-cellulose I. After washing with tap water and drying, the Na-cellulose IV changes into cellulose II. There is a wide peak at (002), which may be comprised of overlapping cellulose I ($2\theta = 22.6°$) and cellulose II ($2\theta = 20.2$ and $22.2°$) peaks. Peak at $(10\bar{1})$ is assigned to cellulose I. The peak at (040) is formed by overlapping cellulose I ($2\theta = 34.5°$) and cellulose II ($2\theta = 34.5°$) peaks. The cell wall swells in various extent depending on the alkali concentration. In the abaca fibers treated with low-concentration alkali solution (5 wt. % NaOH), the large pores in the cellulose crystalline structure were occupied with sodium ions. The Na^+ seems to have a favorable diameter to penetrate the spacing of the lattice planes [45]. With increasing the alkali concentration, Na^+ (0.276 nm in diameter) advances more easily into small spaces [71]. This leads to the formation of new Na-cellulose I lattice with relatively large distances between the cellulose molecules (as shown in Table 5.1). The OH-groups of the cellulose in the lattice are converted into ONa-groups, thus expanding the dimensions of cellulose molecules [73]. Therefore, the alkali treatment causes swelling of the cell wall and enables large molecules to penetrate into crystalline regions. The swelling of the cell wall exerts very large forces [18] onto the weaker Na-cellulose lattice [46], thus the lumen collapses. The cellulose swelling is a complicated process. The cell wall thickening occurs due to the presence of swollen cellulose in the cell wall. Similar results were reported by Amel et al. [74]. After washing with fresh tap water, the Na^+ ions were removed and formed the Na-cellulose IV with larger crystallite lattice which was the result of swelling of the crystalline lattice by the alkali solution [46]. After drying, Na-cellulose IV transforms to cellulose II. The swollen cell wall does not revert to the original shape, therefore the cell wall remains swollen and the lumen is collapsed.

5.4.3 FT-IR analysis of alkali-treated abaca fibers

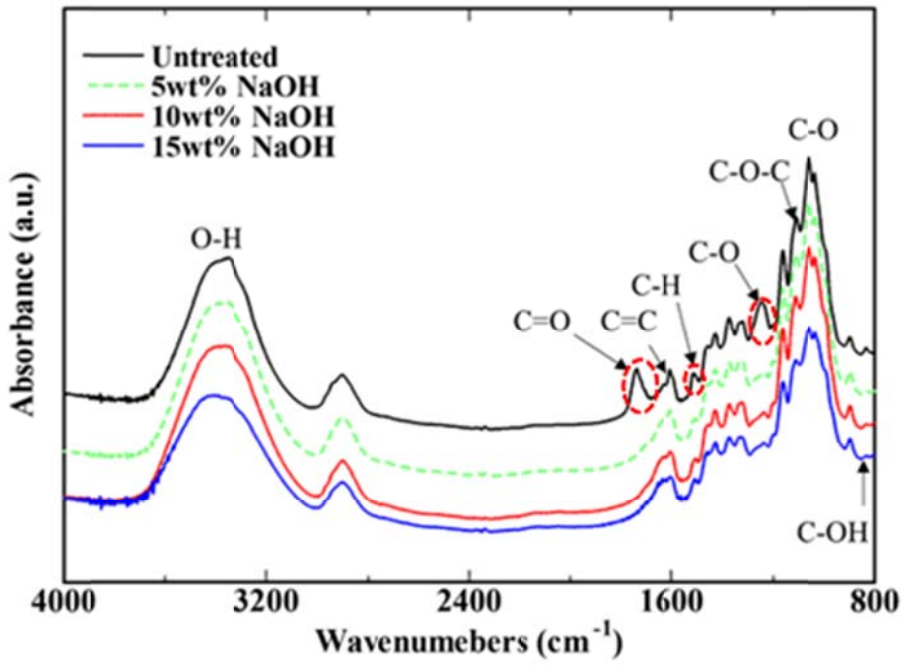

Figure 5.9 FT-IR spectra of abaca fiber bundles before and after alkali treatment for 30 min.

The elementary fibers in an abaca fiber bundle were separated (Figure 5.6(c) - (d)) compared to untreated abaca fibers (Figure 5.6(a)). The fiber bundle separation may be attributed to the removal of the binding materials, such as lignin, pectin and hemicelluloses, from abaca fiber bundles after the alkali treatment. We analyzed the chemical composition of untreated and alkali-treated abaca fibers using FT-IR spectroscopy, as shown in Figure 5.9. The peak assignments of the absorption bands corresponding to various chemical groups are summarized in Table 5.2 [18, 42, 44, 75-77]. The peaks at about 3400, 1742, 1603, 1514, 1242, 1100, 1062 and 896 cm^{-1} are assigned to the (-OH), (C=O), (C=C), (C-H), (C-O), (C-O-C), (C-O), and (C-OH), respectively. The peak observed at 1742 cm^{-1}, representing the C=O bonds of the carboxylic group of hemicelluloses and pectin in the untreated fibers, was no longer visible upon the alkali treatment [75, 78]. In comparison to the untreated abaca fibers, the peak at 1242 cm^{-1} was also no longer observed in the treated abaca fibers. This 1242 cm^{-1} peak belongs to the C-O stretching of acetyl groups of lignin [76]. This indicates

that part of lignin was removed from abaca fibers during alkali treatment. A partial removal of hemicelluloses from the fibers after the NaOH treatment also occurred, as it is evident by the decreased carbonyl peak at 1500 – 1750 cm^{-1} [77]. From these results we conclude that alkali treatment caused the removal of the binding materials, such as hemicelluloses, pectin and lignin, from the abaca fiber bundle. This removal of the binding materials caused a separation into elementary fibers [14].

Table 5.2 Characteristic bands of the infrared spectra of the abaca fiber.

	Functional Group	**Possible Assignment**
3400	-OH	Cellulose, hemicelluloses and lignin
1742	C=O	Hemicelluloses and pectin
1603	C=C	Lignin components
1514	C-H	Hemicelluloses and pectin
1242	C-O	Lignin
1100	C-O-C	Cellulose
1062	C-O	Hemicelluloses and lignin

5.4.4 Effect of morphological changes on the mechanical properties of abaca fibers

In this study, we found that tensile properties of alkali-treated abaca fibers were significantly affected by their morphological changes. Figure 5.10(a) shows typical stress-strain curves of alkali-treated (5, 10 and 15 wt.% NaOH) and untreated abaca fibers. The tensile curves for abaca fibers treated with 10 and 15 wt.% NaOH solution indicates a non-linear behavior in

the strain region of 0.5 – 3%. This non-linear behavior was not observed for untreated and 5 wt.% alkali-treated abaca fibers. The non-linearity appears to be derived from fiber twisting.

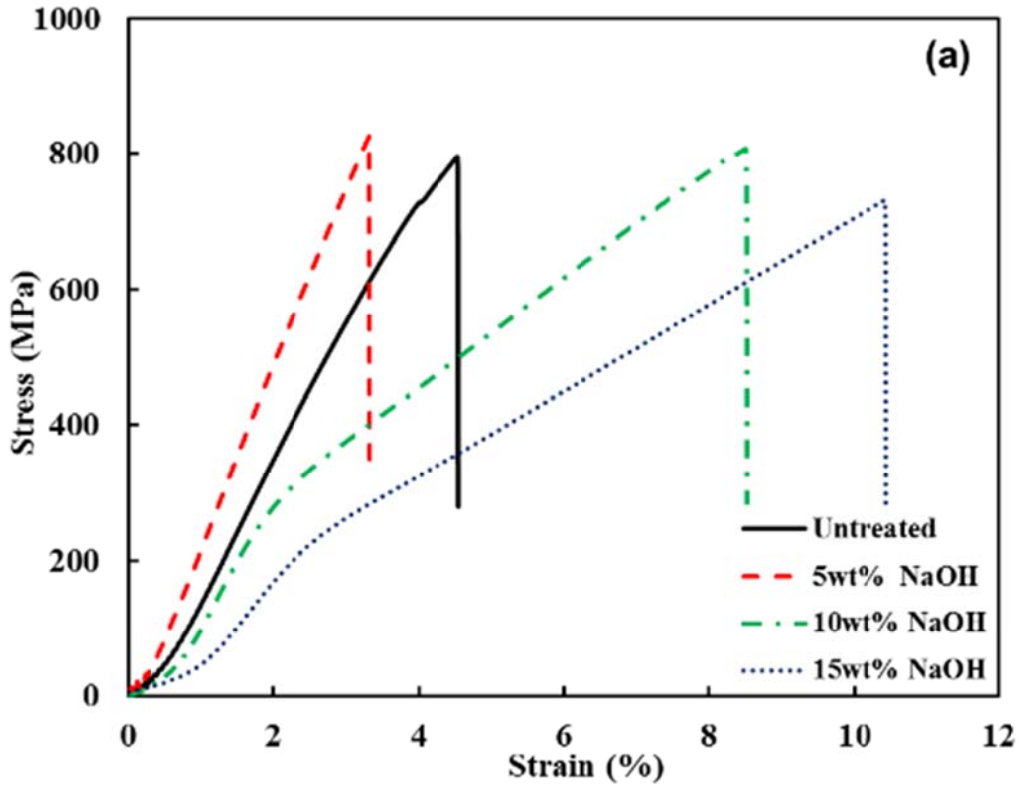

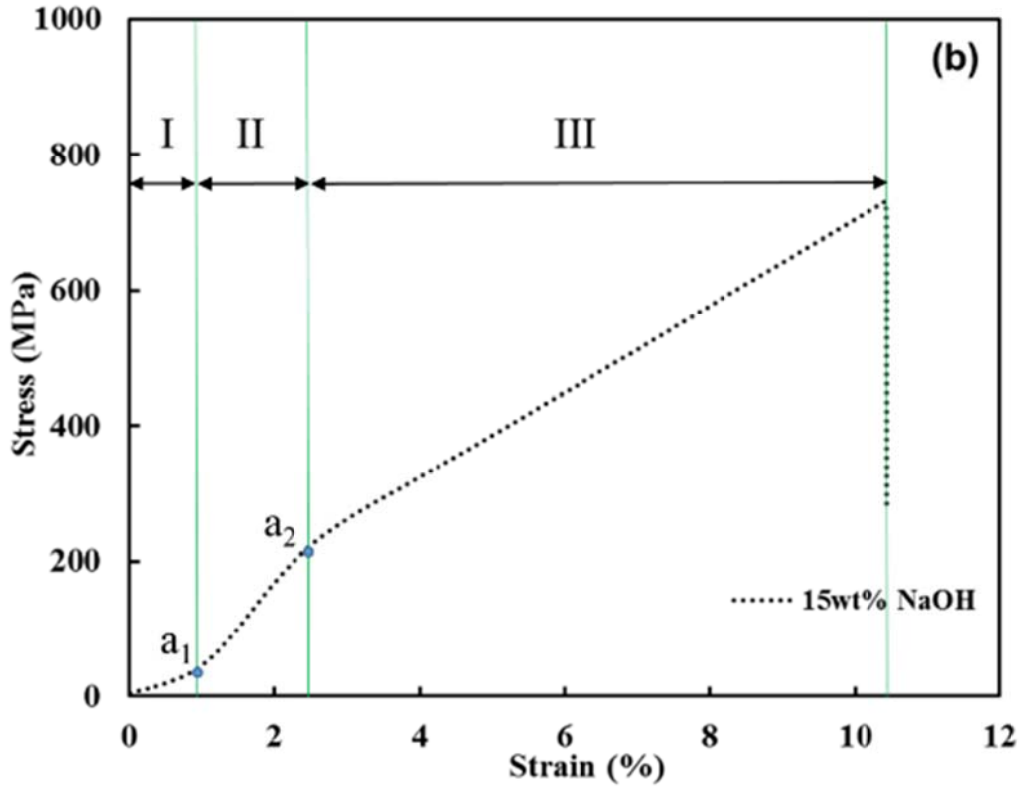

Figure 5.10 Tensile stress-strain curves of abaca fiber bundles:(a) before and after alkali treatment for 30 min and (b) the stress-strain curve is divided into 3 regions by the inflection point a_1 and the yield point a_2.

Figure 5.10(b) shows that the stress-strain curve of 15 wt. % alkali-treated abaca fibers is divided into three distinct regions. In region I, it is known that during tensile tests carried out in the direction of the fiber loading axis, the twisted fiber bundle orientates towards the direction of the load [79-81]. In region II, the twisted elementary fibers organize themselves in parallel to the loading direction, which is parallel to the fiber axis. An elastic behavior is characteristic for the region II. The slope of the curve increases compared to the region I due to a parallel alignment of the elementary fibers in the direction of the fiber axis [81]. The Young's modulus was defined as a slope of the curve in this region [80]. These reorganizations would start to form in the inflection point a_1 [79]. The yield point a_2 appears when the elementary fibers are aligned parallel to the loading direction. In the region III (after yield point a_2), the parallel cellulose microfibrils slide along each other within the fiber bundle axis by shearing the non-crystalline region of the fiber [75, 79, 81]. The slope of the

stress-strain curve in region III drops compared to region II due to the softening of the cellulose microfibrils after alkali treatment (softening may be due to the hydrogen bonds broken by alkali treatment). After strong alkali treatment, the fibers were twisted like a spiral spring (as shown in Figure 5.7) which would lead to the non-linear behavior in the stress-strain curves. Another possible explanation is that the non-linear stress-strain behavior could be induced by non-uniformities in MFA [79].

Table 5.3 Tensile properties of untreated and alkali-treated abaca fiber bundles.

NaOH concentration (wt%)	**Fiber diameter (mm)**	**Tensile strength (MPa)**	**Young's modulus (GPa)**
Untreated	0.23 ± 0.03	760 ± 90	17.1 ± 2.4
5	0.20 ± 0.04	850 ± 70	24 ± 5
10	0.20 ± 0.03	840 ± 60	13 ± 2
15	0.19 ± 0.04	840 ± 80	12 ± 3

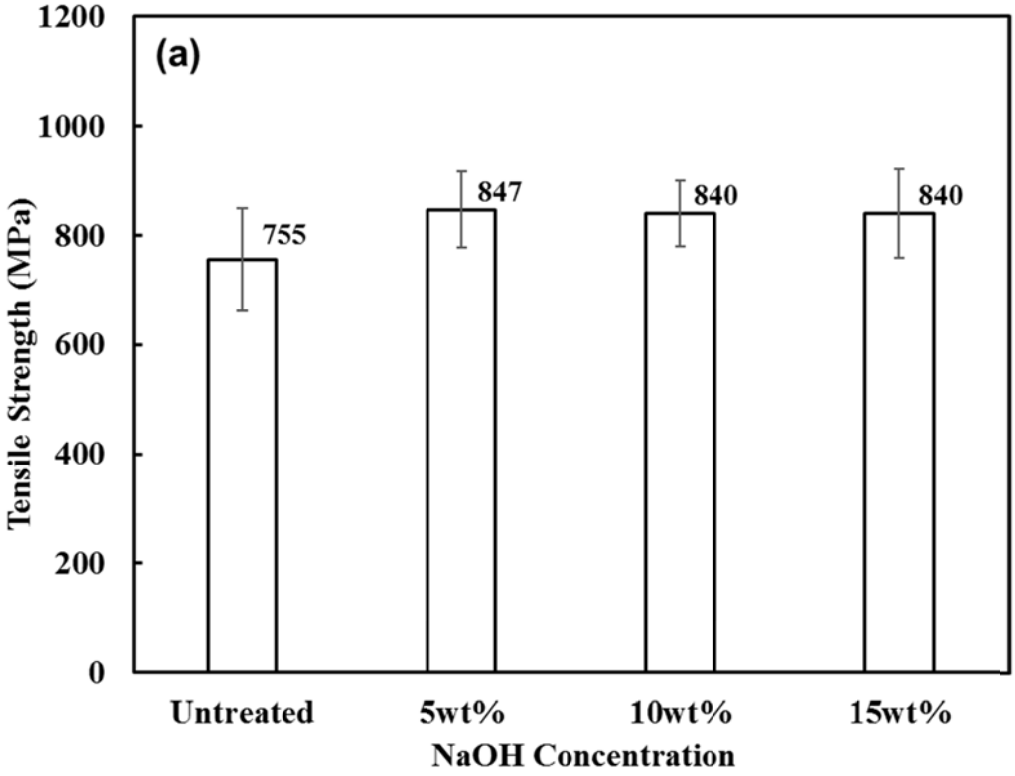
(a)
Tensile Strength (MPa)
1200
1000
800
600
400
200
0
755
847
840
840
Untreated
5wt%
10wt%
15wt%
NaOH Concentration

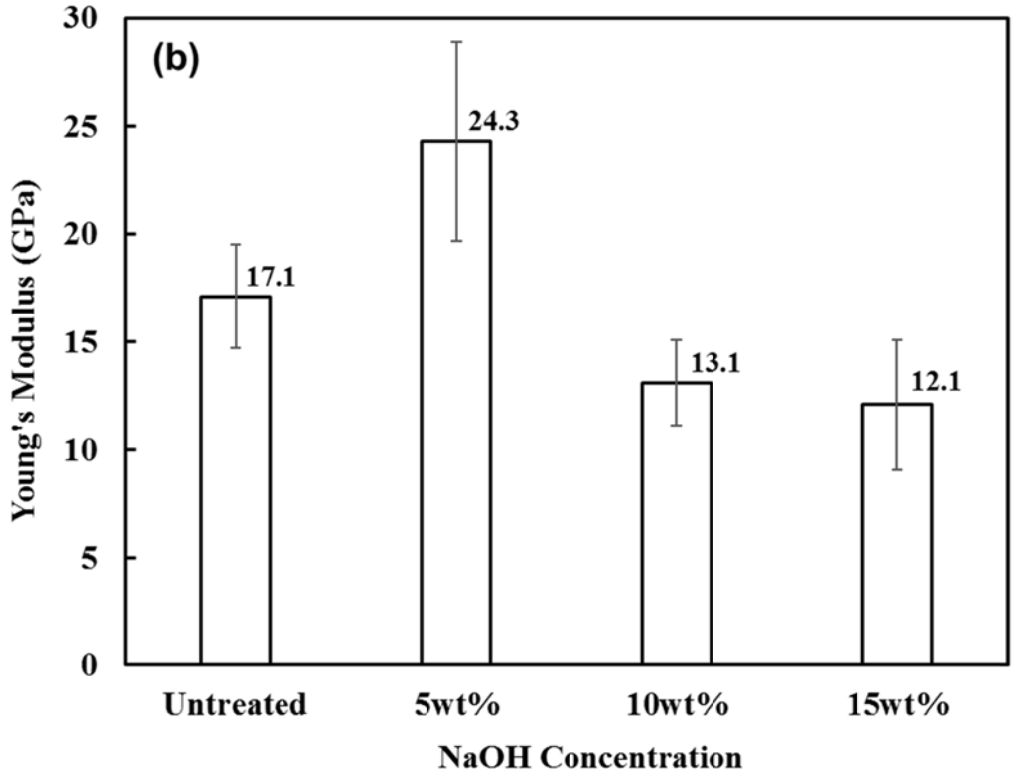
(b)
Young's Modulus (GPa)
30
25
20
15
10
5
0
17.1
24.3
13.1
12.1
Untreated
5wt%
10wt%
15wt%
NaOH Concentration

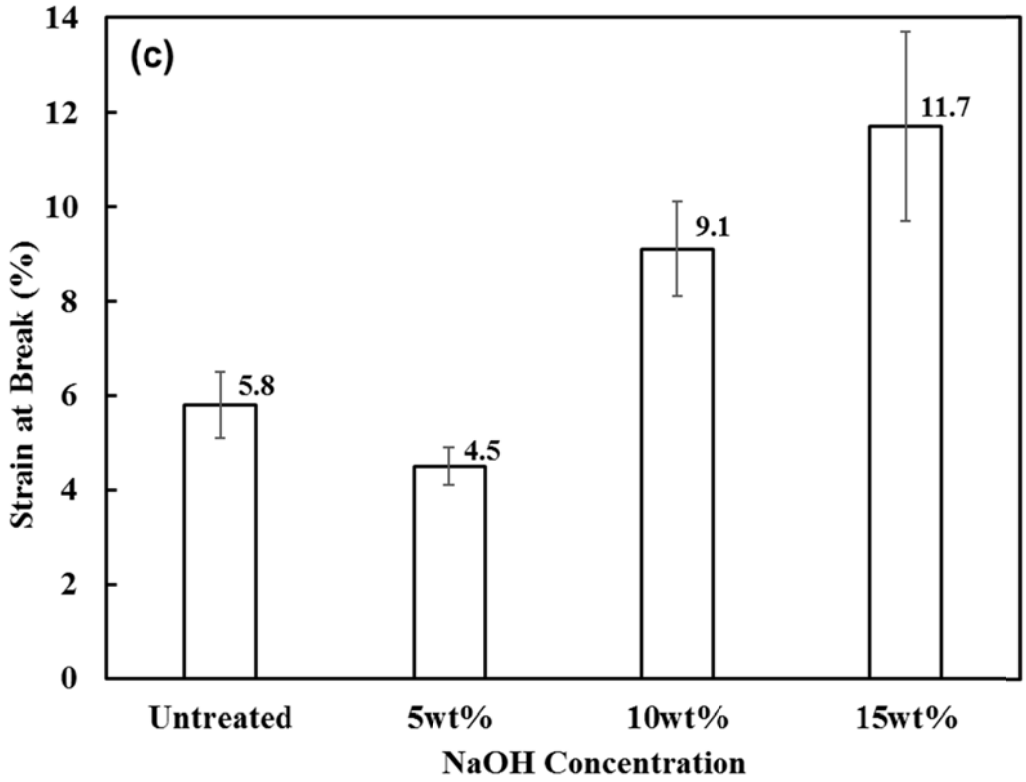

Figure 5.11 Mechanical properties of abaca fiber bundles before and after alkali treatment for 30 min. (a) tensile strength, (b) Young's modulus and (c) strain at break.

Figure 5.11(a) - (c) show the tensile properties of untreated and treated abaca fibers. The diameter of abaca fibers decreased by 10 – 20% after 5, 10 and 15 wt. % alkali treatment, (Table 5.3). The tensile strength did not significantly change after alkali treatment with different NaOH concentration (Figure 5.11(a)). The Young's modulus of the 5 wt. % NaOH treated abaca fibers increased by 41%, but decreased by 24% and 29% in the fibers treated with 10 and 15 wt. % NaOH solution, respectively. The strain at break improved 60 – 100% after alkali treatment with 10 and 15 wt. % NaOH solution, whereas it was reduced by 20% in the fibers treated with 5 wt. % alkali concentration in comparison to the untreated abaca fibers. The increase in the Young's modulus after 5 wt. % NaOH treatment, compared to untreated fiber bundles (Figure 5.11(b)), might be derived from a decrease in the fiber diameter after NaOH treatment. The decrease in the Young's modulus and the increase in the strain at break occurred when treated with alkali solution higher than 10 wt. % NaOH (Figure

5.11(b) - (c)). Nakagaito and Yano [82] have reported that the Young's modulus of the cellulose nanofibers were decreased by the strong alkali treatment with 20 wt.% NaOH solution. Ishikura et al. [47] determined that the changes in the structure of the wood fiber; such as MFA and cellulose crystallinity, are major factors that influence the mechanical properties in the longitudinal direction of the wood fibers. The alkali treatment leads to a removal of hydrogen bonds in the cross-linked networks of cellulose and lignin structure [14, 83], and this makes the fibers soft [38], resulting in large elongation and reduction in Young's modulus [83]. Another possible reason is that the MFA increased with decreasing crystallinity of the fiber, which consequently influenced the mechanical properties of the fibers [38, 81].

5.5 Conclusions

The effects of alkali concentration on internal microstructure and mechanical properties of abaca fibers were investigated. The results obtained are summarized as follows:

1. The cross sectional area of abaca fiber bundles decreases significantly with alkali treatment, which can be attributed to collapse of the lumen through the swelling of the cellulose microfibrils, and also the solubilisation of lignin, hemicelluloses and pectins in the native fibers. In addition, the abaca fiber bundles become twisted with strong alkali treatment (10 and 15 wt. % NaOH).

2. Hemicelluloses, pectin and lignins, were completely removed from the abaca fiber bundles after treatment for 30 minutes in 10 or 15 wt. % NaOH solutions.

3. Alkali treatment affects the tensile properties of the abaca fiber bundles. After strong alkali treatment (10 or 15 wt. % NaOH), the associated fiber twisting and softening resulted in non-linear stress-strain behavior, a lower Young's modulus and higher strain at break, compared to untreated abaca fibers.

4. The tensile strength of abaca fiber bundles did not significantly change with alkali concentration (0, 5, 10 or 15 wt. % NaOH). However, both the Young's modulus and the strain at break were dependent on the alkali concentration. Results suggest that by varying the alkali concentration, it is possible to tailor the tensile properties of abaca fiber bundles for specific applications.

Chapter 6 Influence of Alkali Treatment on Interfacial Bonding in Abaca Fiber-reinforced Composites

6.1 Abstract

Chemically modified abaca fibers demonstrate enormous potential as natural reinforcing agents in composite materials. In this study, a series of alkali-treated abaca fibers were first prepared by immersion of abaca fibers in 5, 10 and 15 wt. % sodium hydroxide (NaOH) solutions for 2 h. The crystallinity index, microstructure, surface morphology, chemical components, interfacial adhesion with epoxy and mechanical characteristics of the untreated and alkali-treated abaca fibers were then evaluated. Results show that the degree of crystallinity in the abaca fibers increased by 6% following 5 wt. % NaOH treatment. This treatment also increased the tensile strength and the Young's modulus (increased by 37.8 %) of the fibers. However, the Young's modulus of abaca fibers decreased by 34 % and 49 % after 10 and 15 wt. % NaOH treatments, respectively, indicating that strong alkali treatments negatively impacted fiber stiffness and suitability for use in composite applications. The 5 wt. % NaOH treatment improved the interfacial shear strength (IFSS) of abaca fiber reinforced epoxy by 32%. It can be concluded that pre-treatment of raw abaca fibers with 5 wt. % NaOH is highly beneficial for the fabrication of abaca fiber-reinforced composites.

6.2 Introduction

The use of natural plant fibers as reinforcing agents in composite materials has attracted widespread scientific and industrial interest over the past decade [1, 84-86]. This interest originates from the natural abundance and low cost of such fibers, and inherent physical properties such as their light weight and high specific modulus [33]. Amongst the various plant fibers under consideration for use in polymer composites, abaca (i.e., Manila hemp)

produced in the Philippines possesses the most desirable mechanical properties. Abaca fiber contains 56-64% cellulose, 25-29% hemicelluloses, 11-14% lignin and a small proportion of fats, pectin, ash and waxes [87, 88].

Abaca fiber-reinforced composites have been used in automotive applications, including under-floor protection in passengers vehicles (e.g. Daimler AG series) [53]. Abaca fiber was the first plant fiber to meet the stringent quality requirements of road transportation, which can be attribute to its resistance to influences such as dampness, exposure to the elements, and stone strike [52]. Obtaining large quantities of high quality abaca fiber with consistent characteristics is essential for the industrial composite applications (e.g. variations in fiber quality form batch-to-batch or year-to-year is highly undesirable as this could yield composites with low or unpredictable strength). The most important factor in obtaining good plant fiber reinforcement in a composite is the interfacial adhesion between the matrix polymer and the fiber [89]. However, a common shortcoming of many plant fiber-reinforced composites is weak interfacial adhesion with the matrix, which generally can be traced to the hydrophilic nature of plant fibers. Therefore, in order to develop composites with improved mechanical properties, it is necessary to impart a degree of hydrophobicity to the fibers by suitable chemical treatments [14, 90, 91].

Alkali treatment (i.e., Mercerization) is one of the most useful methods for surface modification of cellulose fibers. A considerable body of work has been reported on this topic [42, 92, 93]. Hossain et al. [94] compared sugarcane fiber bundles treated with 1 wt.% and 5 wt.% alkali solutions, and found that fibers treated with 5 wt.% alkali solution possessed the best mechanical properties. Alkali treatment has been shown to selectively remove lignin and amorphous hemicelluloses from the natural fibers, leaving behind the stiffer and more crystalline cellulose fibers [95]. Accordingly, the mechanical properties of composites containing alkali-treated fibers are generally greatly superior to composites containing raw

fibers [41]. Alkali modification of abaca fiber improves the mechanical and physical properties of the fiber, and the associated chemical modification enables stronger fiber surface adhesion to the surrounding matrix. Optimizing interfacial adhesion between natural fibers and matrix polymers is critical for obtaining high performance composites, and it is a very active field of research.

In the present work, we investigate the effect of different alkali treatments on the tensile properties of abaca fibers and then explore the interfacial adhesion of the obtained fibers with an epoxy resin. SEM, XRD and FT-IR were used to follow structural and chemical changes in the fibers after alkali treatment. Tensile strength tests on the fibers, together with interface shear strength tests on raw fiber and treated fiber reinforced epoxy composites, guide the development of new and improved processes for the surface modification of natural fibers for advanced composite applications.

6.3 Materials and Experimental

6.3.1 Materials

Abaca fibers were obtained from the Philippines, and cut to a length of 20 mm. The abaca fibers were treated with each one of three different aqueous NaOH solutions (5, 10 and 15 wt. %) for 2 h under vacuum (around 13 kPa or 98 Torr) to ensure good penetration of the alkali solutions into the fiber bundles. The fibers were subsequently removed from the alkali solution and washed several times using fresh tap water until the pH was around 7 to completely remove NaOH from the abaca fibers. Finally, the abaca fibers were dried in a vacuum oven at 80 ^{o}C for 2 h.

6.3.2 X-ray Diffraction

Wide-angle X-ray diffraction patterns for all samples were obtained on a Rigaku MultiFlex X-ray Diffractometer (Rigaku Corporation, Japan). The measurements were carried with the

Cu X-ray tube operating at 40 kV and 20 mA, with a detector placed on a goniometer scanning the range from 5º to 40º at scan speed of 2º/min.

6.3.3 FT-IR

Fourier transform infrared spectra of untreated and alkali-treated fibers were performed by dispersing the powdered fiber samples on KBr pellets (mass ratio; abaca fiber:KBr = 1:100), and measured using a Bio-Rad VARIANFTS 3000MXT spectrometer (Varian, Inc., USA).

6.3.4 SEM

Morphology of the untreated and alkali-treated fibers was examined using a scanning electron microscope JEOL-JSM-6390 (JEOL Ltd., Japan). For the SEM study, the fiber samples were lightly coated with Pt-Pd to minimize specimen charging under electron beam. Specimens were imaged at an accelerating voltage of 1.5 kV.

6.3.5 Fiber tensile tests

The mechanical properties of the fibers, including tensile strength, Young's modulus and strain at break, were determined using an Instron model 5567 (Instron Corporation, USA). The abaca fiber bundle was glued on a paper frame with 10 mm gauge length (Figure 6.1). The tensile tests were performed using a load cell of 500 N at a cross head speed of 1.0 mm/min. Before each tensile test, the edge of the supporting paper frame was cut in the middle.

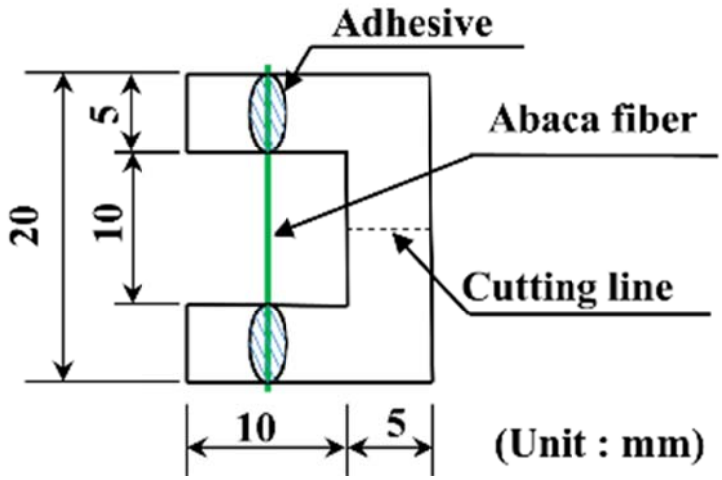

Figure 6.1 Tensile specimen of abaca fiber bundle was glued on a paper frame.

6.3.6 Single fiber pull-out tests

The single fiber pull-out test is an experimental method commonly used to measure the interfacial shear strength (IFSS) between a single fiber and a bulk of matrix material that surrounds the fiber [96]. A single fiber was threaded through the eye of a sewing needle. The needle, together with the fiber, was then punctured into the wall of a silicon rubber box. After the needle was removed, one end of the fiber was left on the inner wall of the box, with the embedded length ranging from 500 μm to 1000 μm. Epoxy mixed with curing agent and accelerator was poured into the box and cured at room temperature for 24 h. Afterward the specimens were carefully removed from the box and post-cured at 60^{o}C for 2 h. The test system is shown in Figure 6.2(a), the test sample is detailed in Figure 6.2(b) along with a schematic of the pull-out test (Figure 6.2(c)).

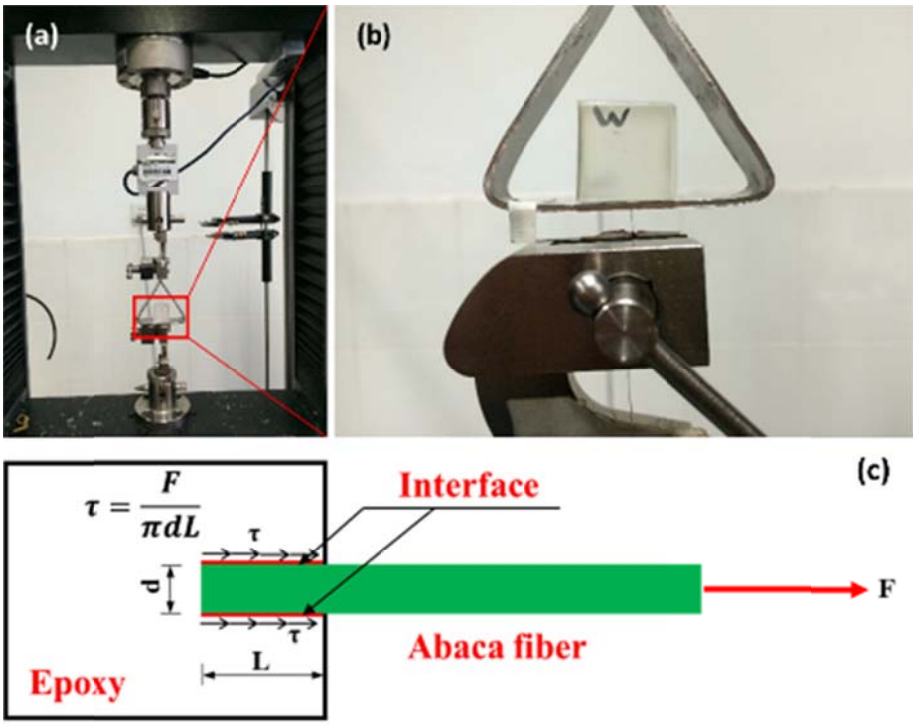

Figure 6.2 Pull-out test specimen of abaca-reinforced epoxy composite

The IFSS between the fiber and matrix material was calculated as follows [56, 97]:

Interfacial shear stress, $\tau = \frac{F_{max}}{\pi \times d \times L}$ (1)

where F_{max} is the maximum force recorded by the load cell, d is the diameter of the fiber, and L is the embedded length in the matrix.

6.4 Results and Discussion

6.4.1 Surface morphologies of alkali-treated abaca fibers

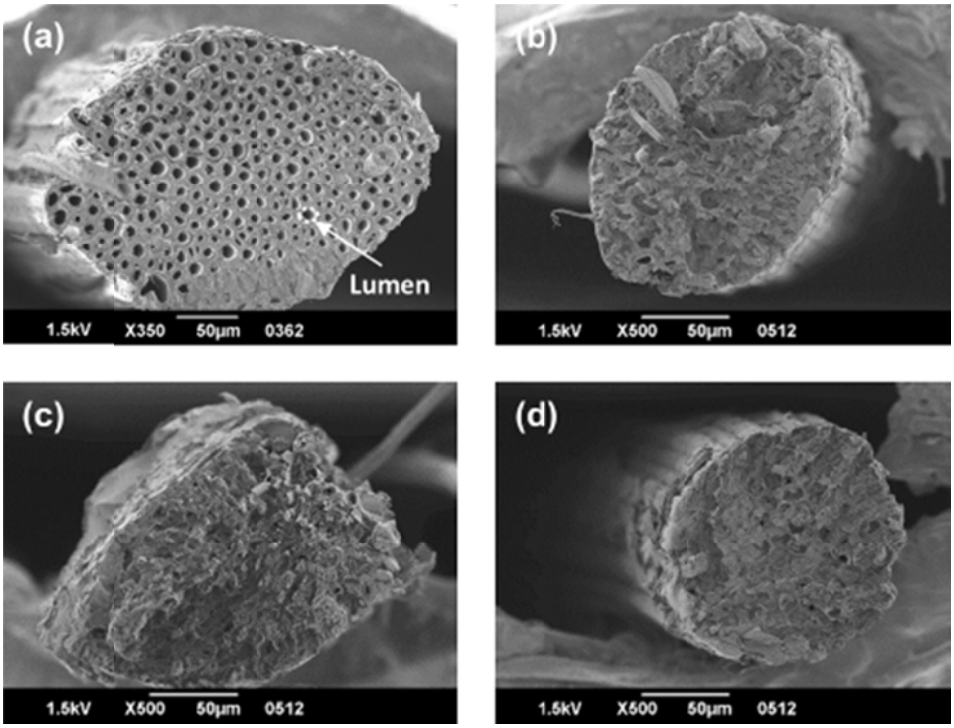

Figure 6.3 SEM images of fractured surfaces of abaca fiber bundles after tensile test: (a) untreated abaca fiber bundle; (b)-(d) abaca fiber bundles treated with 5, 10, and 15 wt. % NaOH solution for 2 h.

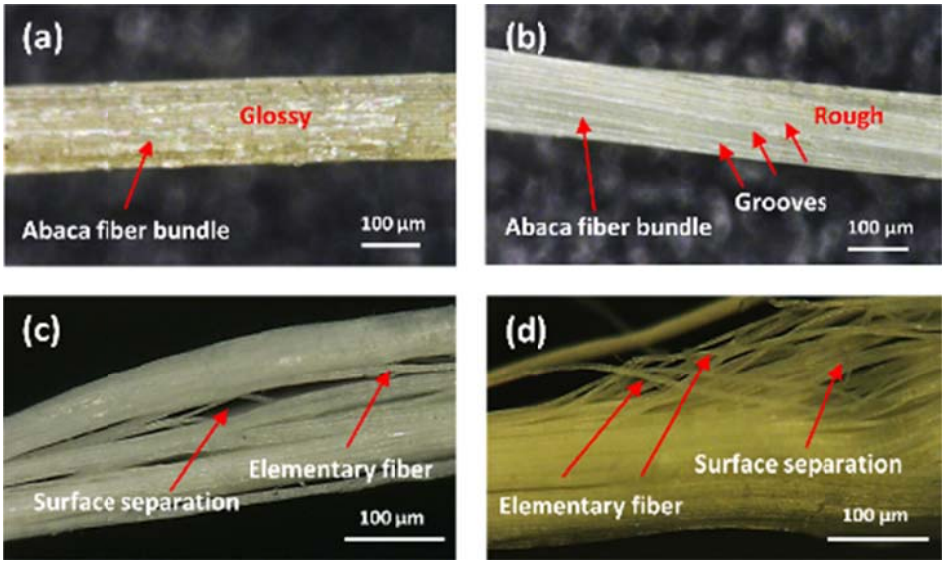

Figure 6.4 Digital images of the surface of the abaca fiber bundles: (a) untreated abaca fiber bundle, (b)-(d) abaca fiber bundles treated with 5, 10, and 15 wt. % NaOH solution for 2 h.

Untreated and alkali-treated abaca fibers cross sections are shown in Figure 6.3. In the cross section of the untreated fiber (Figure 6.3(a)), the hollow lumen is visible in the center of

every elementary fiber cell. The untreated fiber diameters were typically in the range of 250-300 μm. For the alkali-treated fibers (Figure 6.3(b)-(d)), the lumen had almost disappeared which may have been a consequence of fibers swelling or the lumen collapsing in the alkali solutions. Swelling agent is thought to result from the incorporation of sodium ions into the cellulose structure which breaks bonds between cellulose sheets [45, 71]. In addition, the fiber diameters were generally smaller following alkali treatment. The NaOH treatment of abaca fibers caused significant shrinkage and weight loss, as shown in Table 6.1. Both shrinkage and weight loss increased with increasing NaOH concentration. This may be a result of stripping of the lignin and hemicelluloses from the fibers in alkali solution [40, 90].

Table 6.1 Shrinkage and weight loss of alkali-treated abaca fibers.

NaOH concentration (wt. %)	**Average fiber diameter (μ m)**	**Cross section shrinkage (%)**	**Weight loss (%)**
0	270 ± 60	-	-
5	200 ± 40	36 ± 16	17.7
10	200 ± 30	47 ± 9	27.7
15	190 ± 50	44 ± 12	30.5

Figure 6.4 shows the surface morphology of untreated and alkali-treated abaca fibers. The untreated fiber consists of bundles of elementary fibers covered with binding components which are likely hemicelluloses, lignin, pectin and other substances (Figure 6.4(a)). In comparison the 5 wt. % NaOH treated fiber bundles were free of such surface material (Figure 6.4(b)) and appeared as bundles of slightly twisted fibers. The well-defined grooves between individual fibers in the bundles could be expected to aid adhesion with composite matrices. After 10 and 15 wt. % NaOH-treatments, most of the binding material between the individual fibers in the bundles was removed (Figure 6.4(c)-(d)), resulting in bundle fibrillation (breakdown of the fiber bundle into elementary fibers) [40, 90]. From images of Figure 6.4, it can be concluded that 10 and 15 wt. % NaOH alkali treatments compromise the integrity of the fiber bundles and induce twisting. Accordingly, 10 and 15 wt. % NaOH

treatments for 2 h were deemed unsuitable for treating abaca fibers for composite applications.

6.4.2 FT-IR analysis

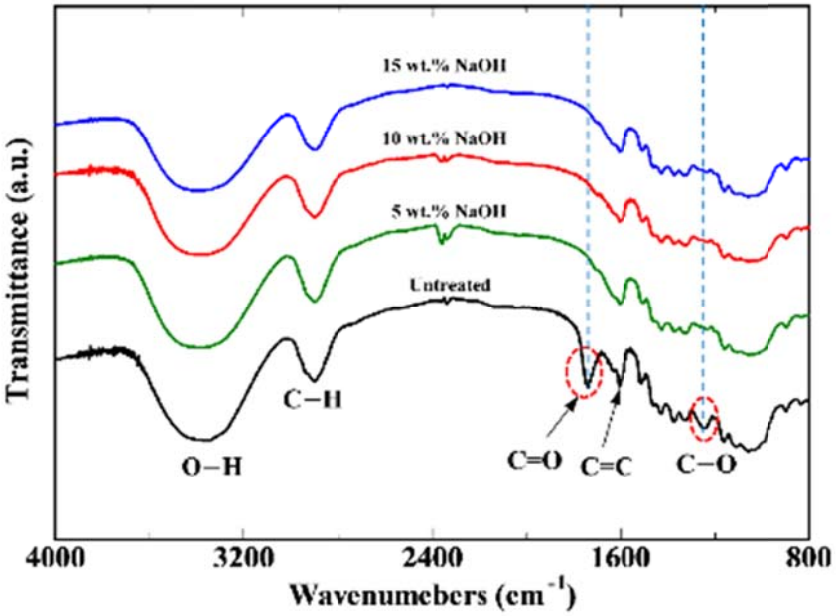

Figure 6.5 FT-IR spectra of untreated and alkali-treated abaca fiber bundles.

Figure 6.5 shows FT-IR transmittance spectra for the untreated and alkali-treated abaca fiber bundles. The spectra have been offset vertically for clarity. The FT-IR spectra for the abaca fibers treated with NaOH at concentrations of 5-15 wt.% were near identical, and were consistent with literature data reported for cellulose [18, 32, 65, 76, 78]. The cellulose peaks were also present in the spectrum of the untreated fiber, along with additional peaks at 1742 and 1242 cm^{-1} which are readily assigned to C=O and C-O stretching modes, respectively. The peak observed at 1742 cm^{-1} is characteristic for the carbonyl stretch of carboxylic groups in hemicelluloses and pectin. The peak at 1242 cm^{-1} can also be readily assigned to the C-O stretching mode of acetyl groups in lignin [76]. The disappearance of the 1742 cm^{-1} and 1242 cm^{-1} peaks after alkali treatment indicates that either the carboxylic acid and and acetyl groups were destroyed by the alkali treatment or the macromolecules containing these functional groups were selectively dissolved from the fiber bundles under strong alkali

conditions [77]. The latter scenario is supported by the SEM and optical images of Figure 6.3 and Figure 6.4, respectively, which showed that the binding materials around the primary fibers in the abaca bundles were removed by alkali treatment. Thus, differences in the FT-IR spectra between the untreated and alkali-treated abaca fibers (Figure 6.5) is attributed to the removal of the binding materials, such as hemicelluloses, pectin and lignin, from the abaca fiber bundle [98].

6.4.3 X-ray diffraction analyses of the abaca fibers

Cellulose crystallinity is an important characteristic of plant fibers. For composite applications, plant fibers with high cellulose crystallinity are demanded since the crystallinity correlates with fiber strength and stiffness. Any procedure used to prepare plant fibers for composite applications should not compromise the native cellulose crystallinity of the fibers. Cellulose is characterized by XRD peaks at 2θ = 15.5, 16.5 and 22.8º when using a Cu Kα X-ray source, corresponding to $(10\bar{1})$, (002) and (004) reflections, respectively. The (002) reflection is the major crystalline peak of cellulose I. The fiber crystallinity index (CrI) of abaca fiber was determined by using the Segal empirical method [99]. This method offers a quick and simple calculation of the crystallinity index using the following equation.

$$\mathrm{CrI} = \frac{(I_{002} - I_{am})}{I_{002}} \times 100$$

where I_{002} is the maximum intensity of the (002) crystalline peak and I_{am} is the minimum intensity of the amorphous material between $(10\bar{1})$ and (002) peaks as shown in Figure 6.6.

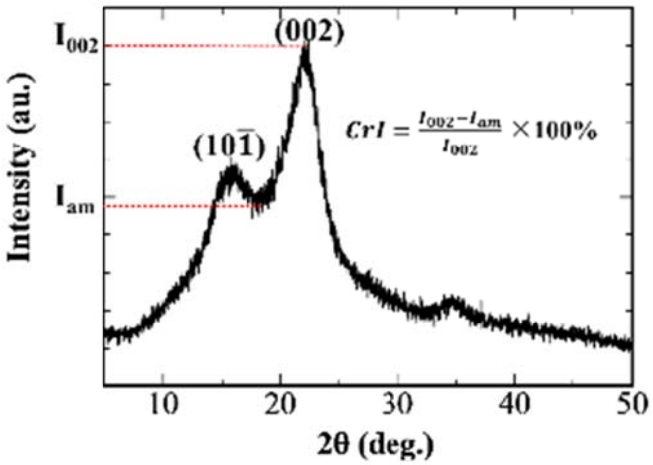

Figure 6.6 Determination of the degree of crystallinity of abaca fibers

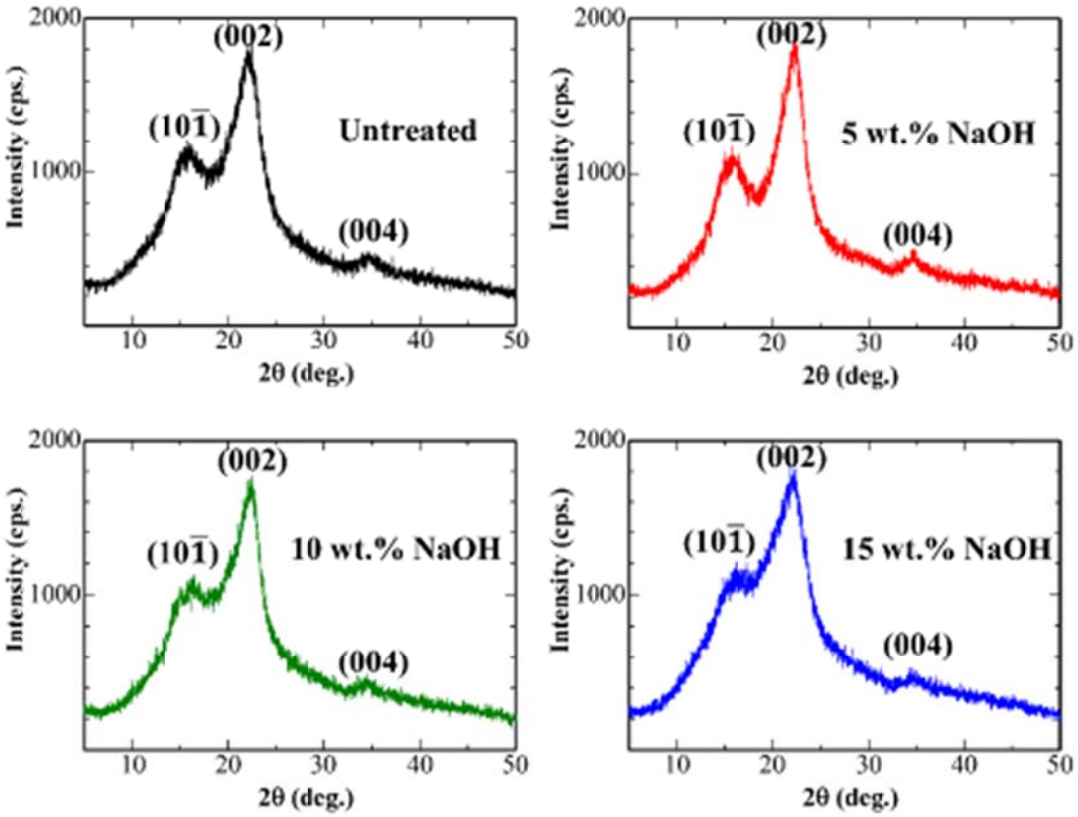

Figure 6.7 XRD diffractograms of the untreated and alkali-treated abaca fiber bundles.

X-ray diffraction patterns for untreated and alkali-treated abaca fiber are shown in Figure 6.7. The crystallinity indexes calculated for each sample from the XRD patterns are summarized in Table 6.2. The crystallinity indexes of untreated and 5, 10 and 15 wt. % NaOH treated

abaca fibers were approximately 52%, 58%, 50% and 47%, respectively. The data shows that the degree of crystallinity increased after 5 wt. % NaOH treatment, which is expected since this treatment removed hemicelluloses, lignin and other non-cellulosic material from the fiber bundles. At higher alkali concentrations, the cellulose fibers themselves may be attacked, resulting in a loss of structural conformation and crystallinity [100]. On the basis of the XRD data and calculated fiber crystallinity indices, it would appear that the fibers treated with 5 wt. % NaOH would be most suitable for composite applications.

Table 6.2 Mechanical properties of abaca fibers before and after NaOH treatment.

NaOH concentration (wt. %)	Crystallinity of cellulose (%)	Tensile strength (MPa)	Young's modulus (GPa)	Strain at break (%)
Untreated	52	720 ± 80	18.6 ± 1.9	4.2 ± 0.2
5	58	770 ± 120	25 ± 6	3.2 ± 0.5
10	50	680 ± 80	12 ± 3	9.9 ± 2.5
15	47	670 ± 26	9.4 ± 1.0	12.4 ± 1.2

6.4.4 Mechanical properties

The tensile properties of untreated and alkali-treated abaca fibers are summarized in Figure 6.8 and Table 6.2. The untreated abaca fiber had a tensile strength of 717 MPa and a Young's modulus of 18.6 GPa. After 5 wt. % NaOH treatment, the tensile strength of abaca fiber improved by ~8% and the Young's modulus by 36% with respect to the untreated abaca fiber. The strain at break decreased slightly following 5 wt. % NaOH treatment. The data is consistent with an increase in the stiffness and brittleness of the fiber after mild alkali treatment. The improvements in tensile strength and Young's modulus may result from improved ordering of cellulose crystalline chains along the fiber direction. Fibers treated with 10 and 15 wt. % NaOH maintained good tensile strength. However, the Young's modulus decreased by 34% and 49%, respectively. Interestingly, the strain at break increased by 136% and 200%, respectively, compared to the untreated abaca fiber. As hemicelluloses are leached out from the fibers, the cellulose chains in the fibers can adopt a more closely packed

arrangement, which explains the higher strain at break observed for the 10 and 15 wt. % NaOH treated fibers [90].

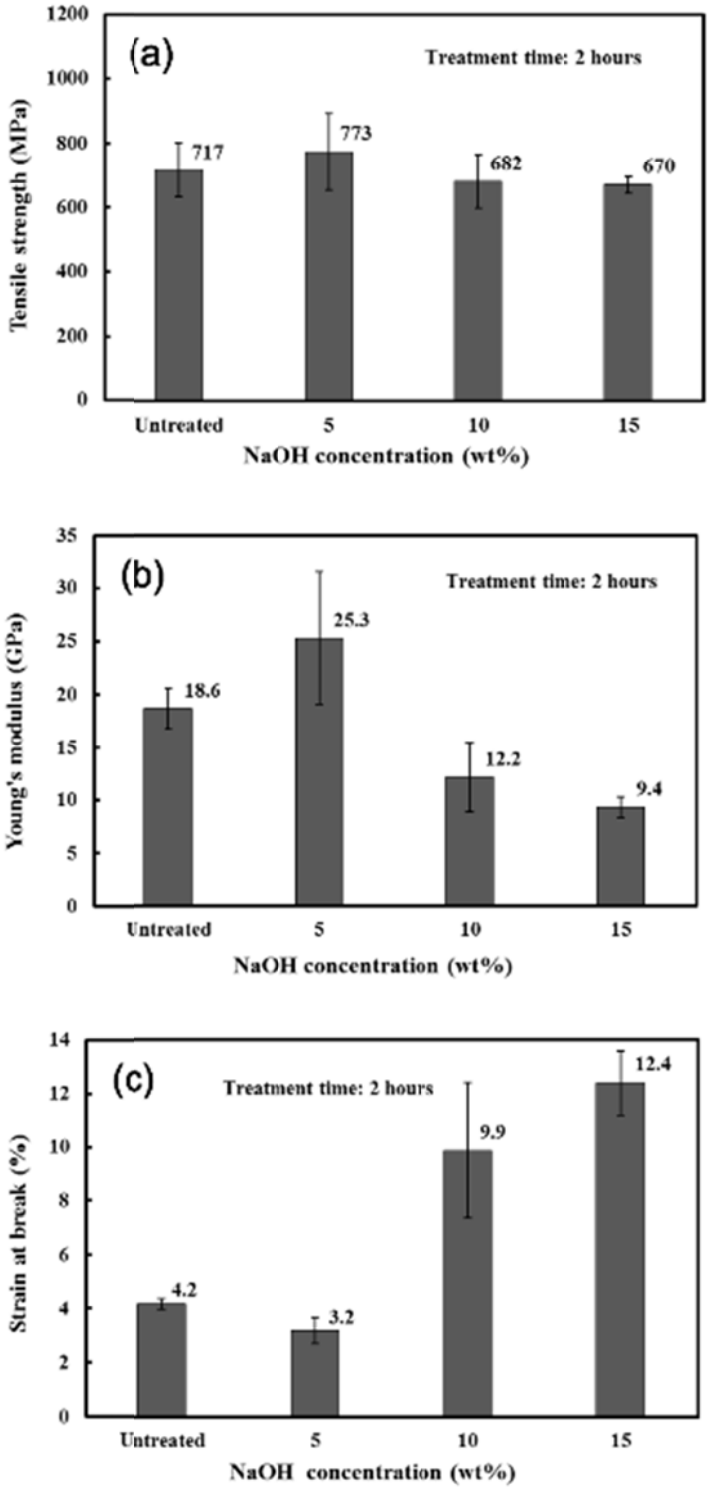

Figure 6.8 Mechanical properties of abaca fiber bundles before and after alkali treatment: (a) tensile strength, (b) Young's modulus, and (c) strain at break.

Figure 6.9 shows representative stress-strain curves for the untreated and alkali-treated (5, 10 and 15 wt. % NaOH) abaca fibers. Following 5 wt. % NaOH treatment, the stiffness of the fiber increased and toughness decreased compare to untreated fiber. The tensile curves for abaca fibers treated with 10 and 15 wt. % NaOH solution displayed non-linear behavior, showing an initial steep increase followed by a weaker linear increase with strain above 1.5%. The non-linear behavior may be the result of fiber twisting, which has been studied in detail in a previous work [40].

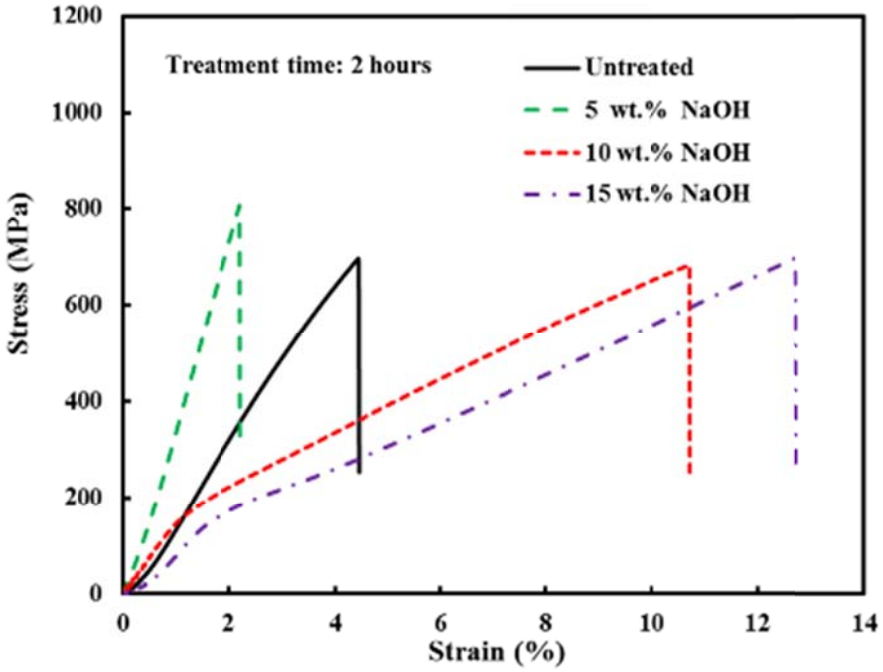

Figure 6.9 Tensile stress-strain curves of abaca fiber bundles before and after alkali treatment.

6.4.5 Structure of abaca fiber reinforced epoxy composite

Abaca fiber reinforced epoxy composites were prepared to examine the effect of the different alkali treatments on the interfacial bonding characteristics of the fibers. Figure 6.10 shows representative SEM micrographs for the abaca fiber-epoxy composites following the pull-out tests described in section 6.3.6.

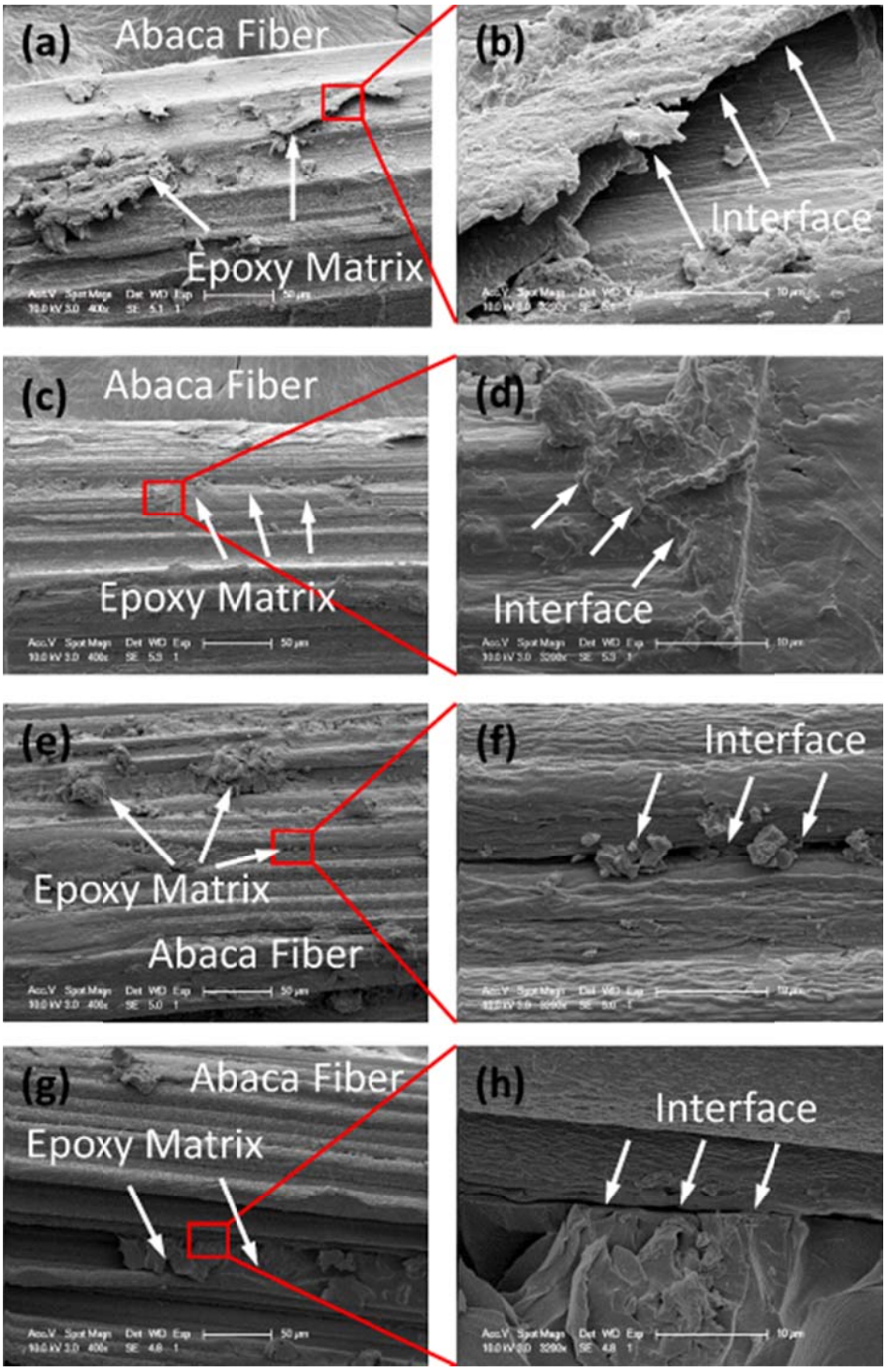

Figure 6.10 SEM images of abaca fiber reinforced epoxy matrix after pull-out tests. (a) and (b) untreated, (c) and (d) 5 wt. % NaOH, (e) and (f) 10 wt. % NaOH, and (g) and (h) 15 wt. % NaOH solution-treated.

The SEM images show that the bonding of the epoxy to the fibers differs considerably depending on the fiber pretreatment. For composites prepared using untreated fibers, visible gaps can be seen between fiber and epoxy matrix (Figure 6.10(a) and (b)), suggesting poor

interfacial adhesion. This presumably arises because of the incompatibility between hydrophilic fibers and hydrophobic epoxy matrix, and is probably compounded further by the presence of the impurities and topographical irregularities on the abaca fiber surface (as shown in Figure 6.4(a)). This was supported by the fact that the untreated abaca fiber could be easily pulled out of the epoxy matrix with little resistance. For composites prepared using 5 wt. % NaOH treated abaca fibers, excellent interfacial bonding between the epoxy resin and abaca fiber was observed (Figure 6.10(c) and (d)). In Figure 6.4(b), it was observed that 5 wt. % NaOH treatment yielded abaca fibers with clean and roughness surfaces (Figure 6.4(b)) that resulted in a better mechanical interlocking, which clearly presents a more suitable substrate for the epoxy adhesion than the untreated fibers. Fibers treated at higher NaOH concentrations twisted and fibrillated, which reduced epoxy adhesion. Figure 6.10 (e) - (h), show that fibrillation creates gaps between the individual fibers in each bundle. Epoxy binds well to each fiber, but poorly across such gaps, resulting in an overall poor epoxy adhesion to the fiber bundle.

6.4.6 Interfacial shear strength measurement

The single fiber pull-out test was used to quantify the interfacial adhesion between the abaca fibers and the epoxy matrix. Figure 6.11 (a) shows the relationship between the peak force and the embedded abaca fiber surface areas. After applying a linear regression to the plots, passing through the origin, IFSS was calculated from the slopes ($\tau = F/A$, where F is the peak force, and A is the embedded fiber surface area).

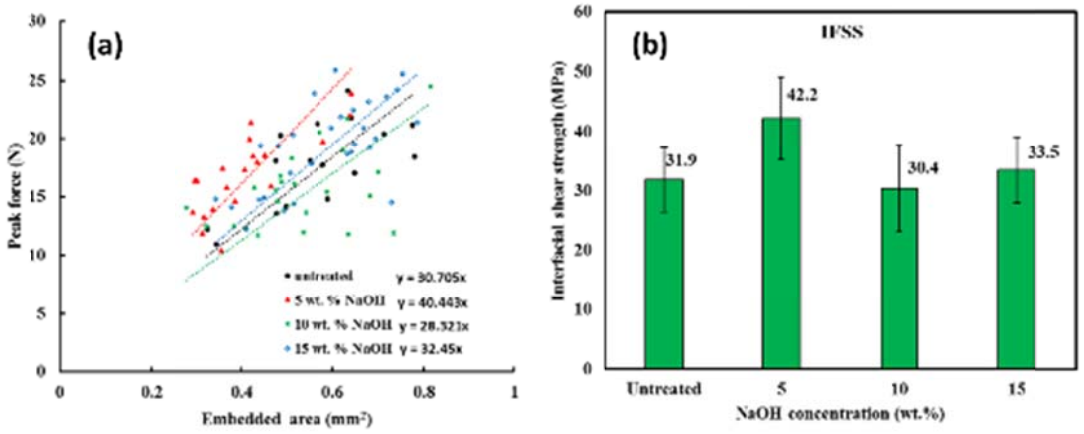

Figure 6.11 Interfacial shear strength of untreated and alkali-treated abaca fiber reinforced epoxy composites.

Figure 6.11 (b) shows IFSS values determined for untreated and alkali-treated abaca fibers. It can be seen that the IFSS of 5 wt. % NaOH treated fiber-reinforced epoxy composites was considerably higher than that of the untreated group. The average IFSS value of 42.2 MPa obtained for the abaca fiber treated with 5 wt. % NaOH was 32% higher than that of untreated fiber. There are two possible reasons. In the first case, the fiber surface became cleaner and rougher by 5 wt. % alkali treatment which resulted in a better mechanical interlocking for the composites (Figure 6.10(c) and (d)). In another case, the fiber is subjected to an axial force and this results in a Poisson contraction in the radial direction and the normal radial stress on the fiber resulting from matrix shrinkage may be reduced [101]. However, IFSS for 10 and 15 wt. % NaOH treated fiber-reinforced epoxy composites were almost the same as that of composites prepared using untreated abaca fibers. It is because the high alkali concentration treatment led to the fibrillation and increases the defects in the composite. The data clearly indicates that 5 wt. % NaOH is the near optimum concentration to maximize the IFSS of abaca fiber-reinforced epoxy composites [102,103].

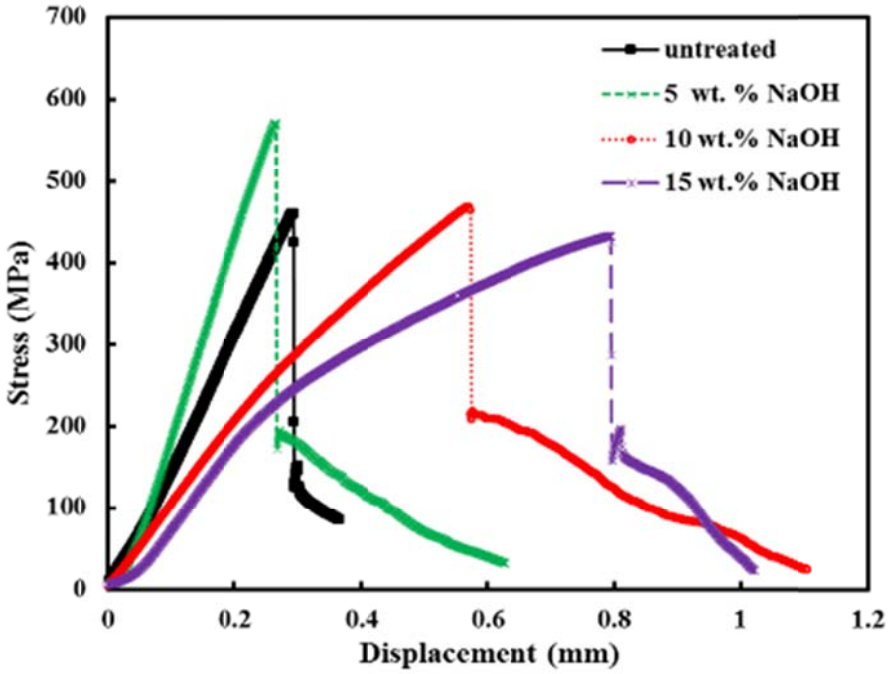

Figure 6.12 Typical stress-displacement curves from pull-out tests for untreated and alkali-treated abaca fiber-reinforced epoxy composites.

Representative stress-displacement curves obtained from the single fiber pull-out tests for the untreated and alkali-treated abaca fiber reinforced epoxy composites are shown in Figure 6.12. All the samples show the same general behavior, which can be described by an initial increase with stress to a maximum, where the fiber de-bonds along the full embedded length from the matrix, followed by a sudden drop to a lower stress value [101]. In the post drop region, the fiber is simply sliding along a hole in the epoxy matrix until the fiber is completely pulled out of epoxy matrix. The 5 wt. % NaOH treated abaca fiber epoxy composite shows far higher interfacial shear strength compared with the other composites. This can be attributed to the high roughness of 5 wt. % NaOH -treated fiber surface leading to better interfacial fiber-matrix bond. However, high alkali concentrations (10 and 15 wt. % NaOH) were not beneficial in improving the IFSS, for reasons evident in Figure 6.4 and Figure 6.10 relating to fiber fibrillation and subsequently poor adhesion with the epoxy matrix.

6.5 Conclusions

Alkali treatments modify the structure and chemical composition of abaca fibers, with the degree of modification increasing with alkali concentration. Immersion of abaca fibers in 5-15 wt. % NaOH solution for 2 h results in solubilization of hemicelluloses and lignin from abaca fibers, and changes the internal structure and surface morphology of the fibers. Abaca fiber bundles treated in 5 wt. % NaOH showed high cellulose crystallinity and minimal fibrillation, and displayed excellent interfacial adhesion with epoxy resin. Higher NaOH concentrations decreased the cellulose crystallinity and caused fibrillation of the abaca fiber bundles, which along with possible further surface chemistry changes to the fibers weakened the adhesion with the epoxy resin. Results suggest that low concentration alkali treatments are highly beneficial for improving the surface properties and performance of abaca fibers for advanced composite applications.

Chapter 7 Conclusions and Suggestions for Future Work

7.1 Concluding remarks

This thesis studied the effects of different alkali treatments on the microstructure and mechanical properties of abaca fibers. Their chemical composition and crystalline structures relate to alkali treatment. The major results and salient conclusions are summarized below:

1. Alkali treatments modify the microstructure and tensile properties of abaca fibers, with the degree of modification increasing with alkali concentration. Immersion of abaca fibers in 3 - 15 wt. % alkali solution for 5 min. resulted in the lumen size decreased with increasing alkali concentration above 7 wt. %. Meanwhile, the mechanical properties increased after alkali treatments. Young's modulus and tensile strength reached the highest value after 7 wt. % NaOH treatment for 5 min.

2. The effect of alkali treatment time on the microstructure and tensile properties of abaca fibers was investigated. Immersion of abaca fiber in 5, 10 and 15 wt. % alkali solutions for 5, 10, 15, 20, 25, 30 min. resulted in the lumen size decreased with increasing alkali concentration and treatment time. Moreover, the tensile strength increased slightly after 5 and 10 wt. % and maintained after 15 wt.% alkali treatment. The Young's modulus increased after 5 wt. % and decreased after 10 and 15 wt.% alkali treatments. The strain at break decreased after 5 wt. % and remarkably increased after 10 and 15 wt.% alkali treatments. The effect of treatment time is not evident compared to the effect of alkali concentration.

3. The mechanism of the effect of alkali treatment on the microstructure and mechanical properties was analyzed. Immersion of abaca fiber in 5, 10, and 15 wt. % alkali solutions for 30 min. resulted in the cross- sectional area of abaca fiber bundles decreasing significantly with alkali treatment, which can be attributed to collapse of the lumen through the swelling of the cellulose microfibrils, and also the solubilisation of lignin, hemicelluloses, and pectins in

the native fibers. The chemical components such as pectin, lignin, and hemicelluloses were removed from the abaca fiber by alkali treatments. In addition, the abaca fiber bundles become twisted with strong alkali treatment (10 and 15 wt. % NaOH). Alkali treatment affects the tensile properties of the abaca fiber bundles. After strong alkali treatment (10 or 15 wt.% NaOH), the associated fiber twisting and softening resulted in non-linear stress-strain behavior, a lower Young's modulus and higher strain at break, compared to untreated abaca fibers. The tensile strength of abaca fiber bundles did not significantly change with alkali concentration (0, 5, 10 or 15 wt. % NaOH). However, both the Young's modulus and the strain at break were dependent on the alkali concentration.

4. The interfacial adhesion of the abaca fiber reinforced epoxy using alkali treated fibers was assessed. Abaca fiber bundles treated in 5 wt. % NaOH showed high cellulose crystallinity and minimal fibrillation, and displayed excellent interfacial adhesion with epoxy resin. Higher NaOH concentrations decreased the cellulose crystallinity and caused fibrillation of the abaca fiber bundles, which along with possible further surface chemistry changes to the fibers weakened the adhesion with the epoxy resin. Results suggest that low concentration alkali treatments are highly beneficial for improving the surface properties and performance of abaca fibers for advanced composite applications.

7.2 Suggestions for future work

Although the research completed in the current investigation has successfully demonstrated in this project, it is still recognized that there are some investigations in the field of alkali modification of abaca fiber-reinforced composites that requires further studies in the future.

Further efforts to understand the role of interfaces on composite properties will require additional quantitative characterization work on the interface properties of composites. It could contribute to establish a suitable multi-scale mechanical model that can accurately

predict bulk mechanical properties of composites with the consideration of macroscopic and microcosmic interface adhesion.

The microscopic characterization of abaca fiber structure can be conducted using advanced analytical techniques such as atomic force microscopy (AFM) and nanoindentation. The macroscopic characterization of abaca fiber-reinforced composites can be investigated by tensile, bending and interlaminar shear tests.

In addition, it is important to understand the effects of interface adhesion on durability and long-term mechanical behavior of composites, such as hydrothermal ageing and fatigue properties. Furthermore, advances in recyclability and better accounting of a variety of life cycle cost options for natural fiber composites for high-value applications.

Appendix

Appendix of Chapter 3

This section contains additional results in detail.

Stress-strain curves of untreated and alkali-treated abaca fibers

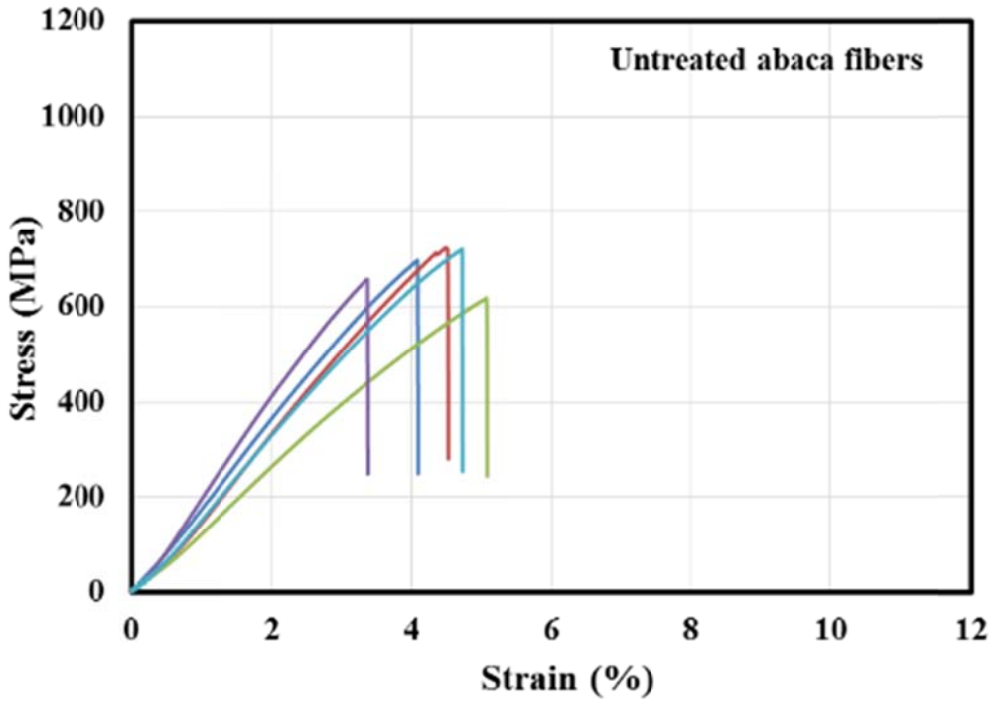

Figure 1 Stress-strain curves of untreated abaca fibers.

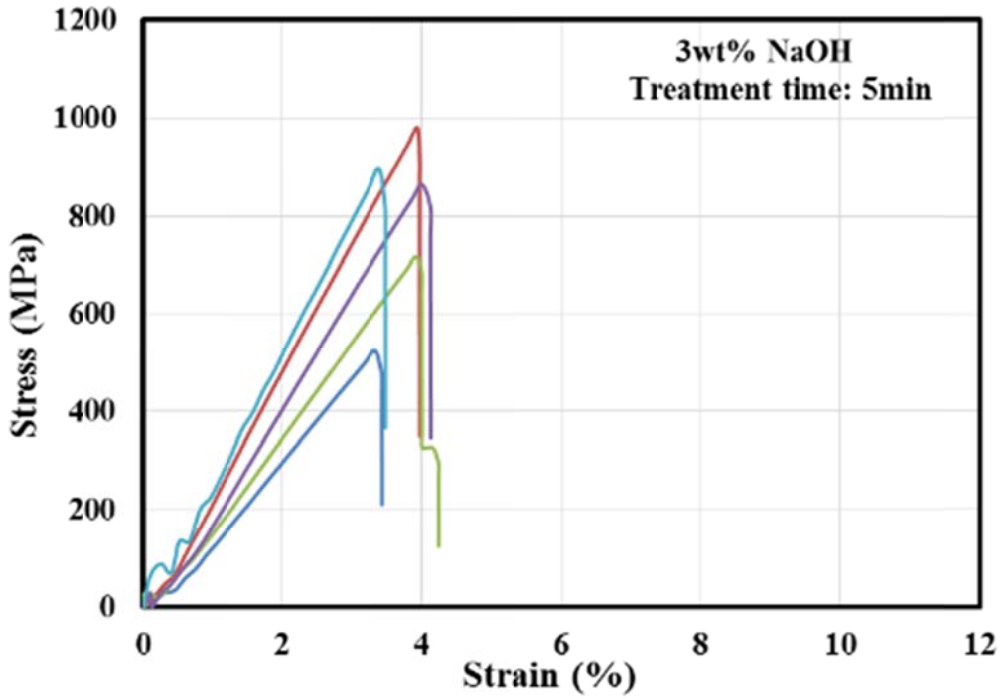

Figure 2 Stress-strain curves of 3 wt. % NaOH-treated abaca fibers.

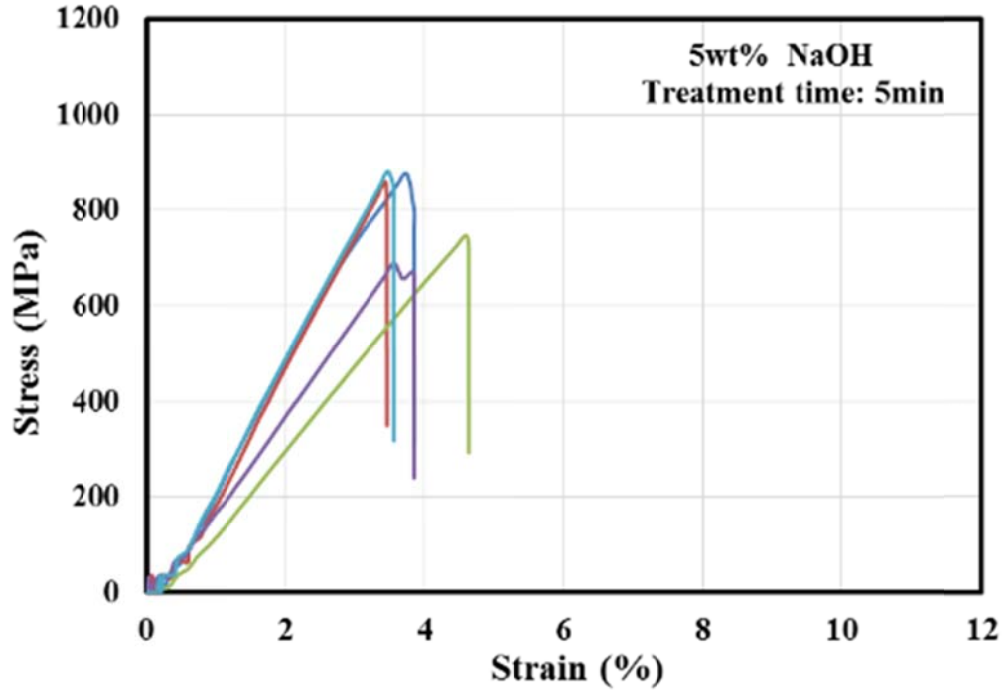

Figure 3 Stress-strain curves of 5 wt. % NaOH-treated abaca fibers.

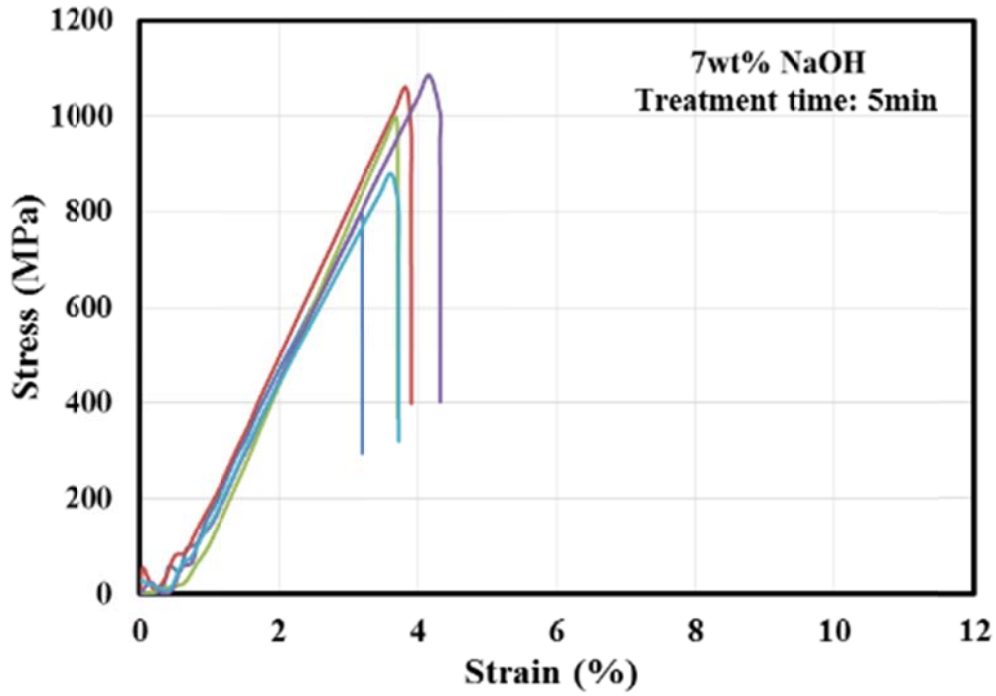

Figure 4 Stress-strain curves of 7 wt. % NaOH-treated abaca fibers.

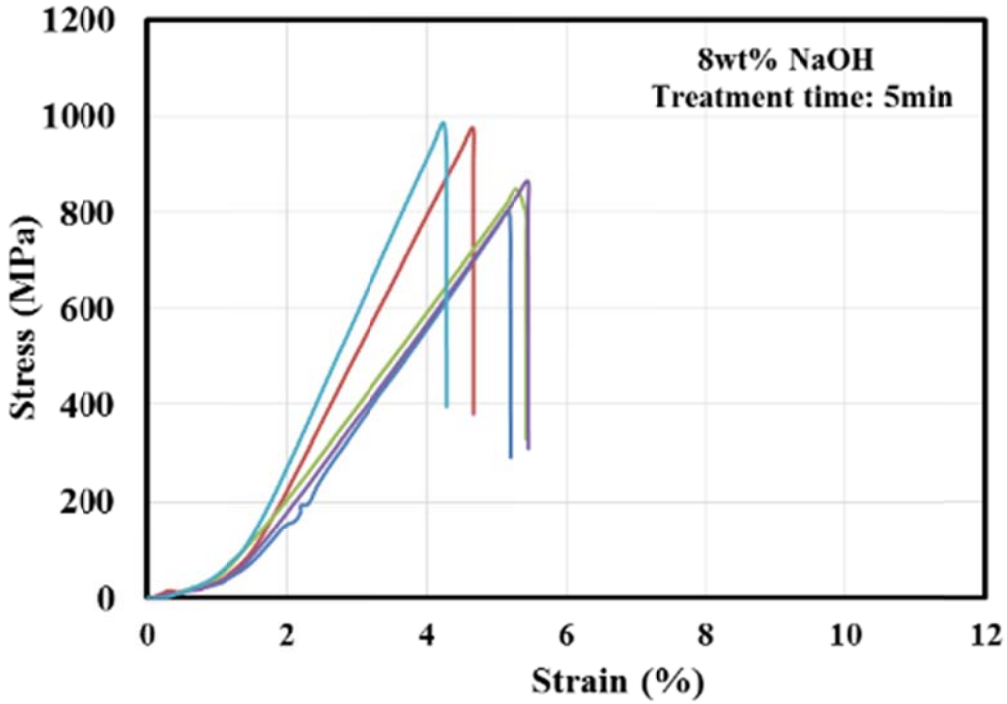

Figure 5 Stress-strain curves of 8 wt. % NaOH-treated abaca fibers.

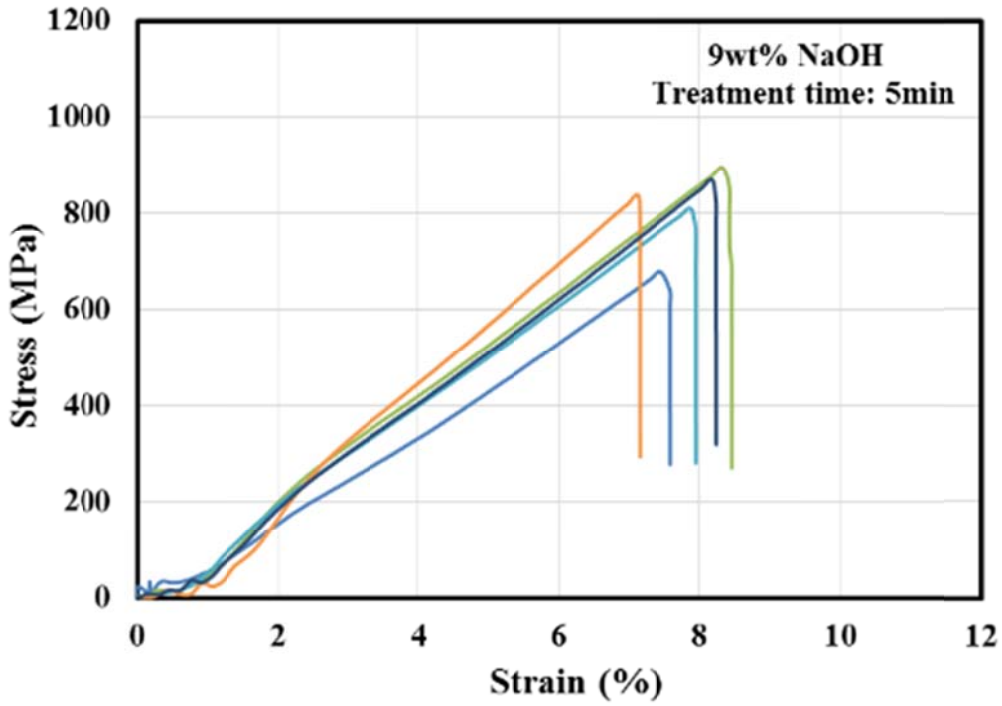

Figure 6 Stress-strain curves of 9 wt. % NaOH-treated abaca fibers.

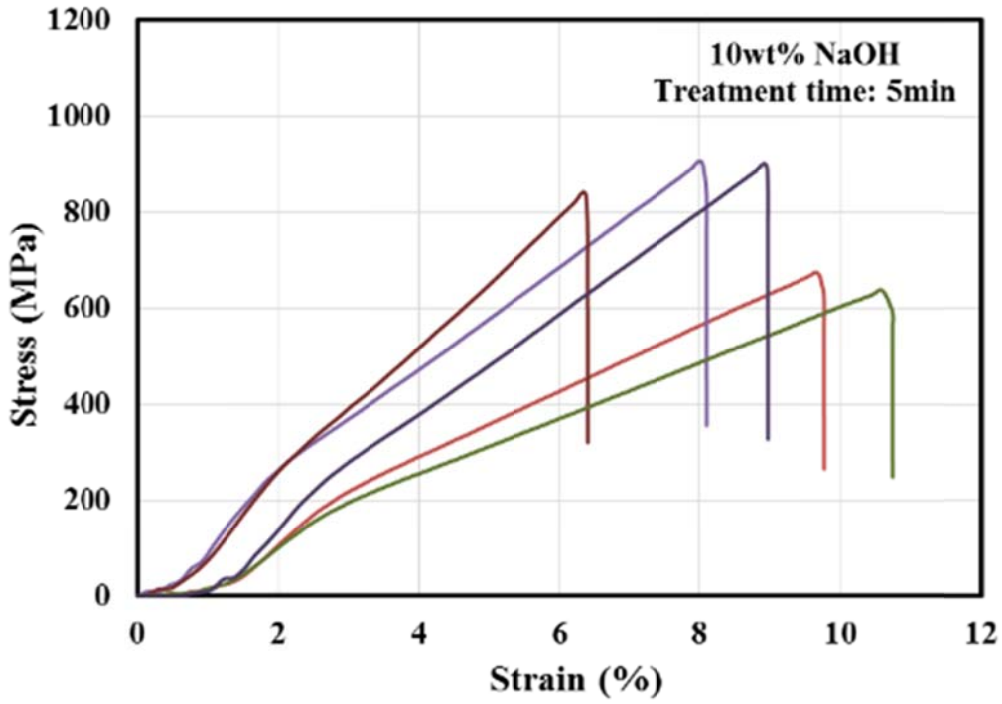

Figure 7 Stress-strain curves of 10 wt. % NaOH-treated abaca fibers.

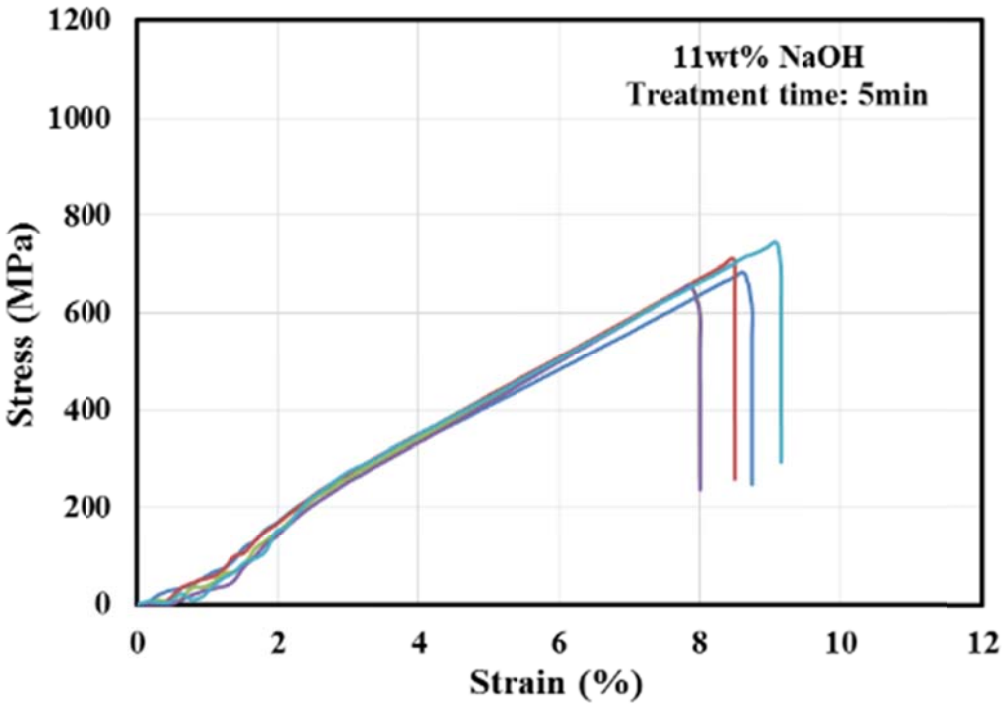

Figure 8 Stress-strain curves of 11 wt. % NaOH-treated abaca fibers.

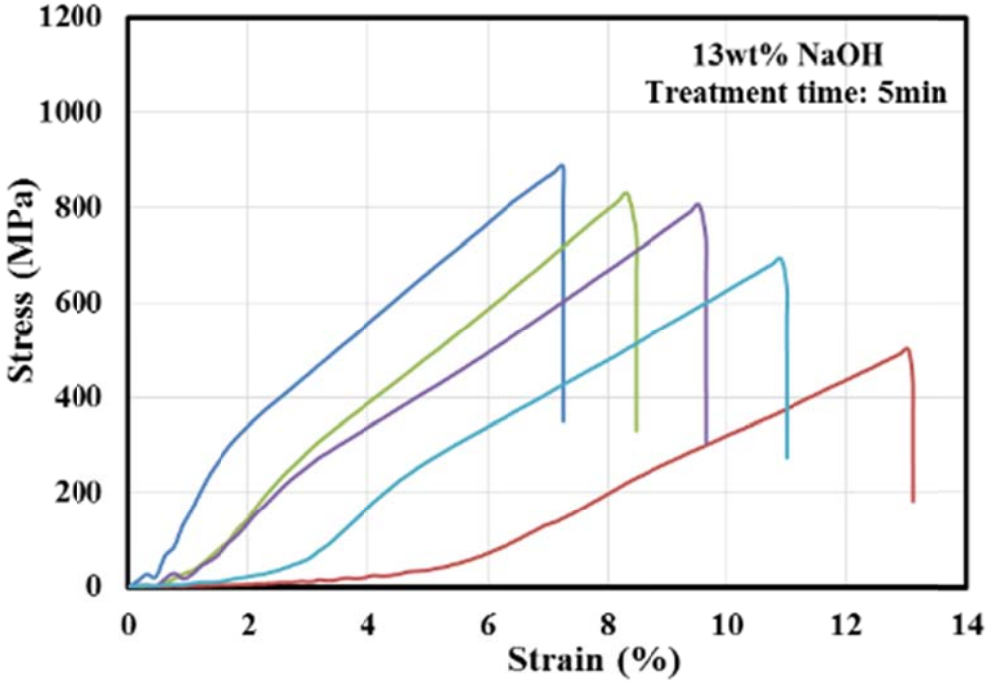

Figure 9 Stress-strain curves of 13 wt. % NaOH-treated abaca fibers.

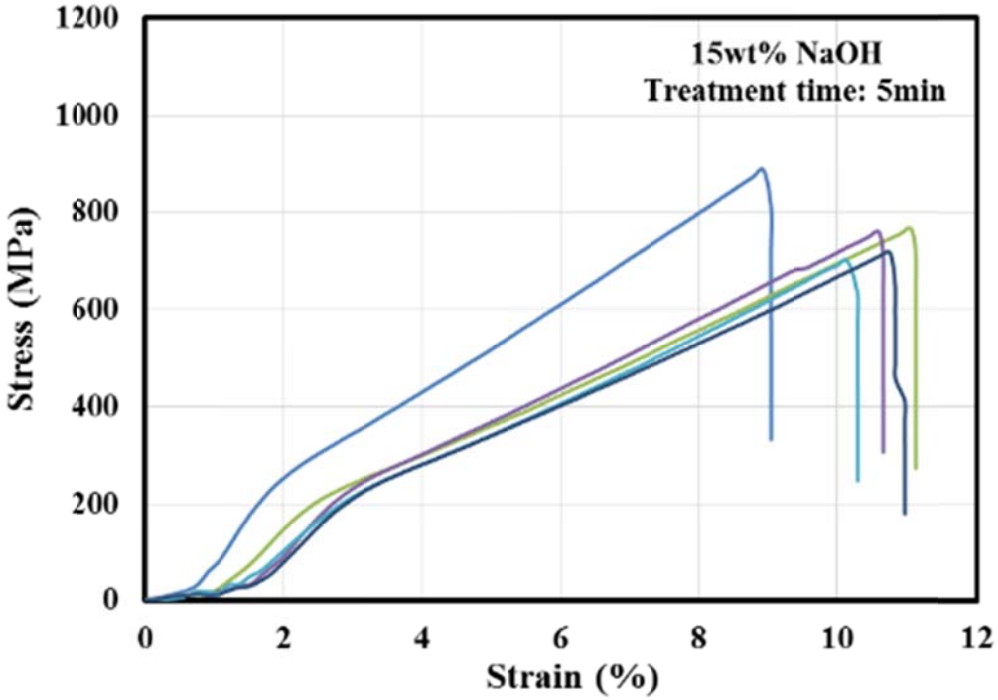

Figure 10 Stress-strain curves of 15 wt. % NaOH-treated abaca fibers.

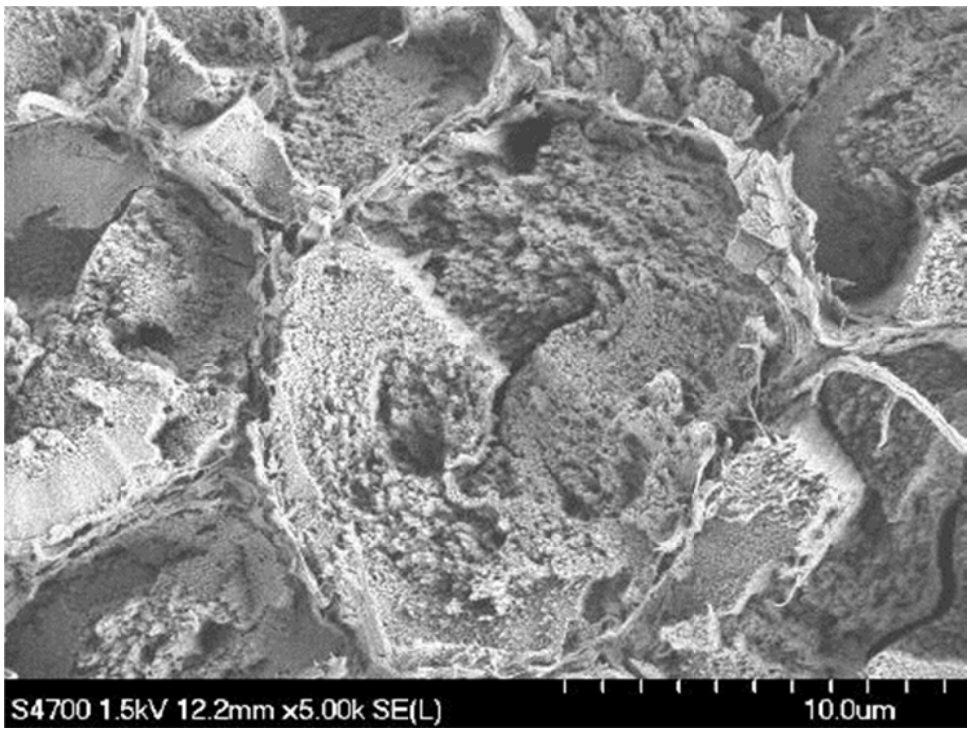

Figure 11 SEM of 10 wt. % NaOH-treated abaca fibers after washing for 1hour.

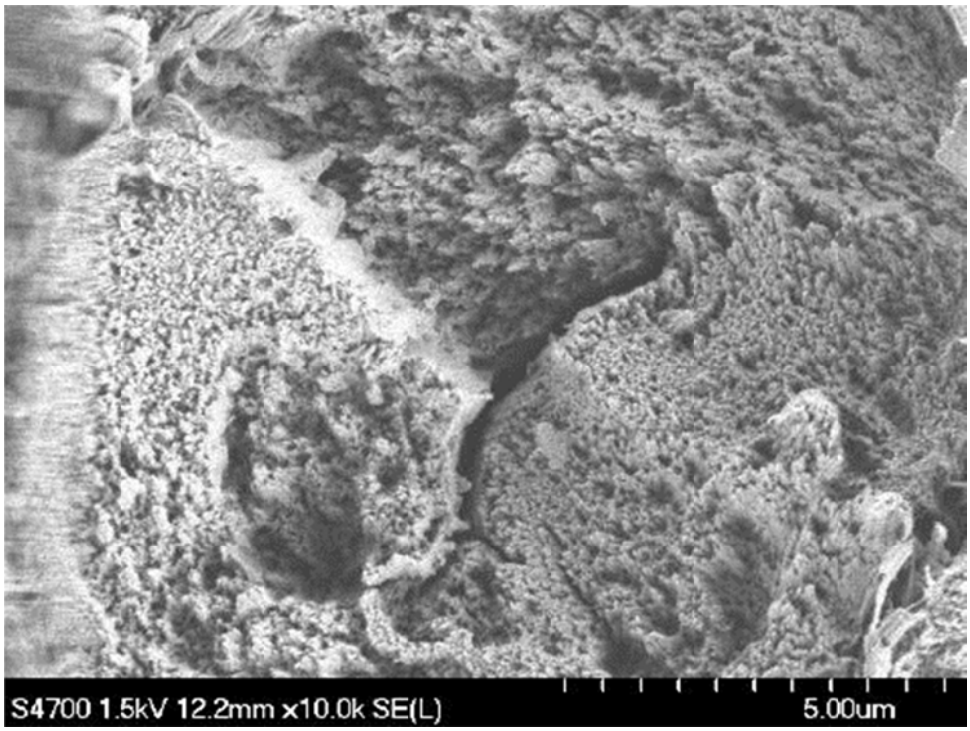

Figure 12 SEM of 10 wt. % NaOH-treated abaca fibers after washing for 1hour.

References

[1] Takagi H, Asano A. Effects of processing conditions on flexural properties of cellulose nanofiber reinforced “green” composites. Composites Part A: Applied Science and Manufacturing. 2008;39(4):685-9.
[2] Yan Li Y-WM, Lin Ye. Sisal fibre and its composites a review of recent developments.pdf. Composites Science and Technology. 2000;60(11):18.
[3] Thakur VK, Thakur MK. Processing and characterization of natural cellulose fibers/thermoset polymer composites. Carbohydr Polym. 2014;109:102-17.
[4] Thakur VK, Thakur MK. Recent trends in hydrogels based on psyllium polysaccharide: a review. Journal of Cleaner Production. 2014;82:1-15.
[5] Pandey JK, Ahn SH, Lee CS, Mohanty AK, Misra M. Recent Advances in the Application of Natural Fiber Based Composites. Macromolecular Materials and Engineering. 2010;295(11):975-89.
[6] Zhang Y, Li Y, Ma H, Yu T. Tensile and interfacial properties of unidirectional flax/glass fiber reinforced hybrid composites. Composites Science and Technology. 2013;88:172-7.
[7] Liu K, Takagi H, Osugi R, Yang Z. Effect of physicochemical structure of natural fiber on transverse thermal conductivity of unidirectional abaca/bamboo fiber composites. Composites Part A: Applied Science and Manufacturing. 2012;43(8):1234-41.
[8] Holbery J, Houston D. Natural-fiber-reinforced polymer composites in automotive applications. Jom. 2006;58(11):80-6.
[9] Gurunathan T, Mohanty S, Nayak SK. A review of the recent developments in biocomposites based on natural fibres and their application perspectives. Composites Part A: Applied Science and Manufacturing. 2015;77:1-25.
[10] Sangappa, Rao BL, Asha S, Kumar RM, Somashekar R. Physical, chemical, and surface properties of alkali-treated Indian hemp fibers. Composite Interfaces. 2014;21(2):153-9.
[11] Liu L, Yu J, Cheng L, Qu W. Mechanical properties of poly(butylene succinate) (PBS) biocomposites reinforced with surface modified jute fibre. Composites Part A: Applied Science and Manufacturing. 2009;40(5):669-74.
[12] Munawar SS, Umemura K, Kawai S. Characterization of the morphological, physical, and mechanical properties of seven nonwood plant fiber bundles. Journal of Wood Science. 2007;53(2):108-13.
[13] Kabir M, Wang H, Aravinthan T, Cardona F, Lau K-T. Effects of natural fibre surface on composite properties: A review. Proceedings of the 1st International Postgraduate Conference on Engineering, Designing and Developing the Built Environment for Sustainable Wellbeing (eddBE2011): Queensland University of Technology; 2011. p. 94-9.
[14] Kalia S, Kaith B, Kaur I. Pretreatments of natural fibers and their application as reinforcing material in polymer composites—a review. Polymer Engineering & Science. 2009;49(7):1253-72.
[15] Liu K, Takagi H, Osugi R, Yang Z. Effect of lumen size on the effective transverse thermal conductivity of unidirectional natural fiber composites. Composites Science and Technology. 2012;72(5):633-9.
[16] Li X, Tabil LG, Panigrahi S. Chemical treatments of natural fiber for use in natural fiber-reinforced composites: a review. Journal of Polymers and the Environment. 2007;15(1):25-33.
[17] Kumar SP, Sharma S. Effect of alkali treatment on jute fibre composites 2007.
[18] Mwaikambo LY, Ansell MP. Chemical modification of hemp, sisal, jute, and kapok fibers by alkalization. Journal of Applied Polymer Science. 2002;84(12):2222-34.

[19] Marais S, Gouanvé F, Bonnesoeur A, Grenet J, Poncin-Epaillard F, Morvan C, et al. Unsaturated polyester composites reinforced with flax fibers: effect of cold plasma and autoclave treatments on mechanical and permeation properties. Composites Part A: Applied Science and Manufacturing. 2005;36(7):975-86.
[20] Venkateshwaran N, Perumal AE, Arunsundaranayagam D. Fiber surface treatment and its effect on mechanical and visco-elastic behaviour of banana/epoxy composite. Materials & Design. 2013;47:151-9.
[21] Wu C-S, Liao H-T. The mechanical properties, biocompatibility and biodegradability of chestnut shell fibre and polyhydroxyalkanoate composites. Polymer Degradation and Stability. 2014;99:274-82.
[22] Manalo AC, Wani E, Zukarnain NA, Karunasena W, Lau K-t. Effects of alkali treatment and elevated temperature on the mechanical properties of bamboo fibre-polyester composites. Composites Part B: Engineering. 2015.
[23] Gassan J, Bledzki AK. Possibilities for improving the mechanical properties of jute/epoxy composites by alkali treatment of fibres. Composites Science and Technology. 1999;59(9):1303-9.
[24] Rong MZ, Zhang MQ, Liu Y, Yang GC, Zeng HM. The effect of fiber treatment on the mechanical properties of unidirectional sisal-reinforced epoxy composites. Composites Science and Technology. 2001;61(10):1437-47.
[25] Ilomäki KM. Adhesion between natural fibers and thermosets. 2012.
[26] Chen C, Li Y, Yu T. Interlaminar toughening in flax fiber-reinforced composites interleaved with carbon nanotube buckypaper. Journal of Reinforced Plastics and Composites. 2014;33(20):1859-68.
[27] Kabir M, Wang H, Lau K, Cardona F. Chemical treatments on plant-based natural fibre reinforced polymer composites: An overview. Composites Part B: Engineering. 2012;43(7):2883-92.
[28] Bledzki AK, Gassan J. Composites reinforced with cellulose based fibres. Progress in Polymer Science. 1999;24:221-74.
[29] Wang B. Pretreatment of flax fibers for use in rotationally molded composites. Unpublished masters thesis Saskatoon, SK: Department of Agriculture and Bioresource Engineering, University of Saskatchewan. 2004.
[30] George J, Sreekala M, Thomas S. A Review on Interface Modification and Characterization. Polymer engineering and science. 2001;41(9).
[31] Hill CA, Khalil HA, Hale MD. A study of the potential of acetylation to improve the properties of plant fibres. Industrial Crops and Products. 1998;8(1):53-63.
[32] Punyamurthy R, Sampathkumar D, Srinivasa CV, Bennehalli B. Effect of alkali treatment on water absorption of single cellulosic abaca fiber. BioResources. 2012;7(3):3515-24.
[33] Bledzki AK, Faruk O, Sperber VE. Cars from Bio-Fibres. Macromolecular Materials and Engineering. 2006;291(5):449-57.
[34] Mamun AA, Heim HP, Faruk O, Bledzki AK. 8 - The use of banana and abaca fibres as reinforcements in composites. In: Faruk O, Sain M, editors. Biofiber Reinforcements in Composite Materials: Woodhead Publishing; 2015. p. 236-72.
[35] La Mantia F, Morreale M. Green composites: A brief review. Composites Part A: Applied Science and Manufacturing. 2011;42(6):579-88.
[36] Houston JHaD. natural fiber in the automotive.pdf. JOM-US. 2006;11:6.
[37] Takagi H, Liu K, Osugi R, Nakagaito AN, Yang Z. Heat Barrier Properties of Green Composites. Journal of Biobased Materials and Bioenergy. 2012;6(4):470-4.
[38] Gassan J, Bledzki AK. Alkali treatment of jute fibers: relationship between structure and mechanical properties. Journal of Applied Polymer Science. 1999;71(4):623-9.

[39] Van de Weyenberg I, Ivens J, De Coster A, Kino B, Baetens E, Verpoest I. Influence of processing and chemical treatment of flax fibres on their composites. Composites Science and Technology. 2003;63(9):1241-6.
[40] Cai M, Takagi H, Nakagaito AN, Katoh M, Ueki T, Waterhouse GIN, et al. Influence of alkali treatment on internal microstructure and tensile properties of abaca fibers. Industrial Crops and Products. 2015;65:27-35.
[41] Gomes A, Matsuo T, Goda K, Ohgi J. Development and effect of alkali treatment on tensile properties of curaua fiber green composites. Composites Part A: Applied Science and Manufacturing. 2007;38(8):1811-20.
[42] Boopathi L, Sampath PS, Mylsamy K. Investigation of physical, chemical and mechanical properties of raw and alkali treated Borassus fruit fiber. Composites Part B: Engineering. 2012;43(8):3044-52.
[43] Mylsamy K, Rajendran I. Investigation on physio-chemical and mechanical properties of raw and alkali-treated Agave americana fiber. Journal of Reinforced Plastics and composites. 2010;29(19):2925-35.
[44] Sghaier S, Zbidi F, Zidi M. Characterization of Doum palm fibers after chemical treatment. Textile Research Journal. 2009;79(12):1108-14.
[45] John MJ, Anandjiwala RD. Recent developments in chemical modification and characterization of natural fiber ‐ reinforced composites. Polymer composites. 2008;29(2):187-207.
[46] Kobayashi K, Kimura S, Togawa E, Wada M. Crystal transition from Na–cellulose IV to cellulose II monitored using synchrotron X-ray diffraction. Carbohydrate Polymers. 2011;83(2):483-8.
[47] Ishikura Y, Abe K, Yano H. Bending properties and cell wall structure of alkali-treated wood. Cellulose. 2010;17(1):47-55.
[48] Ishikura Y, Nakano T. Contraction of the microfibrils of wood treated with aqueous NaOH: evidence from changes in the anisotropy of the longitudinal and transverse swelling rates of wood. Journal of Wood Science. 2007;53(2):175-7.
[49] Sgriccia N, Hawley M, Misra M. Characterization of natural fiber surfaces and natural fiber composites. Composites Part A: Applied Science and Manufacturing. 2008;39(10):1632-7.
[50] Biagiotti J, Puglia D, Torre L, Kenny JM, Arbelaiz A, Cantero G, et al. A systematic investigation on the influence of the chemical treatment of natural fibers on the properties of their polymer matrix composites. Polymer Composites. 2004;25(5):470-9.
[51] Liu W, Mohanty A, Drzal L, Askel P, Misra M. Effects of alkali treatment on the structure, morphology and thermal properties of native grass fibers as reinforcements for polymer matrix composites. Journal of Materials Science. 2004;39(3):1051-4.
[52] Bledzki AK, Mamun AA, Faruk O. Abaca fibre reinforced PP composites and comparison with jute and flax fibre PP composites. eXPRESS Polymer Letters. 2007;1(11):755-62.
[53] Knothe J, Rebstock K, Schlosser T. Natural fibre reinforced plastics in automotive exteriour applications. In: Proceedings of In: 3rd International wood and natural fibre composites symposium. Kassel, Germany, Conference, Conference 2000. p. 1-12.
[54] Liu K, Takagi H, Yang Z. Evaluation of transverse thermal conductivity of Manila hemp fiber in solid region using theoretical method and finite element method. Materials & Design. 2011;32(8-9):4586-9.
[55] Saenghirunwattana P, Noomhorm A, Rungsardthong V. Mechanical properties of soy protein based “green” composites reinforced with surface modified cornhusk fiber. Industrial Crops and Products. 2014;60:144-50.

[56] Li Y, Hu C, Yu Y. Interfacial studies of sisal fiber reinforced high density polyethylene (HDPE) composites. Composites Part A: Applied Science and Manufacturing. 2008;39(4):570-8.
[57] Yu T, Jiang N, Li Y. Study on short ramie fiber/poly(lactic acid) composites compatibilized by maleic anhydride. Composites Part A: Applied Science and Manufacturing. 2014;64:139-46.
[58] Takagi H, Ichihara Y. Effect of Fiber Length on Mechanical Properties of Green Composites Using a Starch-Based Resin and Short Bamboo Fibers. JSME International Journal, Series A: Solid Mechanics. 2004;47(4):551-5.
[59] Liu K, Takagi H, Yang Z. Dependence of tensile properties of abaca fiber fragments and its unidirectional composites on the fragment height in the fiber stem. Composites Part A: Applied Science and Manufacturing. 2013;45:14-22.
[60] Shibata M, Ozawa K, Teramoto N, Yosomiya R, Takeishi H. Biocomposites Made from Short Abaca Fiber and Biodegradable Polyesters. Macromolecular Materials and Engineering. 2003;288:35-43.
[61] Müssig J, Fischer H, Graupner N, Drieling A. Testing methods for measuring physical and mechanical fibre properties (plant and animal fibres). In: Müssig J, editor. Industrial Applications of Natural Fibres-Structure, Properties and Technical Applications. John Wiley & Sons, Chichester2010. p. 269-309.
[62] Liu L, Yu J, Cheng L, Qu W. Mechanical properties of poly (butylene succinate)(PBS) biocomposites reinforced with surface modified jute fibre. Composites Part A: Applied Science and Manufacturing. 2009;40(5):669-74.
[63] Bledzki AK, Mamun AA, Jaszkiewicz A, Erdmann K. Polypropylene composites with enzyme modified abaca fibre. Composites Science and Technology. 2010;70(5):854-60.
[64] Fu S-Y, Feng X-Q, Lauke B, Mai Y-W. Effects of particle size, particle/matrix interface adhesion and particle loading on mechanical properties of particulate–polymer composites. Composites Part B: Engineering. 2008;39(6):933-61.
[65] Boopathi L, Sampath P, Mylsamy K. Investigation of physical, chemical and mechanical properties of raw and alkali treated Borassus fruit fiber. Composites Part B: Engineering. 2012;43(8):3044-52.
[66] Yang W, Li Y. Sound absorption performance of natural fibers and their composites. Science China Technological Sciences. 2012;55(8):2278-83.
[67] Spence JCH, Zuo JM. Electron Microdiffraction. New York: Plenum Publishing Corporation; 1992.
[68] Nakano T, Sugiyama J, Norimoto M. Contractive force and transformation of microfibril with aqueous sodium hydroxide solution for wood. Holzforschung. 2000;54(3):315-20.
[69] Nakano T. Mechanism of microfibril contraction and anisotropic dimensional changes for cells in wood treated with aqueous NaOH solution. Cellulose. 2010;17(4):711-9.
[70] El Oudiani A, Chaabouni Y, Msahli S, Sakli F. Crystal transition from cellulose I to cellulose II in NaOH treated Agave americana L. fibre. Carbohydrate Polymers. 2011;86(3):1221-9.
[71] Borysiak S, Doczekalska B. X-ray diffraction study of pine wood treated with NaOH. Fibres Text East Eur. 2005;13(5):87-9.
[72] Nishiyama Y, Kuga S, Okano T. Mechanism of mercerization revealed by X-ray diffraction. Journal of wood science. 2000;46(6):452-7.
[73] Moon RJ, Martini A, Nairn J, Simonsen J, Youngblood J. Cellulose nanomaterials review: structure, properties and nanocomposites. Chemical Society reviews. 2011;40(7):3941-94.

[74] Amel BA, Paridah MT, Sudin R, Anwar UMK, Hussein AS. Effect of fiber extraction methods on some properties of kenaf bast fiber. Industrial Crops and Products. 2013;46:117-23.
[75] Alix S, Philippe E, Bessadok A, Lebrun L, Morvan C, Marais S. Effect of chemical treatments on water sorption and mechanical properties of flax fibres. Bioresource technology. 2009;100(20):4742-9.
[76] Lu N, Swan RH, Ferguson I. Composition, structure and mechanical properties of hemp fiber reinforced composite with recycled high-density polyethylene matrix. Journal of Composite Materials. 2011;0(0):11.
[77] Sun R, Fang JM, Goodwin A, Lawther JM, Bolton AJ. Fractionation and characterization of polysaccharides from abaca fibre. Carbohydrate Polymers. 1998;37(4):351-9.
[78] Sain M, Panthapulakkal S. Bioprocess preparation of wheat straw fibers and their characterization. Industrial Crops and Products. 2006;23(1):1-8.
[79] Placet V, Cissé O, Lamine Boubakar M. Nonlinear tensile behaviour of elementary hemp fibres. Part I: Investigation of the possible origins using repeated progressive loading with in situ microscopic observations. Composites Part A: Applied Science and Manufacturing. 2014;56:319-27.
[80] Duval A, Bourmaud A, Augier L, Baley C. Influence of the sampling area of the stem on the mechanical properties of hemp fibers. Materials Letters. 2011;65(4):797-800.
[81] Baley C. Analysis of the flax fibres tensile behaviour and analysis of the tensile stiffness increase. Composites Part A: Applied Science and Manufacturing. 2002;33(7):939-48.
[82] Nakagaito AN, Yano H. Toughness enhancement of cellulose nanocomposites by alkali treatment of the reinforcing cellulose nanofibers. Cellulose. 2007;15(2):323-31.
[83] Rahman MM, Khan MA. Surface treatment of coir (Cocos nucifera) fibers and its influence on the fibers' physico-mechanical properties. Composites Science and Technology. 2007;67(11-12):2369-76.
[84] Li Y, Ma H, Shen Y, Li Q, Zheng Z. Effects of resin inside fiber lumen on the mechanical properties of sisal fiber reinforced composites. Composites Science and Technology. 2015;108:32-40.
[85] Li Y, Li Q, Ma H. The voids formation mechanisms and their effects on the mechanical properties of flax fiber reinforced epoxy composites. Composites Part A: Applied Science and Manufacturing. 2015;72:40-8.
[86] Dong C, Takagi H. Flexural properties of cellulose nanofibre reinforced green composites. Composites Part B: Engineering. 2014;58:418-21.
[87] Richter S, Stromann K, Müssig J. Abacá (Musa textilis) grades and their properties—A study of reproducible fibre characterization and a critical evaluation of existing grading systems. Industrial Crops and Products. 2013;42(0):601-12.
[88] Armecin RB, Coseco WC. Abaca (Musa textilis Nee) allometry for above-ground biomass and fiber production. Biomass and Bioenergy. 2012;46(0):181-9.
[89] Nam TH, Ogihara S, Tung NH, Kobayashi S. Effect of alkali treatment on interfacial and mechanical properties of coir fiber reinforced poly(butylene succinate) biodegradable composites. Composites Part B: Engineering. 2011;42(6):1648-56.
[90] Roy A, Chakraborty S, Kundu SP, Basak RK, Majumder SB, Adhikari B. Improvement in mechanical properties of jute fibres through mild alkali treatment as demonstrated by utilisation of the Weibull distribution model. Bioresource technology. 2012;107:222-8.
[91] Min Zhi Rong MQZ, Yuan Liu, Gui Cheng Yang, Han Min Zeng. The effect of fiber treatment on the mechanical properties of unidirectional sisal-reinforced epoxy composites. Composites Science and Technology. 2001;61:10.

[92] Uma Maheswari C, Obi Reddy K, Muzenda E, Guduri BR, Varada Rajulu A. Extraction and characterization of cellulose microfibrils from agricultural residue – Cocos nucifera L. Biomass and Bioenergy. 2012;46:555-63.
[93] Rawal A, Sayeed MMA. Tailoring the structure and properties of jute blended nonwoven geotextiles via alkali treatment of jute fibers. Materials & Design. 2014;53:701-5.
[94] Hossain MK, Karim MR, Chowdhury MR, Imam MA, Hosur M, Jeelani S, et al. Comparative mechanical and thermal study of chemically treated and untreated single sugarcane fiber bundle. Industrial Crops and Products. 2014;58:78-90.
[95] Mohanty AK, Misra M, Drzal LT. Surface modifications of natural fibers and performance of the resulting biocomposites: An overview. Composite Interfaces. 2001;8(5):313-43.
[96] Li Y, Chen C, Xu J, Zhang Z, Yuan B, Huang X. Improved mechanical properties of carbon nanotubes-coated flax fiber reinforced composites. Journal of Materials Science. 2014;50(3):1117-28.
[97] Yang L, Thomason JL. Development and application of micromechanical techniques for characterising interfacial shear strength in fibre-thermoplastic composites. Polymer Testing. 2012;31(7):895-903.
[98] Kalia S, Kaith BS, Kaur I. Pretreatments of natural fibers and their application as reinforcing material in polymer composites-A review. Polymer Engineering & Science. 2009;49(7):1253-72.
[99] L.Segal JJC, A.E.Martin, Jr., and C.M.Conrad. An Empirical Method for Estimating the Degree of Crystallinity of Native Cellulose Using the X-Ray Diffractometer.pdf. Textile Research Journal. 1959;October:8.
[100] Oudiani AE, Chaabouni Y, Msahli S, Sakli F. Crystal transition from cellulose I to cellulose II in NaOH treated Agave americana L. fibre. Carbohydrate Polymers. 2011;86(3):1221-9.
[101] A. Valadez-Gonzalez JMC-U, R. Olayo, P.J. Herrera-Franco. Effect of fiber surface treatment on the fiber-matrix bond strength of natural fiber reinforced composites. composites Part B: Engineering. 1999;30:11.
[102] Cai M, Takagi H, Nakagaito AN, Kusaka K, Katoh M. Influence of alkali concentration on morphology and tensile properties of abaca fibers. Advanced Materials Research. 2015;1110:302-5.
[103] Cai M, Takagi H, Nakagaito AN, Li Y, Waterhouse GIN. Effect of alkali treatment on interfacial bonding in abaca fiber-reinforced composites. Composites：Part A. 2016;90:589-97.